1. Report No. FHWA/TX-09/0-5820-1	2. Government Accession No.	3. Recipient's Catalog No.
4. Title and Subtitle USING CEMENT PASTE RHEOLOGY TO PREDICT CONCRETE MIX DESIGN PROBLEMS: TECHNICAL REPORT		5. Report Date November 2008 Published: July 2009
		6. Performing Organization Code
7. Author(s) Anal K. Mukhopadhyay and Sehoon Jang		8. Performing Organization Report No. Report 0-5820-1
9. Performing Organization Name and Address Texas Transportation Institute The Texas A&M University System College Station, Texas 77843-3135		10. Work Unit No. (TRAIS)
		11. Contract or Grant No. Project 0-5820
12. Sponsoring Agency Name and Address Texas Department of Transportation Research and Technology Implementation Office P. O. Box 5080 Austin, Texas 78763-5080		13. Type of Report and Period Covered Technical Report: September 2006-August 2008
		14. Sponsoring Agency Code

15. Supplementary Notes

Project performed in cooperation with the Texas Department of Transportation and the Federal Highway Administration.
Project Title: Using Cement Paste Rheology to Predict Concrete Mix Design Problems
URL: http://tti.tamu.edu/documents/0-5820.pdf

16. Abstract

The complex interaction between cement and chemical/mineral admixtures in concrete mixture sometimes leads to unpredictable concrete performance in the field, which is generally defined as concrete incompatibilities. Cement paste rheology measurements instead of traditional workability tests can have a great potential to detect those incompatibilities in concrete before the concrete is placed to avoid setting time, workability, and curing-related issues, which sometimes leads to severe early-age cracking especially in severe weather conditions. The objective of the present study was to examine the applicability of the Superpave Dynamic Shear Rheometer (DSR) to measure cement paste rheology in one hand and identify cement and mineral/chemical admixtures incompatibilities based on cement paste rheological behavior on the other hand.

Based on the extensive laboratory investigation, it is observed that DSR in modified form can measure cement paste rheology with permissible repeatability and sensitivity and has a great potential to identify cement and mineral/chemical admixture incompatibilities. The heat of hydration data from isothermal calorimeter test and setting time results for the studied mixtures have strongly supported the rheology-based observations. A procedure to formulate rheology-based acceptance criteria has been developed based on the available test results. Further refinement of these acceptance criteria based on detailed work covering a wide range of incompatibilities and validation through implementation efforts is warranted. This will ultimately help concrete producers and district laboratories to detect problematic combinations of concrete ingredients during the mixture design process. The researchers also investigated the feasibility of the mini slump cone test as an alternative or supporting tool for the rheology test.

17. Key Words Cement Paste, Concrete, Chemical Admixture, Incompatibility, Rheology, Plastic Viscosity, Yield Stress, Setting Time, Heat of Hydration, Stiffening, Workability, Mini Slump	18. Distribution Statement No Restrictions. This document is available to the public through NTIS: National Technical Information Services Springfield, Virginia 22161 http://www.ntis.gov	
19. Security Classif.(of this report) Unclassified	20. Security Classif.(of this page) Unclassified	21. No. of Pages 154	22. Price

Form DOT F 1700.7 (8-72)   **Reproduction of completed page authorized**

USING CEMENT PASTE RHEOLOGY TO PREDICT CONCRETE MIX DESIGN PROBLEMS: TECHNICAL REPORT

by

Anal K. Mukhopadhyay
Associate Research Scientist
Texas Transportation Institute

and

Sehoon Jang
Graduate Assistant Researcher
Texas Transportation Institute

Report 0-5820-1
Project 0-5820
Project Title: Using Cement Paste Rheology to Predict Concrete Mix Design Problems

Performed in cooperation with the
Texas Department of Transportation
and the
Federal Highway Administration

November 2008
Published: July 2009

TEXAS TRANSPORTATION INSTITUTE
The Texas A&M University System
College Station, Texas 77843-3135

DISCLAIMER

The contents of this report reflect the views of the authors, who are responsible for the facts and the accuracy of the data presented herein. The contents do not necessarily reflect the official view or policies of the Texas Department of Transportation and/or the Federal Highway Administration. The report does not constitute a standard, specification, or regulation. The scientist in charge of the project was Dr. Anal K. Mukhopadhyay.

ACKNOWLEDGMENTS

TABLE OF CONTENTS

<div align="right">**Page**</div>

TABLE OF CONTENTS (Continued)

Page

LIST OF FIGURES

Figure   **Page**

LIST OF FIGURES (Continued)

Figure   **Page**

LIST OF TABLES

Table   **Page**

LIST OF TABLES (Continued)

Table   **Page**

CHAPTER 1

INTRODUCTION

Research Background

    The use of various chemical and mineral admixtures in portland cement concrete is a common practice, which sometimes deliberately or non-deliberately alters the hydration process and chemical interaction that leads to unexpected concrete behavior. Complex chemical interaction between C_3A in cements, sulfate contents in pore solution, supplementary cementitious materials (SCM), and chemical admixtures along with temperature change sometimes creates poor cement-admixture compatibility and can give rise to inadequate early workability or premature loss of workability along with setting time (early stiffening or excessive retardation) and heat evolution abnormalities.

    For that reason, it is necessary to identify those concrete incompatibilities before concrete placement in order to avoid the problems in the placing and curing process. The measurement of rheological properties of cement pastes yields crucial information on (i) the evolution of hydrating cementitious systems, (ii) microstructural changes and particle interaction in cement paste, (iii) the relative performance of different chemical admixtures (e.g., water-reducing admixture)—the optimum dosage and the consequences of excessive dosages, and (iv) the compatibility of various cement, chemical, and mineral admixtures combinations. Therefore, cement paste (cement + supplementary cementitious materials + chemical admixtures + water) rheological measurements have a great potential to identify those incompatibilities before concrete placement. However, a successful application of the rheology approach needs a standard user-friendly device (e.g., rheometer) to measure paste rheology.

    Cement paste rheology studies using parallel plate fluid rheometer and rotational viscometers were conducted by several researchers in the past (Chapter 2). It has been observed that mixtures with different admixture dosages and water to cementitious material ratio (w/cm) can clearly be distinguished based on paste rheological parameters such as viscosity and yield stress. Therefore, identifying cement-admixtures (chemical and mineral) incompatibilities through the measurement of paste rheological parameters instead of concrete rheological parameters is a sound concept. Cement paste rheology measurement tests have the following advantages: (i) much smaller amounts of testing materials, (ii) representative sample preparation

by user-friendly preparation techniques, (iii) less testing time, (iv) more accurate results as it records true engineering properties of viscosity and yield stress, (v) less labor intensive than tests performed on concrete—existing concrete rheometers are large in size and heavy and are not suitable for outdoor application. Moreover, aggregate effects in real concrete can be simulated during cement paste rheology measurements by some suitable means, e.g., using a high shear mixing procedure to simulate aggregate shearing effects in concrete and setting a suitable plate gap in rheology test to represent an average gap between aggregate particles in real concrete.

Research Objectives

The objective of this research is (i) to develop a Dynamic Shear Rheometer (DSR) based on an easy-to-use rheometer, which can measure cement paste rheology with permissible repeatability and sensitivity, and (ii) to investigate whether potential cement-mineral/chemical admixtures incompatibilities can clearly be identified through the direct measurement of cement paste rheology using the developed rheometer through laboratory testing program.

The ultimate goal, in this regard, is to develop an easy-to-use, relatively inexpensive field laboratory test and equipment to predict potential concrete mixture incompatibilities such as those between the sulfate system and mineral and chemical admixtures through the direct measurement of cement paste rheology.

Scope of Research

The research team has proposed the project work in the following sequence in order to achieve the above objectives.

- Identify the areas of modification to make DSR suitable for measuring cement paste rheology based on literature review and expertise on rheometers with parallel plate configuration.
- Adopt those areas of modifications and upgrade DSR to measure cement paste rheology.
- Conduct preliminary investigation to optimize DSR test conditions and develop a DSR based rheology test procedure.

2

- Perform extensive laboratory investigation using the modified DSR based rheology test procedure with varieties of cements, supplementary cementitious materials (SCMs), and different types and dosages of commonly used chemical admixtures under different temperature conditions. The researchers will select the materials based on the available historical information so that some incompatibilities can be generated in the laboratory.

- Develop a procedure to formulate rheology based acceptance criteria. Acceptance criteria will be developed based on the test results available from the above laboratory investigation.

- Conduct field demonstrations. The DSR based rheology test method will be demonstrated in TxDOT or some other laboratory to show the repeatability as well as sensitivity to identify incompatibilities.

Further refinement of these acceptance criteria based on more specific work covering a wide range of incompatibilities and field laboratory validation through implementation efforts are beyond the scope of the present research. This will ultimately help material suppliers, concrete producers, and other users to detect problematic combination of concrete ingredients before the concrete is placed and thereby, to avoid concrete cracking and other durability issues due to incompatibilities.

This project was divided into a number of parts, which are explained in the following chapters. Chapter 2 gives the background information based on literature review and personal communication with the national experts on cement paste rheology. Chapter 3 explains the applicability of DSR to measure cement paste rheology including modifications and optimization of the test conditions and development of a mixing procedure and rheology test procedure. Chapter 4 describes material characterization and selection procedure. Chapter 5 presents the experimental design and updated test procedure for the main laboratory test program. Chapter 6 presents laboratory test results, analysis, and discussion. Chapter 7 describes a procedure to formulate rheology-based acceptance criteria. Chapter 8 presents the field demonstration program. Finally, Chapter 9 contains the conclusions and recommendations from this project.

CHAPTER 2
LITERATURE REVIEW

Many practices in the construction of highway pavements are less than ideal. Placement during hot weather, short mixing times, transport in non-agitating trucks, excessive or insufficient vibration, and poor timing of control joint sawing all contribute to unsatisfactory performance. Some materials and combinations of materials are more sensitive to these practices and aggravate unsatisfactory performance as an additional material factor. In particular, some combinations of cement, SCMs, and chemical admixtures have the potential for incompatibility, leading to early stiffening or excessive retardation along with heat evolution abnormalities (*1*). A complex interaction between C_3A in cement, sulfate in pore solution, SCMs, and chemical admixtures sometimes creates poor cement-admixture compatibility (*2, 3*). Therefore, it is necessary to identify those incompatibilities before the actual placement to avoid the problems in the placing and curing process. It is anticipated that cement paste (cement + SCMs + chemical admixtures + water) rheology measurements could be a good indicator to identify those incompatibilities.

The information collected on these issues was reviewed and highlighted. An extensive literature review was conducted addressing three major categories, i.e., (i) theoretical background of rheology, (ii) rheology as an indicator of mineral admixtures – chemical admixtures – sulfate (from SCMs) incompatibilities, and (iii) existing information pertaining to the applicability of parallel plate rheometer (dynamic shear rheometer and other related fluid rheometer) in measuring rheological parameters of cement paste and concrete.

Theoretical Background of Rheology in Connection with Cement Paste and Concrete

Rheology is the science of the deformation and flow of matter, and the emphasis on flow means that it is concerned with the relationships between stress, strain, rate of strain, and time. Concrete in its fresh state can be considered a fluid and therefore the basic principles of rheology can be applied to this material (*4*).

Bingham Model

For a diluted suspension of solids in a liquid, there is no interparticle force, and the effect of small increases in the amount of suspended solid is merely to increase the coefficient of viscosity. However, for a concentrated suspension (e.g., concrete), there are forces acting between the particles. These forces do not merely change the viscosity but actually change the type of flow. Tattersall and Banfill carried out systematic investigations in the rheology of concrete (5). They found that there was a linear relationship between torque and the rotation speed of the viscometer after a certain torque had been exceeded. They stated that concrete flow could be expressed by the Bingham model and can be written as:

$$\tau = \tau_0 + \mu\dot{\gamma}$$
Equation (1)

where τ (in Pa) is the shear stress, τ_0 is the yield stress, μ (Pa·s) is the plastic viscosity, and $\dot{\gamma}$ (in s^{-1}) is the shear strain rate. Unlike the Newtonian model, concrete has a yield stress, which indicates the minimum stress to start a flow in concrete material. The plastic viscosity measures the resistance of concrete against an increased speed of movement. It is possible that two mixtures may have the same slump or yield stress but exhibit a different behavior at a higher shear rate (e.g., different plastic viscosity) as shown in Figure 2.1 (A). On the other hand two mixtures may behave similarly at an applied shear rate, but the yield stress may be completely different, as shown in Figure 2.1 (B). Therefore, measurement of both yield stress and plastic viscosity is necessary to get a complete picture of flow behavior of paste or concrete.
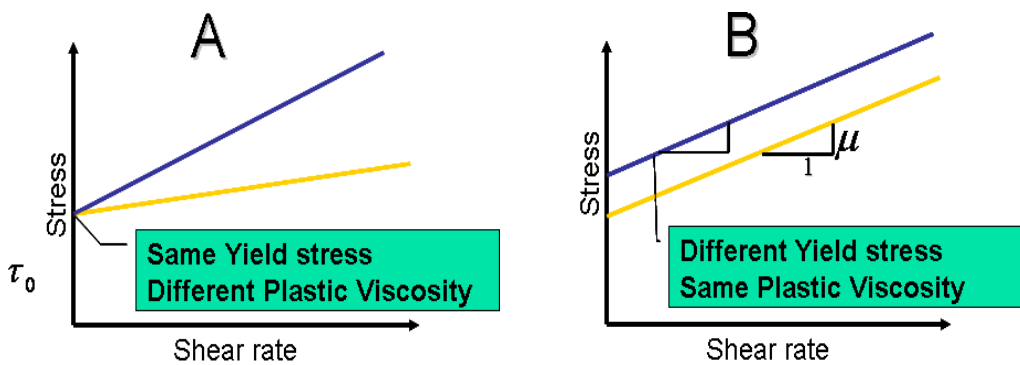
Figure 2.1. Characteristics of Two Rheological Parameters.

The Nature of Rheological Parameters

Table 2.1 shows the range of rheological parameters of paste, mortar, and different types of concretes (*6*). From cement paste to concrete, the yield stress and plastic viscosity increase as the particle size increases. Banfill and Tattersall pointed out that this increase occurs because the aggregate could resist stresses without deformation. Since the aggregate occupies up to 70—80 percent of concrete volume, the yield stress of concrete is higher than cement paste, which has no aggregate inside. Mortar yield stress is in between paste and concrete yield stress. In general, due to the increased interparticle contact and surface interlocking, the plastic viscosity of concrete is higher than that at paste. When concrete is subjected to a shear stress, the shear rate within the solid aggregate particles is zero, since the solid aggregate particles cannot deform (*7*). As a result, in order to have a certain shear rate in the whole composite, the shear rate in paste is higher compared to the material with just pure cement paste. This higher shear rate results in a higher stress and resistance to flow in the cement paste that in turn accounts for the increase in measured plastic viscosity of the bulk material (*8*).

Table 2.1. Rheological Parameters of Cementitious Materials (*6*).

Material	Paste	Mortar	Self-compacting concrete	Flowing concrete	Pavement concrete
Yield Stress (Pa)	10-100	80-400	50-200	400	500-2000
Plastic Viscosity (Pa·s)	0.01-1	1-3	20-100	20	50-100

Cement-Admixture Incompatibilities

The mechanism of incompatibility between the cement, chemical admixtures, and SCMs is described below. The availability of the sulfate ion in pore solution might be completely different depending on the type of sulfate (e.g., anhydrite, hemi-hydrate, and gypsum) although portland cements have the same total SO_3 content (*9*). Some SCMs (e.g., Class C fly ash and slag) can serve as an additional source of sulfate besides the cement itself. The level of sulfate concentration (e.g., low, optimum, high) in the pore solution strongly influences the adsorption of certain chemical admixtures (e.g., water-reducing admixture) during the first minutes of

hydration (10). Consequently, it may also affect the rheological properties of cement paste, which can be explained by the competitive adsorption by the hydrating C_3A between the sulfate ions and the chemical admixture molecules. If the sulfate concentration is too low, a high quantity of admixture molecules is adsorbed and may be incorporated into the cement hydrates during the initial hydration reactions, consequently losing their dispersing effect. On the other hand, if the sulfate concentration is too high, a smaller amount of the admixture is adsorbed due to the competitive adsorption of the sulfate ions. In sulfate deficient systems, the hydration of C_3A yields calcium aluminate hydrates, which rapidly leads to a flash setting, whereas in the presence of excessive sulfate, nucleation and growth of gypsum crystals can lead to false setting behavior (11). Setting time retardation due to abnormal cement-chemical admixture interaction (especially lignin-based water reducing admixture) often occurs in fresh concrete. Excessive retardation may also occur if high volumes of fly ash are incorporated into concrete especially when using Type V cement. It is reported that a cement/mineral/chemical system becomes more complicated and unpredictable with high or low ambient temperature conditions (12).

Rheology as an Indicator of Incompatible Mixture

Since admixtures mainly affect the flow behavior of the cement paste without altering the composition or behavior of the aggregate it seems reasonable to select chemical and mineral admixtures by measuring cement paste rheology (13). However, a successful use of cement paste rheology for identifying any incompatibilities relies on the fact that the rheological parameters (i.e., yield stress and plastic viscosity) should be sensitive enough to differentiate between abnormal and normal mixtures. The most important factors that cause incompatibilities of concrete can be summarized as:

- the amount of C_3A,
- the type and amount of sulfate-bearing phases in cement and SCMs,
- the water-soluble alkalis (Na^+, K^+) from both cement and SCMs,
- the type and dosage of both chemical as well as mineral admixtures,
- cement paste temperature, and
- w/cm.

The sensitivity of the rheological parameters to the above-mentioned factors was reported by several researchers (*14, 15, 16*). Figure 2.2 shows the yield stress and viscosity for cement paste mixtures with varying dosages of high-range water-reducing admixture (HRWRA) as well as SCMs in tests conducted at NIST (*17*). The amounts of the various mineral admixtures replacement by mass of cement are also listed in Figure 2.2. The change of rheological parameters (yield stress and viscosity) as a function of type of mineral admixtures and the HRWRA dosage is clearly manifested in Figure 2.2. Therefore, the use of cement paste rheological parameters as an indicator for identifying concrete incompatibilities is a sound concept.
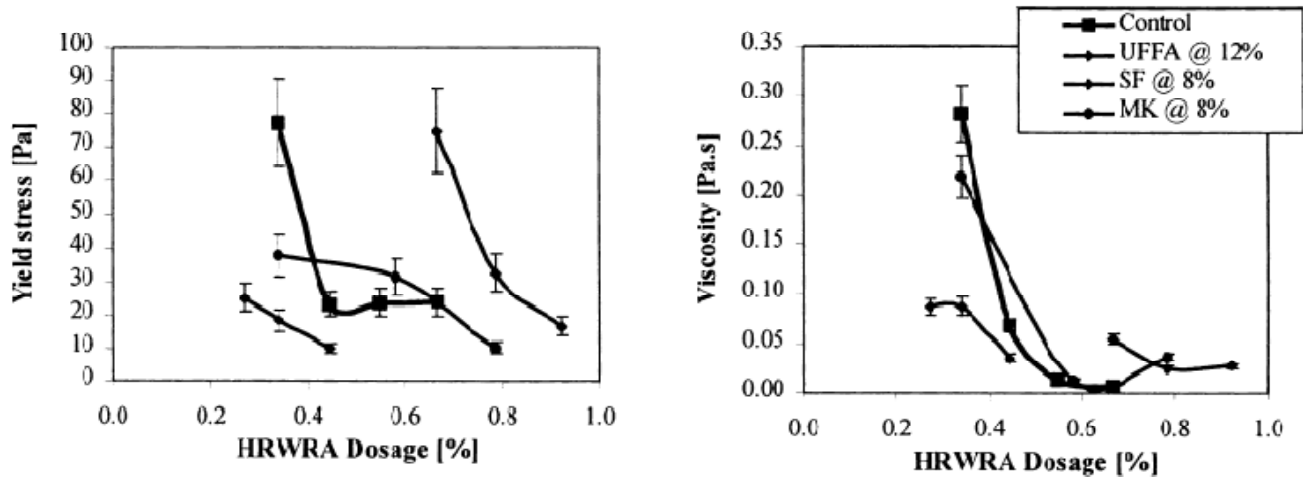
Note: W/C 0.35, UFFA: ultra fine fly ash, SF: silica fume, MK: Metakaolin

Figure 2.2. Dosage of HRWR and Its Effect on Rheological Parameters (*17*).

Areas of Modification of Dynamic Shear Rheometer to Measure Cement Paste Rheology

The applicability of DSR is discussed based on the available information on:

- NIST research on the application of a parallel plate rheometer to measure cement paste rheology,
- issues pertaining to the adoption of DSR to measure cement paste rheology,
- areas of modification of DSR to fit into cement paste rheology measurement, and
- influence of mixer type and mixing procedure.

Dynamic shear rheometer could be a potential test equipment to characterize rheological parameters of cement paste. Struble, Schultz, and Lei reported interesting results using the cement paste and the small amplitude oscillatory shear techniques (*18, 19, 20, 21*). Recently, the use of small shear rate sweeping mode is reported to monitor the stiffening process of dispersed cementitious mixtures using the Bingham model. The cement paste sample is sandwiched between two parallel plates. The shear stress and strain of specimen are measured when the upper plate is oscillating as shown in Figure 2.3.
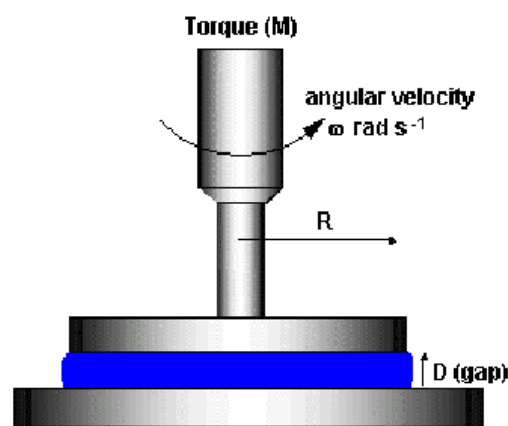
Figure 2.3. Principle of Rheometer with Parallel Plate System.

Issues Pertaining to the Adoption of DSR to Measure Cement Paste Rheology

According to several literatures published by NIST, changes in the rheology of cement paste clearly affect the concrete rheology, although the relationship between cement paste and concrete rheology has not been completely established. NIST is developing a method to predict concrete rheology based on cement paste rheology measured under simulated shearing condition. The cement paste rheology is typically measured under conditions that are not experienced by the cement paste in concrete. The values usually reported in the literature for cement paste do not take into account the contribution of the aggregates (*22*). Determining the correct method for measuring cement paste rheology requires simulation of the conditions that cement paste experiences in concrete. NIST addressed the following factors in designing the proposed test procedure:

- The aggregates cause shearing effects in the cement paste during the mixing process. The distance between the aggregates (varying with the paste content in concrete) in concrete has an important influence on the degree of shearing effects. The distances between aggregates can be represented by setting a proper gap between two parallel plates. Therefore, rheometer with parallel plate geometry is suitable to simulate the aggregate shearing effects by selecting a proper gap between two plates.

- The mixing of cement paste must imitate the shear stresses experienced in concrete. Portland Cement Association (PCA) and several different research institutes reported the use of a high shear mixer for preparing cement paste to simulate this shearing effect (23).

Therefore, selecting an optimum gap between two plates and application of high shear mixing procedure is necessary to simulate the shearing effects that cement paste experiences in concrete due to aggregates.

Areas of Modification for DSR to Fit into Cement Paste Rheology Measurement

The DSR was designed to characterize the viscous and elastic behavior of asphalt binders. Therefore, modification of DSR by changing several features is necessary to measure cement paste rheology. Ferraris and her collaborators have been evaluating cement paste since 1991 by using fluid rheometers with parallel plate geometry (24, 25). They modified the faces of the parallel plates as serrated or cross-hatched to avoid slippage. In the same manner, the smooth surfaces of both upper and lower parallel plate in DSR can be grooved (26). The schematic pictures of both smooth and serrated parallel plates are shown in Figure 2.4.

Nehdi and Rahman investigated the effect of both smooth and serrated parallel plates on the rheological parameters (27). They reported that smooth parallel plates did not depict fundamental changes in rheological properties imparted by the addition of different types of SCMs whereas serrated plates showed obvious changes. The parallel plates with smooth surfaces gave lower storage modulus values for cement paste compared with those of the serrated plate, probably due to the smooth parallel plates' relatively lower friction capability and increased likelihood of slippage. The dependence of the storage modulus on the friction capacity of the parallel plates generally decreased with the increase of the water to total cementitious material ratio (w/cm) for all tested cement paste. This is believed to be due to the

11

effect of slippage smooth plate especially with high w/cm. This leads to doubt on the suitability of parallel plates with smooth surfaces to measure rheological properties of cement pastes.
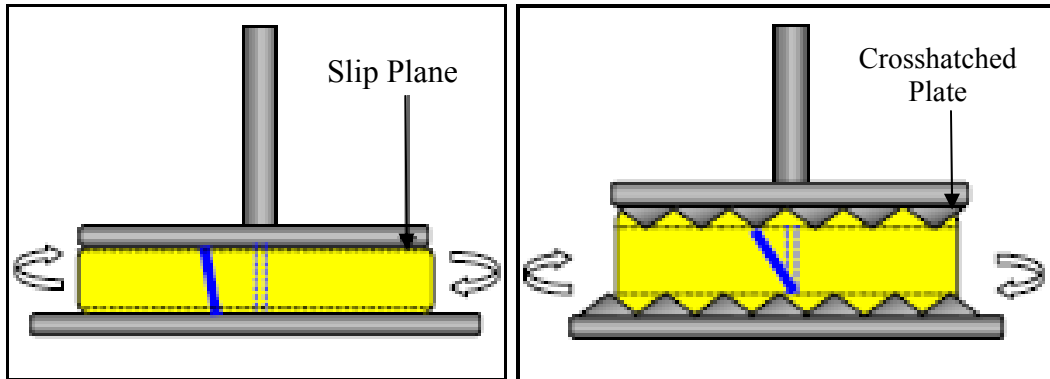
Figure 2.4. (Left) Smooth Parallel Plates, (Right) Serrated Parallel Plates.

Secondly, DSRs used at state Departments of Transportation (DOTs) have mostly open water circulation systems for temperature control where the specimen directly comes in contact with water. Since the fresh cement paste is a water-sensitive material, unlikely asphalt binder, another arrangement such as a Peltier heating-cooling system or closed system water circulation system needs to be instrumented for temperature controlling. In most of the previous studies on cement paste rheology, temperature control during mixing instead of temperature control in the rheometer was considered as a means to study the effect of temperature. However, temperature control in both mixing and rheometer testing stages is necessary in order to study the effect of temperature precisely.

Influence of the Mixer Type and Mixing Procedure

The first use of a high speed shear mixer to make cement paste was reported by Kantro (*28*) in connection with the development of his mini slump cone test. Since Kantro used a high speed shear mixer, many researchers have used this mixing method for cement paste rheology in later years. Several researchers have used a blender as a high speed shear mixer (up to 10,000 rpm) and Hobart paddle mixer as a low speed shear mixer (100 rpm) in their cement paste rheology research (*29*). They mentioned that the cement pastes mixed in the blender more accurately represent concrete performance when the results of the rheological parameter, yield

stress in both cement paste tests with two different mixers, were compared with a concrete slump test as shown in Figure 2.5. This confirms a study by Helmuth (30) stating that in concrete, during mixing, the cement paste is sheared with an energy and rate more closely reproduced in a blender as opposed to the low shear rate of the Hobart mixer. Therefore, it is essential to use a high shear mixer to prepare cement paste in order to measure representative rheological parameters (31).

Note: YS: yield stress; Visc: plastic viscosity.
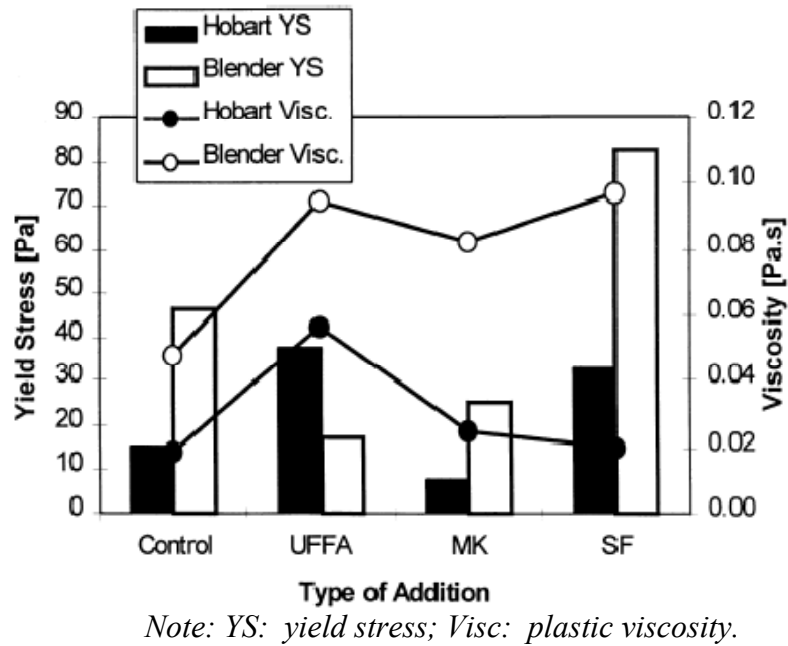
Figure 2.5. Influence of the Mixer on the Rheological Properties of Cement Paste (17).

CHAPTER 3. APPLICABILITY OF DSR
FOR MEASURING CEMENT PASTE RHEOLOGY

The dynamic shear rheometer has been adopted in Superpave to characterize the viscous and elastic behavior of asphalt binders at high and intermediate service temperatures. Most of the Department of Transportation personnel use DSR as a standard test for measuring rheological properties of asphalt binder. DSR is based on parallel plate configuration and has the great potential to be considered as a user-friendly cement paste rheology measurement device after upgrading the device with necessary modifications. The areas of modifications of DSR along with the importance of mixing procedure were discussed in Chapter 2. This chapter presents the modifications and optimization that have been actually made and the test procedure that has been developed. The applicability of DSR to measure cement paste rheology has been verified through a preliminary test program using the modified system and developed test procedure.

Dynamic Shear Rheometer

The dynamic shear rheometer is used to characterize the viscous and elastic behavior of asphalt binders at high and intermediate service temperatures. AASHTO TP5 contains the DSR test procedure. As shown in Figure 3.1 (a) and (b), the asphalt binder sample is sandwiched between a fixed plate and an oscillating plate. Figure 3.1 (c) shows the movement of the oscillating plate when torque is applied as one cycle of oscillation. The frequency of oscillation is expressed as the number of oscillation cycles per second. All Superpave DSR tests are conducted at a frequency of 10 radians per second, which is equivalent to about 1.59 Hz.

The dynamic shear rheometer operates under constant stress and constant strain controlled modes of loading. It applies sinusoidal dynamic loading at a wide range of frequencies (0.1 H to 30 Hz). The system provides the dynamic shear modulus, which is equal to the stress amplitude over the strain amplitude. Also, the system provides the phase angle, which represents the lag between the stress and strain functions. A phase angle of zero indicates an elastic behavior, while a phase angle of 90 indicates a viscous behavior. The cement paste phase angle is expected to be between 0 and 90 radians.

(a) DSR at TTI

(b) Enlarged view of two plates
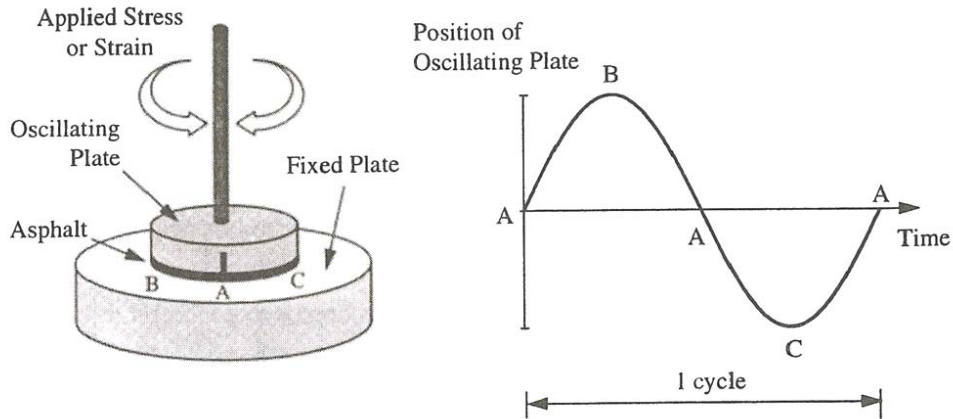
(c) Basics of DSR

Figure 3.1. Dynamic Shear Rheometer at TTI.

Ultimately, the DSR with asphalt binder samples can provide the storage and loss modulus data from the oscillation mode described above. Although these parameters (i.e., storage modulus and loss modulus) have a potential possibility to measure cement paste rheology (*19*), the shear rate sweeping mode was selected for the laboratory test program in accordance with NIST's work on cement paste rheology using parallel plate rheometer. In this mode, the shear stresses are measured with varying shear rate. Since cement paste rheological parameters (i.e., yield stress and plastic viscosity) determined by this mode correlate well with

concrete rheology (*24*), this research has adopted the shear rate sweeping operating mode for DSR to measure cement paste rheology.

Modification of DSR for Measuring Cement Paste Rheology

The following three areas of modifications have been identified from Chapter 2:

- make a serrated surface to avoid slippage,
- install a different temperature controlling system where sample contact with water can be avoided (e.g., Peltier heating-cooling system or closed system water circulation system), and
- install a better evaporation control system.

The three areas of modifications are described below.

Make Serrated Surface

To serrate the parallel plate surface, 240 grit paper with adhesive back was installed on both the upper and lower plates (25 mm diameter for both the plates) in order to prevent slippage. Figure 3.2 shows a schematic representation of attaching 240 grit paper to both the plates. The use of 240 grit paper in a rheometer with parallel plate configuration to prevent slippage effect as well as to simulate aggregate texture effects is reported by several researchers (*9, 10*).
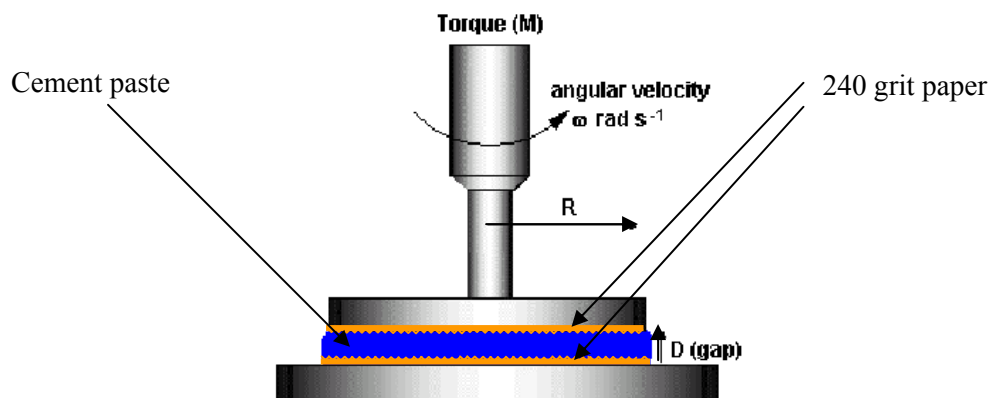
Figure 3.2. Installation of Grit Paper on Both Upper and Lower Plates in DSR.

Temperature Control

A fluid jacket heating/cooling system was installed (Figure 3.3) to avoid direct contact of the specimen (cement paste) with water during testing. Most DSRs used at state Departments of Transportation have open water circulation system for temperature control where a specimen comes in contact with water directly. Since fresh cement paste is a water-sensitive material, unlike asphalt binder, the existing temperature control system needed to be changed. The fluid jacket system operates with a closed system water circulation system to keep the temperature of the cement paste sample constant during the entire time span of the rheological test.

Before Modification   **After Modification**

Figure 3.3. Modified DSR with the Fluid Jacket System.

Evaporation Control

A wet sponge cap was attached to the DSR (Figure 3.4) to prevent the cement paste specimen from moisture loss due to evaporation during the test procedure. Preliminary tests (described later in this chapter) were conducted with the wet sponge cap for evaporation control. However, the wet sponge system did not allow 100 percent evaporation control because of the presence of a little opening in the cap (see Figure 3.4). The research team has continued their efforts to develop a better evaporation control system for the main laboratory tests (described in Chapter 5).

Wet sponge inside the cap
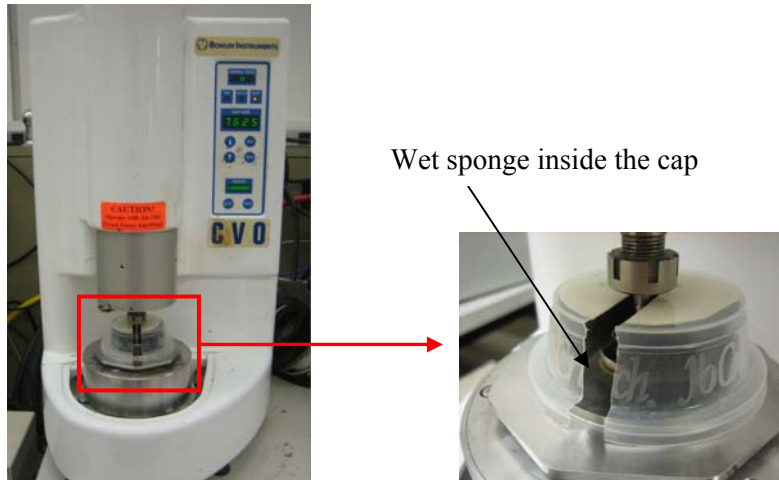
Figure 3.4. Evaporation Control with Wet Sponge.

Test Methods

Table 3.1 summarizes the testing plan in the experimental program. The experimental program is based on four different test methods and equipments: (i) rheological behavior of the cementitious system measured by DSR and AR2000 Rheometer, (ii) heat generation behavior of the cementitious system measured by isothermal micro-calorimeter, (iii) setting behavior of the cementitious system determined by Vicat Apparatus (ACTM C 191), and (iv) flow behavior of cement paste by mini slump cone test. AR 2000 was selected in the preliminary test program to validate and establish DSR results through a comparative assessment between the results of the two rheometers. The test methods for measuring heat of hydration and setting time served as supporting tools for the rheological parameters determined by DSR and AR 2000.

Table 3.1. Test Methods in the Experimental Program.

Test Method	Test Equipment	Measured Properties
Rheological behavior of fresh cement paste	Modified Bohlin CVO Rheometer, DSR (Malvern Instrument)	Rheological parameters (yield stress and plastic viscosity)
Rheological behavior of fresh cement paste	Modified AR2000 Rheometer (TA Instrument)	Rheological parameters (yield stress and plastic viscosity)
Heat generation behavior of the cementitious system (ASTM C 186)	Isothermal conduction calorimeter (OMNICAL)	Heat of Hydration
Setting behavior (ASTM C191)	Vicat needle apparatus	Initial and Final set time

Test Procedure

The test procedure for each type of test equipment (i.e., rheometer, isothermal conduction calorimeter, vicat needle apparatus) is presented below. A temperature controlled high shear mixing procedure is developed as an essential requirement for the cement paste sample preparation for all the rheology tests.

Temperature Controlled Storage and Mixing

All the ingredients (i.e., cement, deionized water, supplementary cementitious materials, and chemical admixtures) were kept under the selected temperatures at least for one day before mixing. A refrigerator was used to store as well as mix the materials at the studied low temperature (i.e., 10°C/50°F) to represent a winter temperature, whereas an oven was used for the same at the studied high temperature (i.e., 35°C/95°F) to represent a summer temperature (as shown in Figure 3.5). Storing materials and mixing inside a lab room with 24°C/75°F temperature represented mixing at intermediate ambient temperature condition. The cement and SCMs (fly ashes, slag, etc.) with predetermined proportions according to the experimental design were dry blended well before being stored.

<div align="center">(a)   (b)</div>

Figure 3.5. (a) Use of a Refrigerator to Mix at Low Temperature (10°C) and (b) Use of an Oven to Mix at High Temperature (35°C).

Mixer Type and Mixing Procedure

The mixing procedure to prepare the cement paste sample was developed by the Texas Transportation Institute based on the procedure developed by Portland Cement Association and later by the National Institute of Standards and Technology. A high-shear mixer, i.e., a kitchen blender (Figure 3.6), was used to develop the mixing procedure. The maximum mixing speed used during mixing procedure was 6000 rpm instead of 10,000 rpm (used by PCA/NIST) in order to reduce high heat generation due to friction. The steps involved in the mixing procedure are presented in Figure 3.7 and are briefly described below:

1. Keep the mixing bowl along with all the ingredients inside the refrigerator/oven/room for pre-conditioning under the selected studied target temperatures.
2. Keep the predetermined quantity of cement and SCM blend in the mixing bowl of the mixer.
3. Pour the water into the mixing bowl containing cement and SCM blend followed by switching on the mixer at 3000 rpm speed for 30 seconds.
4. Stop the mixer, and add the chemical admixture to the cement and water mixture in the container slowly within 50 seconds. Mix again at 3000 rpm setting for another 10 seconds

5. Increase mixing speed to 6000 rpm and continue mixing for another 30 seconds.

6. Stop mixing for 2 minutes and scrape the sides of the mixing bowl with a rubber paddle.

7. Mix again in the same high-shear blender at 6000 rpm for another 30 seconds.

The ingredients kept in the refrigerator or oven were mixed immediately after bringing them outside according to the above mixing procedure and then the mixing bowl with cement paste was put back inside the refrigerator or oven immediately after mixing in order to make the heat gain or loss minimal.

Mixing Speed	1.	2.	3.	4.	5.
Level	Stir	Chop	Mix	Puree	Liquify
RPM	3000	6000	8000	10000	13000

(a)   (b)

Figure 3.6. (a) The High-Shear Mixer, KSB560OB Kitchen Aid Company and (b) RPM Corresponding to Different Mixing Speed Levels.
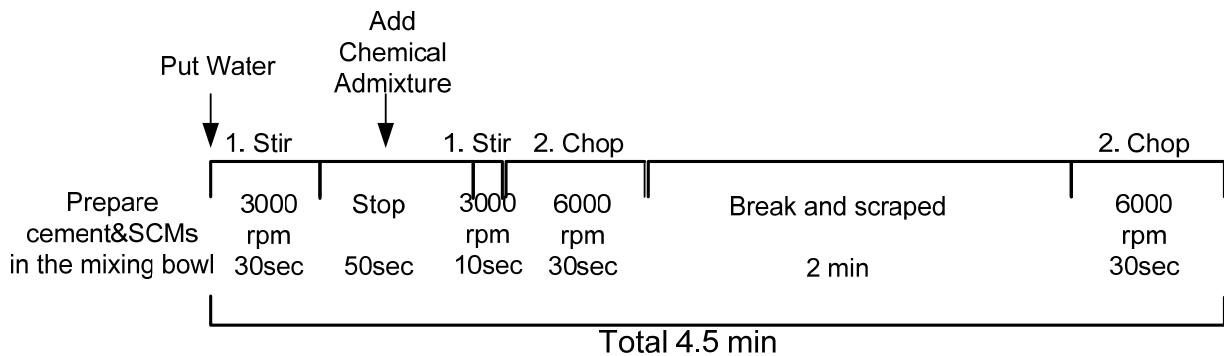
Figure 3.7. Schematic Mixing Procedure.

Rheometer Test Procedure

The studied cement paste was tested for a total of five plate (25 mm diameter) gaps (0.2, .5, 1.0, 1.2, and 1.5 mm). The test was carried out at a controlled temperature 24°C/(75°F), which is the average cement paste temperature during the setting period. A computer program allows the user to customize test parameters, such as the number of readings, the gap of the parallel plate, the sampling interval between the readings, and specimen temperature. The rheometer test procedure is given below:

1. Take cement paste specimen from the mixing bowl using 3 ml syringes immediately after mixing procedure at 24°C/(75°F).
2. Place the predetermined quantity of cement paste (i.e., 1.5 ml) onto the lower plate of the rheometer from the syringe.
3. Sandwich the specimen between the two parallel plates with preselected plate gap and cover the wet sponge cap to prevent water evaporation during the rheology test period.
4. The upper parallel plate starts to rotate and shear with shear rate from 0 to 200/s representing the up curve followed by 200 to 0/s representing the down curve. The shear stress as a function of the shear rate is then recorded. A run with one cycle consisting of one up curve and one down curve takes approximately three minutes.

Calculation of Rheological Parameters

Figure 3.8 (a) presents typical data showing shear rate versus shear stress. The plastic viscosity and yield stress are determined using the Bingham model described in Equation 1 in Chapter 2. Plastic viscosity is calculated from the slope of the linear region of the down curve, whereas yield stress is calculated from the interception as shown in Figure 3.8 (b). Average viscosity and yield stress and their respective coefficient of variation (COV) based on three runs are calculated corresponding to each test and repeated the same calculation for all test runs.
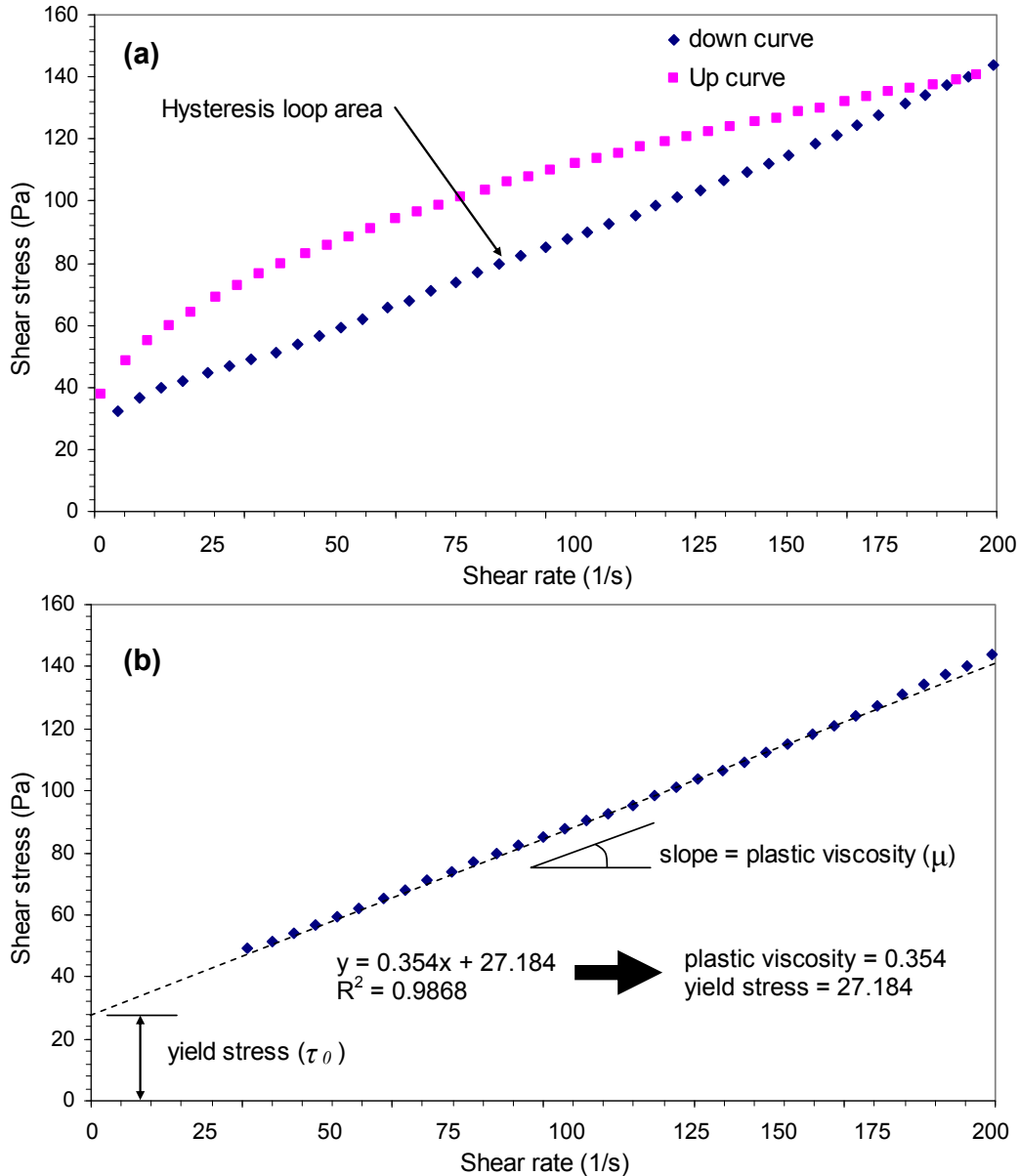
**Figure 3.8. (a) Typical Shear Stress vs. Shear Rate Curve,
(b) Calculation of Rheological Parameters Using Bingham Model.**

Conduction Calorimeter Test Procedure

    A conduction calorimeter (Model Super CRC) manufactured by Omnical Company (Figure 3.9) was used to measure heat of hydration in fresh cement paste. Immediately after completing mixing procedure the cement paste was transferred into a glass cylinder, which was sealed at the top using a plastic layer cap and quickly placed to isothermal calorimeter. The heat evolution data were recorded for 50 hours with 12 seconds intervals.

Figure 3.9. Conduction Calorimeter for Heat of Hydration.

Vicat Apparatus Test Procedure

The setting times for all the studied mixtures were measured by vicat apparatus in Figure 3.10. A specimen of fresh cement paste was prepared with high shear mixer at 24°C/(75°F) constant room temperature. Immediately after mixing, the paste is placed in a frustum of 40 mm (1.57 in.) in height. Initial set is considered as the time when the needle penetration is 25 mm ± 0.5 mm (1.53 in. ± 0.019 in.). The final set corresponds to less than 0.5 mm (0.019 in.) penetration.

Optimization of Rheology Test

The following items are identified for optimization:

- Selecting an optimum gap between two parallel plates to obtain rheological parameters with the lowest variance.
- Reproducibility of the rheological results.
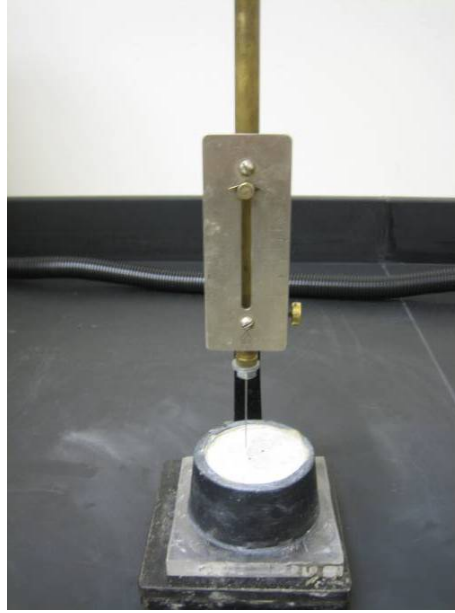
Figure 3.10. Vicat Apparatus for Setting Time *(32)*.

- Use of another advanced rheometer of parallel plate configuration (AR 2000) to validate the DSR rheological test results—AR 2000 is an advanced rheometer (Figure 3.11) based on the same working principle of DSR with parallel plate configuration. It includes a built-in Peltier heating-cooling system and updated software and can be operated with higher torque. The same 240 grit paper was installed to serrate the plate surfaces. AR 2000 was only used in this preliminary investigation to validate the DSR test results and not used in the main test program described later (Chapter 5).

Preliminary Test Program

A preliminary test program based on the above test method was formulated to optimize the DSR with respect to the above listed items. The range of applied shear rate was fixed from 0 to 200/s for all the test runs, which yielded the most reproducible rheological parameters. Note that the DSR operates with shear rate 0-300/s. The cement paste sample placed between two parallel plates tended to suffer a segregation problem (accumulation of more liquid part at the periphery of the plate) as a shear rate greater than 200/s was applied. The plate diameter was fixed to 25 mm based on the literature review *(24, 25)*.
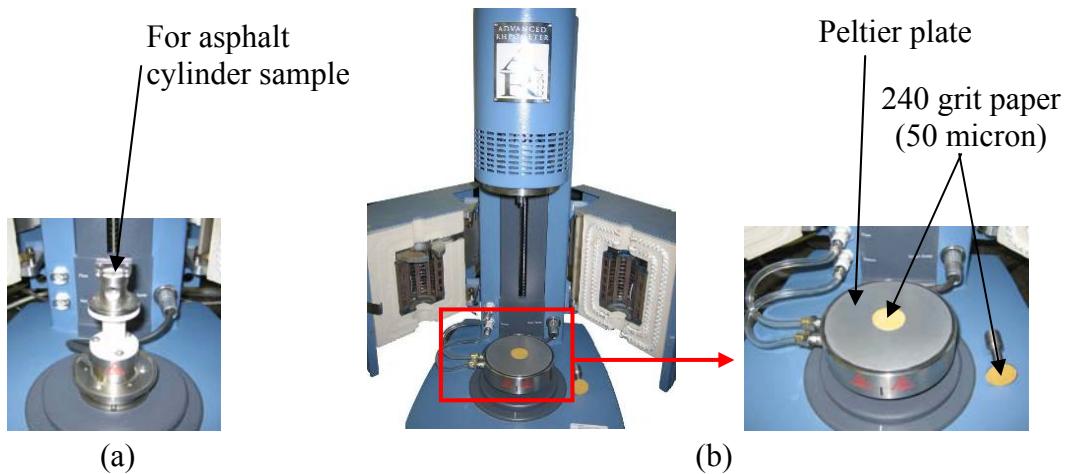
Figure 3.11. (a) Original AR 2000 Rheometer, (b) Modified AR 2000 Rheometer.

Materials and Experimental Design

ASTM Type I portland cement (OPC), a chemical admixture (lignin-based water reducing and retarding admixture (Type B&D), and de-ionized water were used in this preliminary test. Table 3.2 lists three different studied mixtures.

Table 3.2. Mix Design of Cement Paste.

Mixture	Water L/m³ (gal./yd³)	Cement kg/m³ (lb/yd³)	w/c	Chemical Admixture		
				Type	Dosage (%)	Range of Dosage
P1	550 (111)	1375 (2308)	0.4	WRRA	0.2% of cement weight	Typical recommended dosage
P2	550 (111)	1375 (2308)	0.4	WRRA	0.5% of cement weight	Maximum recommended dosage
P3	550 (111)	1375 (2308)	0.4	WRRA	1% of cement weight	Double of the maximum recommended dosage

Note: WRRA= water reducing and retarding admixture

Preliminary Test Results and Discussion

<u>Rheometer Tests</u>

Figure 3.12 (a) and (b) graphically presents the plastic viscosity and yield stress as a function of gap between two parallel plates and dosage of WRRA for all 15 combinations respectively. COV of viscosity and yield stress corresponding to the same 15 combinations are compared in Figure 3.12 (c). A perusal of Figure 3.12 showed the following observations:

- Both plastic viscosity and yield stress corresponding to each cement paste mixture (P1, P2, and P3) decreased obviously with increasing dosage of WRRA for all the five plate gaps – similar trends of paste viscosity and yield stress using high-range water reducing admixture are reported in the literature (*17*), which supports the present observation.

- The greater rate of decrease of both viscosity in Figure 3.12 (a) and yield stress in Figure 3.12 (b) are characteristic of plate gaps of 0.2, 0.5, and 1.0 mm whereas smaller rates of decrease of both the parameters are noticed for plate gaps of 1.2 and 1.5 mm.

- The rheological parameters with large gaps (1.2 and 1.5 mm) showed similar values in accordance with smaller rates of decrease, which did not allow the researchers to distinguish between the three mixtures based on viscosity and yield stress, although reproducibility still remained good.

- COV of both viscosity and yield stress with a 1mm plate gap was found to be less than 10 percent, indicating good reproducibility, whereas the COV for plate gaps smaller than 1 mm (i.e., 0.2 and 0.5 mm) was greater than 10 percent (up to 35 percent) indicating poor reproducibility [see Figure 3.12 (c)].

Similarly, the viscosity, yield stress, and COV as a function of plate gap and WRRA dosage for the same 15 combinations with the AR 2000 rheometer are graphically represented in Figure 3.13 (a), (b), and (c), respectively. Following are some important observations based on the AR 2000 test results. The same decreasing trend of viscosity and yield stress as a function of WRRA dosage was observed in AR 2000 for all the studied mixtures and plate gaps. The same higher COV of viscosity and yield stress with smaller plate gaps (i.e., 0.2, 0.5 mm) and lower sensitivity (especially with yield stress) with the higher plate gaps (i.e., 1.2, 1.5 mm) were also evident in AR 2000 data.
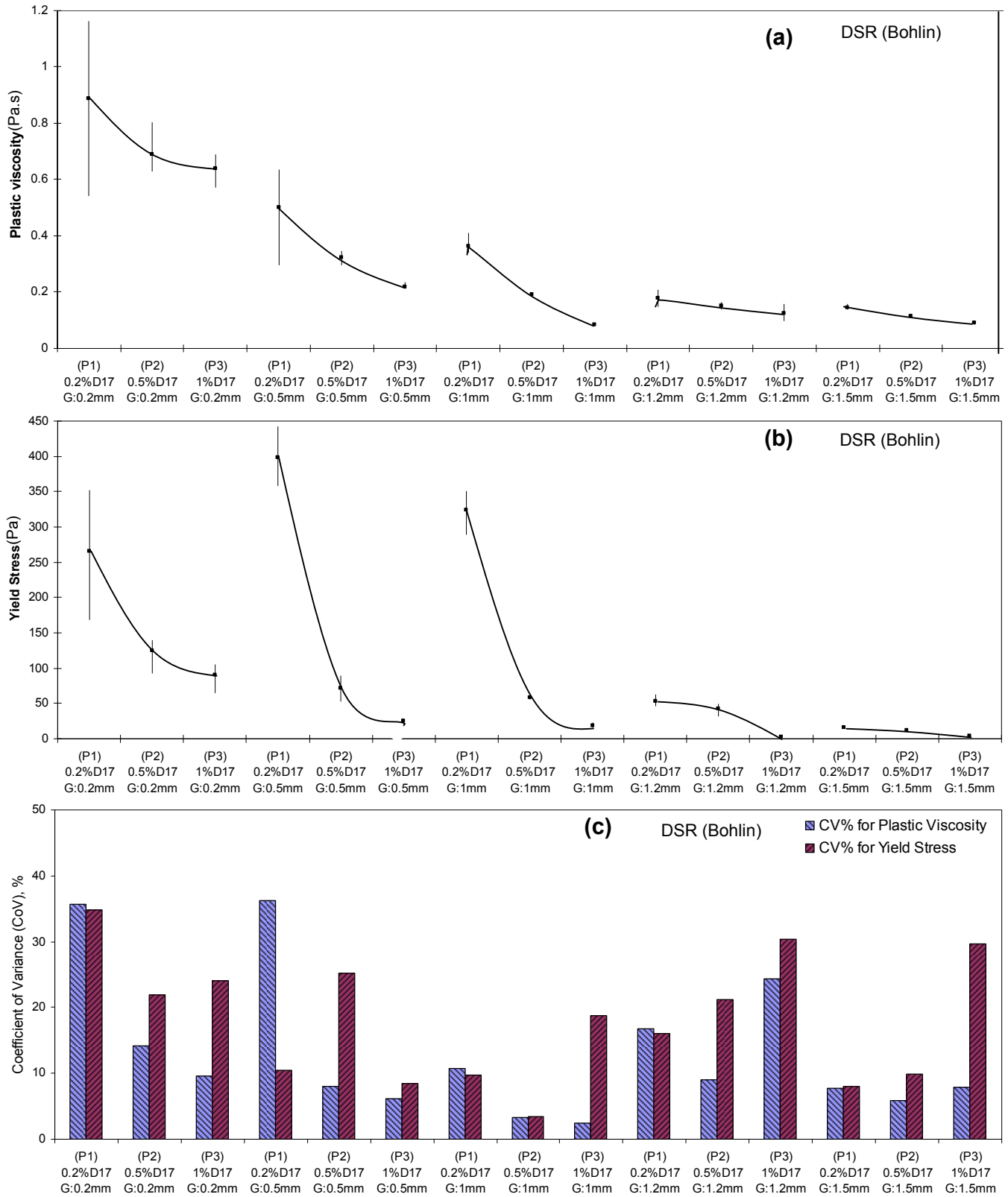
Figure 3.12. (a) Plastic Viscosity, (b) Yield Stress, and (c) COV Data from DSR (Bohlin).
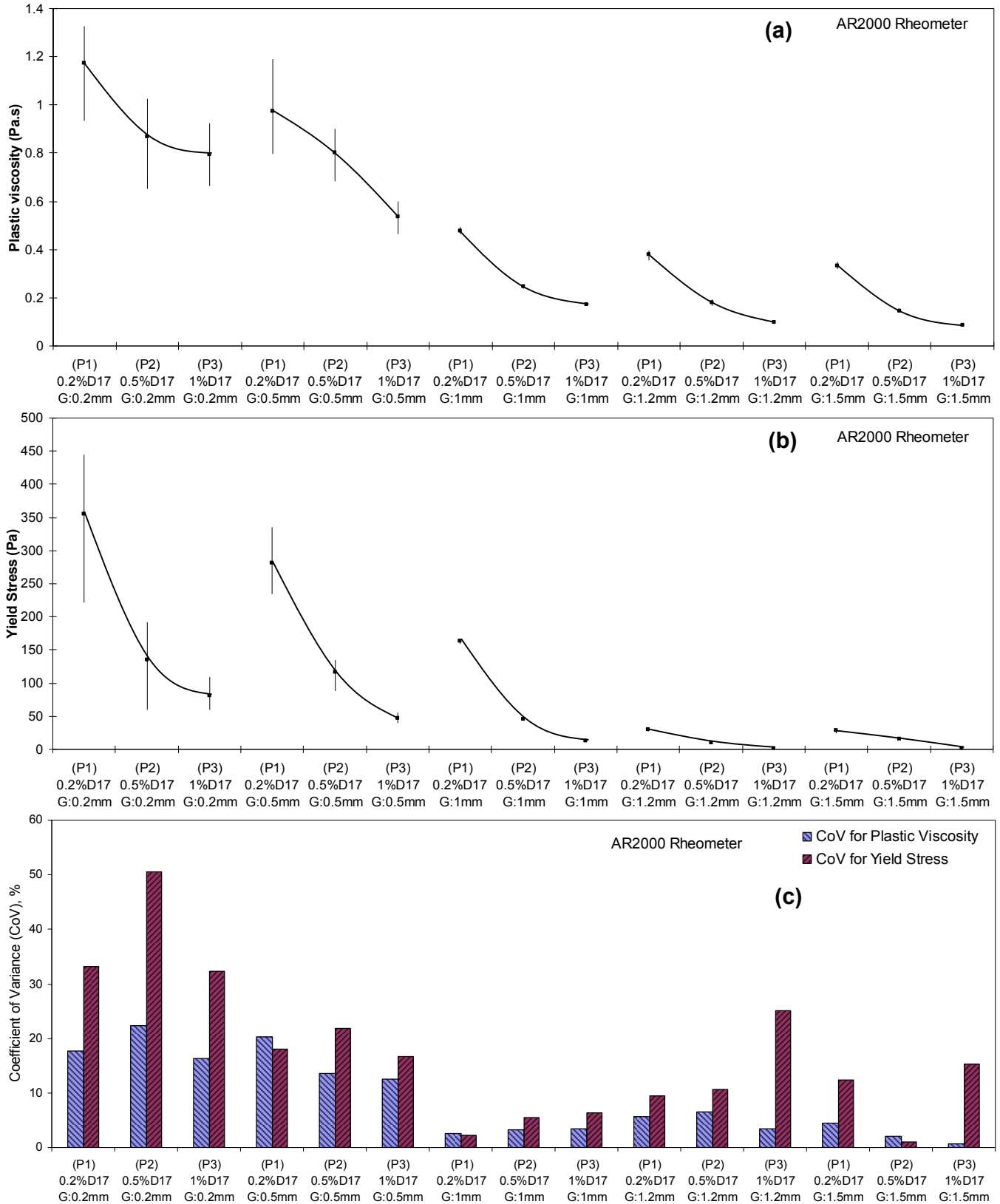
Figure 3.13. **(a) Plastic Viscosity, (b) Yield Stress, and (c) COV Data from AR 2000.**

30

The following key observations were made based on a comparative assessment of the test results from both the rheometers.

- Both the rheometers with 1 mm plate gap can clearly distinguish three mixtures (P1, P2, and P3) with the lowest COV, which implied its better sensitivity and reproducibility.

- Below 1 mm plate gap, the sensitivity still remained good, however, reproducibility became poor as manifested by COV> 10. Permissible reproducibility of low viscous materials (P3) can still be maintained with lower plate gap (e.g., 0.2, 0.5 mm) whereas reproducibility for high viscous materials (P1) with lower plate gap cannot be maintained.

- Above 1 mm plate gap, reproducibility remained good as manifested by COV< 10, however, sensitivity became poor since no such considerable difference between the rheology of three mixtures was noticed.

Therefore, both of the rheometers with 1 mm plate gap have clearly identified these three mixtures with distinct difference in viscosity and yield stress and with permissible reproducibility. The main purpose, i.e., distinguishing an abnormal mixture (P3) from a normal mixture (P1) based on cement paste rheology, is satisfied by both the rheometers. These results validate the results obtained from DSR (Bohlin) although the absolute values of rheological parameters between two rheometers were not exactly the same. It is unlikely that the two different instruments will give the same absolute values although the basic instrumentation remains the same. These results described above ultimately point out the potential feasibility of identifying cement-chemical admixture incompatibilities through the direct measurement of cement paste rheology by DSR alone.

Heat of Hydration Test

The conduction calorimeter tests were performed for these three mixtures (P1, P2, and P3) as a supporting tool. The heat evolution as a function of time and the integrated heat evolution are presented at Figure 3.14 (a) and (b), respectively. Figure 3.14 (a) shows that P1 mixture behaves as a normal mixture, whereas P3 behaves as a problematic one. Figure 3.14 (b) indicates that the integrated heat evolution drastically decreases as the dosage of WRRA increases. Therefore, the three mixtures have clearly been identified as three distinctly different mixtures based on heat evolution characteristics, which support the rheology-based observation in the previous section.
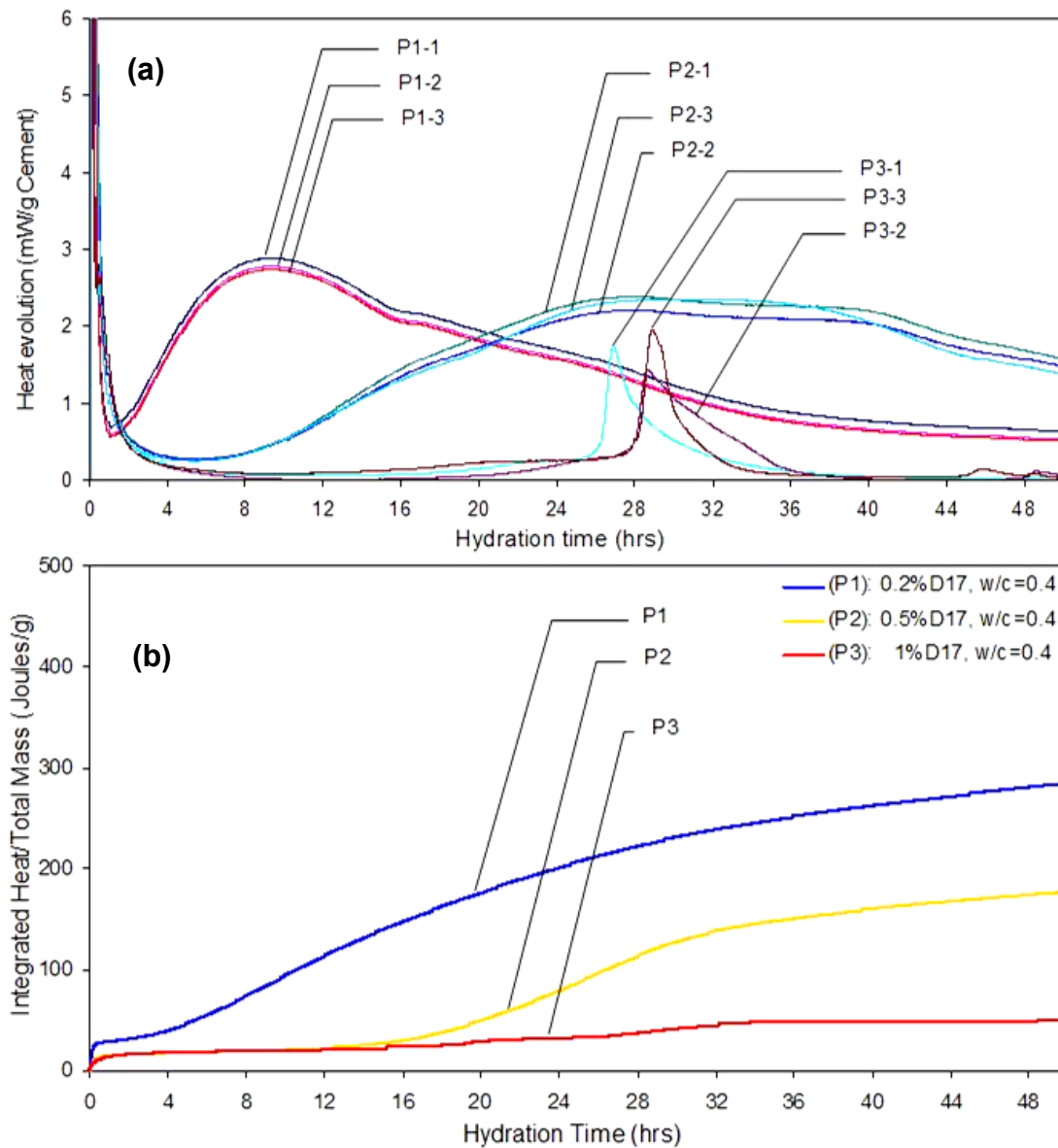
Figure 3.14. (a) Heat Evolution, (b) Integrated Heat Evolution Data as a Function of Time.

32

Setting Measurement with Vicat Apparatus

Vicat Setting time tests were conducted for the studied three mixtures. Figure 3.15 presents the results of initial and final setting times and shows that the initial and final set is drastically retarded with P3 mixture containing a high dosage of WRRA. This phenomenon is in accordance with both heat of hydration and rheological behavior as discussed previously.
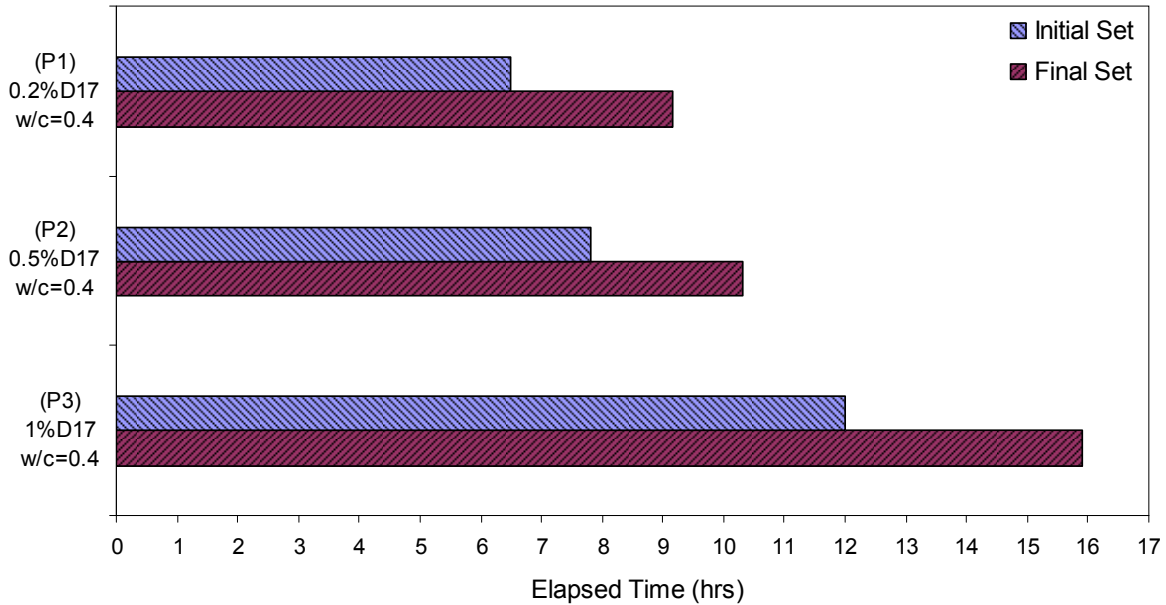
Figure 3.15. Initial and Final Setting Time by Vicat Apparatus.

CHAPTER 4

MATERIALS CHARACTERIZATION AND SELECTION

Material Collection

Historical information pertaining to the specific responsible factors for sulfate-mineral/chemical admixtures incompatibilities under field conditions was collected from past records with the help of TxDOT in order to select the factors and levels in such a way that incompatibilities can be reproduced in the laboratory in a similar manner. Table 4.1 summarizes the most influential factors that affect sulfate-admixtures compatibility in cement paste.

Table 4.1. Most Influential Parameters Related to Incompatibilities in Cement Paste.

	Influential Factors		Possible Effects
1	Type of Cement	C_3A contents	The amount of C_3A content in the cement may affect the incompatibility of concrete mixtures.
		Alkali contents	The amount of water-soluble alkalis content in the cement may affect the incompatibility of concrete mixtures.
2	Type of MWRA		Incompatibility issues caused by lignin-based MWRAs are more than any other type of MWRAs.
3	Dosage of MWRA		Excessively high dosage of MWRA is likely to cause incompatibility issues in concrete. Standard dosage (5–10 fl oz/cwt), high dosage (>15 fl oz/cwt)
4	Type of SCMs		Soluble sulfate, water-soluble alkali and other reactive phases (e.g., C_3A) in SCMs (fly ashes, slag) play an important role in cement-admixture incompatibilities in concrete.
5	Temperature		Excessively high (e.g., > 30°C) or low ambient temperatures (e.g., < 20°C) are reported to be more vulnerable than moderate temperatures to create incompatibilities.

Note: MWRA: mid-range water reducing admixture, SCMs: supplementary cementitious materials

Table 4.2 lists the materials collected based on TxDOT's field evidence of incompatibilities. Seven different types and brands of cements were collected in order (i) to cover a wide range of C_3A contents, sulfate contents (especially gypsum to hemihydrate ratio), and soluble alkali contents in the tested cements on one hand and (ii) to enhance the chances of

getting incompatible mixtures in the lab on the other hand. Three cements from these seven characterized cements will ultimately be selected for the main laboratory tests.

Three SCMs (Class C ash, class F ash, and slag), commonly used in TxDOT concrete pavement construction and suspected to be the cause of creating some problematic mixtures, were selected in order to investigate the role of SCMs in creating incompatibilities. TxDOT typically uses mid-range water reducing admixtures (MWRA) to control water contents in paving concrete. Some Lignin-based MWRAs were found to be the cause of creating concrete incompatibilities in combination with certain mineral admixtures from some field construction projects. Therefore, the researchers considered two lignin-based MWRAs from two different commercial sources in this study.

Therefore, the researchers considered two different commercial sources of lignin-based MWRA as chemical admixtures. Both admixtures are lignin-based MWRAs because it has been frequently reported its incompatibilities in combination with mineral admixtures from field construction. Table 4.2 lists each material's unique code for the convenience of formulating design of experiment.

Table 4.2. Materials Collected.

Materials	Material Code	Type	Sulfate Contents	C$_3$A Contents
Cement	C1	Type I/II	Normal	Normal
	C2	Type I/II	Normal	Normal
	C3	Type I/II	Normal	Normal
	C4	Type V	High	Low
	C5	Type I/II	Medium	Normal
	C6	Type I	Medium	High
	C7	Type I	High	High
Fly ash	C35	Class C fly ash	N/A	N/A
	F35	Class F fly ash		
Slag	S50	Slag		
MRWA (Lignin-based)	D17	WRRA		
	X15	MRWA		

Note: C35- Class C fly ash at 35% cement replacement, F35 - Class C fly ash at 35% cement replacement
S50 - Slag at 50% cement replacement

Material Characterization

The collected cements and SCMs were characterized for their bulk chemical compositions (elemental oxide percentages) and phase compositions. The following analytical tools were used to do chemical and mineralogical characterization of the collected cements, fly ashes, and slag samples.

- Bulk chemical analysis of cements, fly ashes, and slag by X-ray fluorescence (XRF)-TxDOT's Material Lab, Austin.
- Identification of phases presents in cements, fly ashes, and slag by X-ray Diffraction technique (Rigaku MiniFlex X-ray diffractometer in TTI)-The samples were crushed and ground using a mortar and a pestle until they passed 325-mesh (44μm) sieve. Sample holders made of aluminum were used to hold the powder sample during X-ray scanning. The X-ray diffractograms were collected in the range of 5° to 70° 2θ using the CuKα radiation. The step size was 0.02° and the scanning speed was 5° per minute.
- Quantitative estimation of C_3A, gypsum/hemi-hemihydrate in cements were analyzed using the quantitative X-ray diffraction (QXRD)–Construction Materials Consultants, Inc.

Chemical and Mineralogical Compositions of Cements

Chemical and mineralogical compositions of all the selected cements are discussed below. Bulk chemical analyses along with relevant chemical parameters (e.g., gypsum to hemihydrate ratios) and calculated bouge phases of the selected cements are presented in Table 4.3. The summary of XRD results is presented Table 4.4. The XRD diffractograms corresponding to all the studied cements that are generated to identify the phases qualitatively are presented in Appendix B. Cements 1, 2, 3, and 5 belong to Type I/II whereas cements 6 and 7 belong to Type I category with varying gypsum to hemihydrate ratios and C_3A contents. Cement 4 is selected as type V low C_3A cement.

Table 4.3. Oxide Analyses of Cements from XRF Tests.

Chemical Analysis	Percentage of Mass						
	C1	C2	C3	C4	C5	C6	C7
Cement type	I/II	I/II	I/II	V	I/II	I	I
SiO_2	20.349	20.284	20.480	20.422	20.681	19.298	19.830
Al_2O_3	4.501	4.161	4.660	4.057	4.630	5.345	5.121
Fe_2O_3	3.132	3.201	3.772	4.764	3.459	2.306	1.853
CaO	61.534	62.231	63.398	61.959	62.844	63.087	63.912
MgO	3.665	4.168	1.330	0.848	0.796	1.105	1.208
SO_3	2.480	2.456	2.231	3.850	3.053	2.949	3.303
Na_2O	0.101	0.067	0.210	0.298	0.170	0.099	0.115
K_2O	0.627	0.771	0.557	0.232	0.717	0.959	0.474
SrO	0.086	0.042	0.053	0.062	0.176	0.079	0.086
MnO	0.140	0.128	0.037	0.077	0.310	0.041	0.029
TiO_2	0.216	0.260	0.215	0.167	0.233	0.243	0.227
P_2O_5	0.109	0.144	0.067	0.028	0.200	0.279	0.122
L.O.I (950˚C)	1.9	0.8	2.3	1.5	1.7	2.5	2.44
Total	98.84	98.71	99.31	98.26	98.97	98.29	98.72
Alkalies as Na_2O_{eq} *	0.51	0.59	0.54	0.45	0.62	0.73	0.42
Gypsum	2.0	0.2	2.0	0.2	0.2	2.0	5.0
Hemihydrate	3.5	0.2	2.5	1.0	0.2	0.2	0.2
Anhydrate	0	0.2	0	0.2	0.2	0.2	0.2
Gypsum-to-hemihydrate Ratio*	0.57	1.0	0.8	0.2	1.0	10	25
Calculated Compounds per ASTM C 150-02a							
C_3S	54.06	59.65	59.38	51.97	53.90	62.55	63.00
C_2S	17.55	13.16	13.92	19.34	18.63	8.141	9.326
C_3A*	6.628	5.611	5.967	2.692	6.417	10.26	10.44
C_4AF	9.532	9.740	11.48	14.50	10.53	7.018	5.640
LSF	0.9283	0.9474	0.9457	0.9097	0.9238	0.9851	0.9797
Blaine Fineness (cm^2/g)	3730	3660	3920	3840	3670		

Note: * - Key factors which influences cement-admixtures incompatibilities

Table 4.4. Summary of Cement Phases Identified by XRD.

Materials	Identified Phases
Cement 1	Gypsum, hemihydrate, C_3S, C_2S, C_3A, C_4AF
Cement 2	Hemihydrate, C_3S, C_2S, C_3A, C_4AF
Cement 3	Gypsum, C_3S, C_2S, C_3A, C_4AF
Cement 4	Hemihydrate, anhydrate (high peak), C_3S, C_2S, C_3A, C_4AF
Cement 5	Gypsum, hemihydrate C_3S, C_2S, C_3A, C_4AF
Cement 6	Gypsum (high peak), hemihydrate, C_3S, C_2S, C_3A, C_4AF
Cement 7	Gypsum (high peak), hemihydrate, C_3S, C_2S, C_3A, C_4AF

Chemical and Mineralogical Compositions of SCMs

The chemical compositions of the selected SCMs (Class C fly ash, Class F fly ash, and granulated blastfurnace slag) are presented in Table 4.5, and phases identified by XRD are presented at Table 4.6. The XRD patterns of all the SCMs are presented in Appendix B.

Table 4.5. Oxide Analyses of the Studied SCMs.

Chemical Analysis	Percentage of Mass		
	Class C Fly Ash	Class F Fly Ash	Slag
Material Code	C35	F35	S50
SiO_2	38.551	54.123	33.8
Al_2O_3	20.144	25.347	11.1
Fe_2O_3	5.404	3.427	0.8
CaO	22.652	7.501	43.1
MgO	4.312	1.785	6.8
SO_3	1.326	0.326	0.4
Na_2O	1.350	0.462	0.32
K_2O	0.434	0.939	0.30
L.O.I (950˚C)	0.14		
Total	94.313	93.91	96.62
Alkalies as Na_2O	1.636	1.08	0.52
Specific gravity	2.69		

Table 4.6. Summary of SCMs Phases Identified by XRD.

Materials	Identified Phases
Class C fly ash	Predominantly amorphous with quartz, C_3A, $CaFeO_3$, $MgAl_2O_4$ as minor crystalline phases
Class F fly ash	Predominantly amorphous with quartz, mullite as minor crystalline phases
Granulated slag	Mostly amorphous with practically no crystalline phases

Particle Size Distribution of Both Cements and SCMs

Particle size distributions of all collected cements and SCMs were measured using a laser scattering particle size distribution analyzer (PSDA), the Horiba CAPA-700. Each material was dispersed with pure ethyl alcohol (99.9 percent) followed by ultrasonic vibration of 3 minutes (as a part of sample preparation procedure) before starting the actual machine analysis. Figures 4.1 and 4.2 show the results of particle size distribution of cements and SCMs, respectively. Mean and median particle size of cements and SCMs are listed at Table 4.7.

All seven cements (C1–C7) have very similar particle size distributions although Cement 7 has slightly coarser particles than other cements. The SCMs have a slightly wider range of particle size distribution curves than cements have. The granulated slag is finer (mean size 9.8 micron) than all of the tested cements and fly ashes.
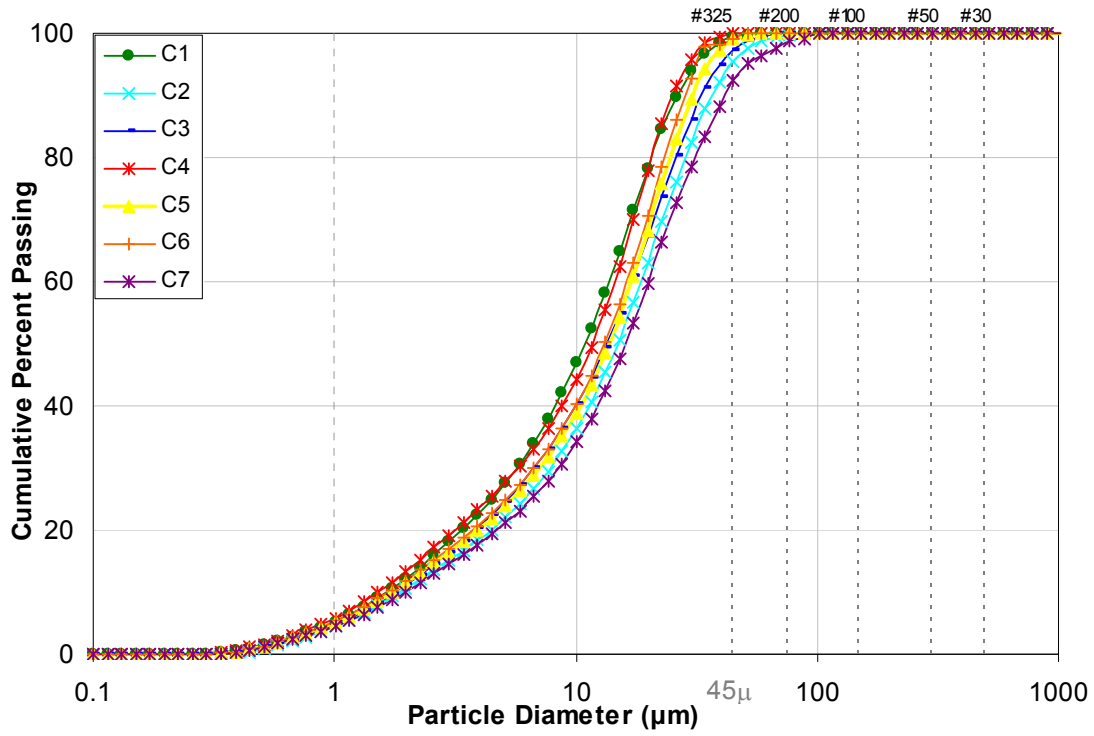
Figure 4.1. Particle Size Distribution Curves of Cements.
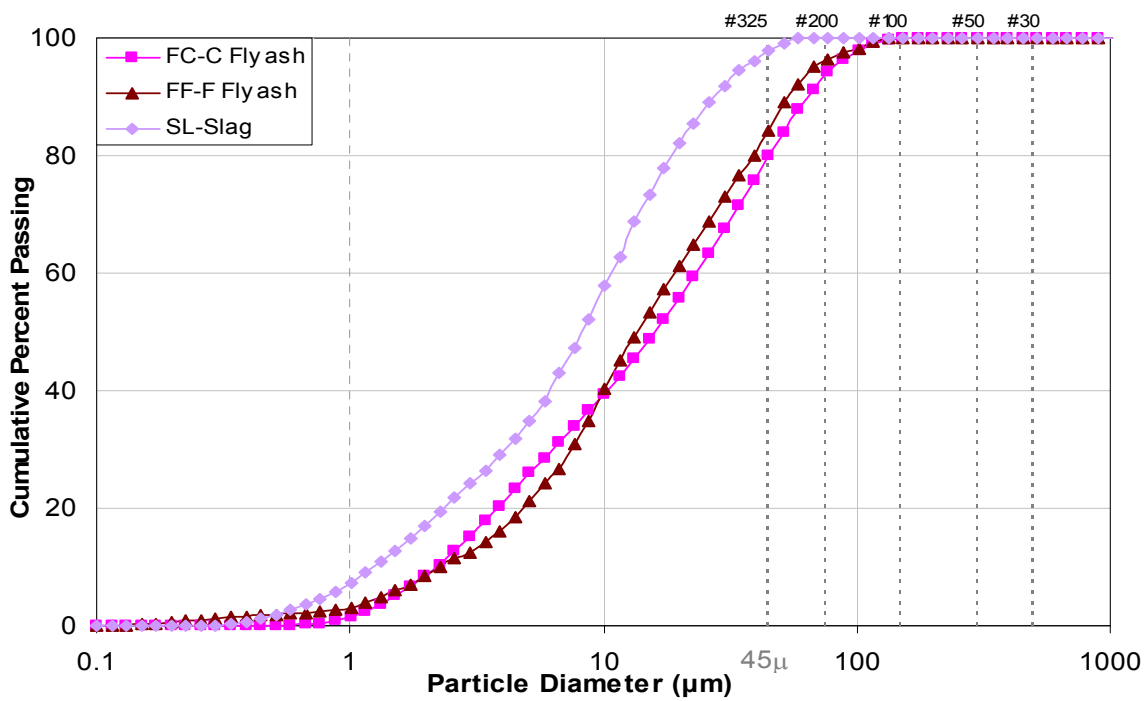
Figure 4.2. Particle Size Distribution Curves of SCMs.

41

Table 4.7. Mean and Median Particle Size of Cements and SCMs.

Size (micron)	Percentage Passing									
	C1	C2	C3	C4	C5	C6	C7	C35	F35	S50
Mean	12.70	17.53	15.80	12.61	15.11	13.98	18.97	17.14	15.42	9.81
Median	10.91	14.92	13.44	11.71	13.76	12.34	16.11	16.38	13.67	8.12

Characteristics of Chemical Admixture

The researchers selected and used the chemical admixtures X15 and D17 in the main laboratory tests. X15 is classified as a Type A & F admixture or Mid-Range Water Reducing Admixture (MWRA), whereas D17 is classified as a Type B & D or Water Reducing and Set Retarding Admixture (WRRA) according to ASTM C 494 *(33)*. X15 is an aqueous solution of lignosulfonate salt specially formulated for use in portland cement concrete-containing pozzolans. D17 is also an aqueous solution of lignosulfonate and compound carbohydrates. Table 4.8 lists the characteristics of the two selected chemical admixtures.

Table 4.8. Characteristics of Chemical Admixtures.

	X15 (MWRA)	D17 (WRRA)
ASTM C 494	Type A & F	Type B & D
Recommended Dosage	196-652 ml/100 kg of cement (3-10 fl oz/cwt)	130-520mL/100kg of cement (2-8 fl oz/cwt)
Typical Dosage	325mL/100kg (5fl oz/cwt)	195mL/100kg (3fl oz/cwt)
Ingredient	Calcium lignosulfonate	Sodium o-phenylphenol
CAS#	8061-52-7	000132-27-4

Selection of Cements for Experimental Test Program

To cover a wide range of C_3A contents, sulfate-bearing phases (especially gypsum to hemihydrate ratio), and soluble alkali contents, seven commercial portland cements, described in

Table 4.3, were initially identified based on chemical and mineralogical compositions. As described previously in Table 4.1, three factors—C_3A content, total soluble alkali content, and gypsum to hemihydrate ratio in cement—are crucial cement parameters in addition to (i) type and dosage of MWRA, (ii) type of SCMs, and (iii) temperature for addressing the cement-chemical/mineral admixtures incompatibilities.

Table 4.9 presents all seven commercial cements classified into three different levels (low, normal, and high) with respect to C_3A content, total soluble alkali content, and gypsum to hemihydrate ratio. The normal level of C_3A content in cement is considered as 5–6 percent. Anything more or less than this normal range is described as high or low. It is believed that high C_3A content could significantly influence cement-admixtures incompatibilities. The normal level of total soluble alkali content is between 0.5 and 0.6 percent. The effect of soluble alkali on cement-admixtures incompatibilities is not fully understood. The normal level of gypsum to hemihydrate ratio is above 1. It is anticipated that any cement with gypsum to hemihydrate ratio below 1 (i.e., more hemihydrates and less gypsum) is more prone to cement-admixtures incompatibilities. In this context, mitigation of concrete incompatibilities with a higher level of gypsum to hemihydrate ratio can be referred (*34*).

Table 4.9. Commercial Portland Cement Characteristics.

Cement	Type	Percentage of C_3A Content (%) (5< Normal< 6)		Percentage of Alkali Content (%) (0.5<Normal< 0.6)		Gypsum-to-Hemihydrate Ratio (0.8<Normal<1.2)	
Cement 1	I/II	6.628	Normal	0.51	Normal	0.57	Close to Normal
Cement 2	I/II	5.611	Normal	0.59	Normal	1.0	Normal
Cement 3	I/II	5.967	Normal	0.54	Normal	0.8	Normal
Cement 4	V	2.692	Low	0.45	Low	0.2	Abnormal
Cement 5	I/II	6.417	Normal	0.62	Normal	1.0	Normal
Cement 6	I	10.26	High	0.73	High	10	Abnormal
Cement 7	I	10.44	High	0.42	Low	25	Abnormal

The researchers selected three representative cements (Table 4.10) from the seven cements to conduct laboratory investigation under Task 6 (Chapter 6) by applying the following analogy:

- Cement 2 has a normal level of C_3A and total soluble alkali contents, while Cements 4 and 6 have low and high levels, respectively.
- In case of calcium sulfate content, Cement 2 has normal level of gypsum to hemihydrates ratio, whereas Cements 4 and 6 have low and high levels, respectively.
- In case of percent of alkali content, Cement 2 has normal level alkali content, whereas Cements 4 and 6 have low and high levels, respectively.

Table 4.10. Three Selected Cements for the Main Experimental Test Program.

Cement	Type	Percentage of C_3A Content (%) (5< Normal < 6)		Percentage of Alkali Content (%) (0.5<Normal< 0.6)		Gypsum-to-Hemihydrate Ratio (0.8<Normal<1.2)	
Cement 2	I/II	5.611	Normal	0.59	Normal	1.0	Normal
Cement 4	V	2.692	Low	0.45	Low	0.2	Abnormal
Cement 6	I	10.26	High	0.73	High	10	Abnormal

It is anticipated that these three cements should be effective to address cement-admixtures incompatibilities. Setting time and heat of hydration characteristics corresponding to Cements 2, 4, and 6 will be determined before conducting the main laboratory testing for rheology. Any addition/rejection of cements (if needed) based on setting time and heat of hydration data (described in Chapter 6) can be made at that time.

CHAPTER 5

EXPERIMENTAL DESIGN AND TEST METHODS

Experimental Design for the Laboratory Testing

Table 5.1 presents the experimental design for the laboratory testing. The following five factors are considered as the most influential factors in the experimental design:

- the type of cement,
- the type of chemical admixture,
- the dosage of chemical admixture,
- the type of SCMs, and
- the testing temperature.

The selected factors and their levels are presented in Table 5.1. Three different types of cements (C2, C6, and C4) were selected in the original design (Chapter 4). Based on the results of preliminary tests, both C2 (type I/II) and C6 (type I) cements have similar mineralogical and chemical compositions and show similar heat of hydration and setting time behaviors. Therefore, C6 cement was removed from the design of experiment. The researchers considered two different commercial sources of lignin-based chemical admixtures with two different dosage levels—manufacturer's typical recommended dosage and double the manufacturer's typical recommended dosage—to be the factors of type and dosage of chemical admixture, respectively (details are given in Chapter 4). Three different types of SCMs were considered: Class F fly ash, Class C fly ash, and slag). Temperature is another controlling factor related to concrete incompatibilities. When concrete is exposed to uncontrolled field conditions such as hot and cold weather, the possibility of getting incompatible mixtures increases. For example, one mix may perform satisfactorily at one temperature (generally at higher temperature such as summer time) but the same mix can behave as incompatible at a lower temperature (e.g., winter time). Three different levels (10, 24, and 35˚C) of testing temperatures were selected to represent winter, summer, and intermediate ambient temperature conditions in this study.

Table 5.1. Design of Experiments.

Total Test Runs	Cement Type	Chemical Admixture Type	Chemical Admixture Dosage	SCMs type	Temp.
96	C2 (Type I/II) C_3A - 5.61%	X15 (Brand X, Lignin based MRWA)	TD (0.25% for X15, 0.2% for D17 of total cement binder weight)	F35 (35% replacement of Class F fly ash)	10°C (50˚F)
				C35 (35% replacement of Class F fly ash)	24°C (75˚F)
	C4 (Type V) C_3A - 2.69%	D17 (Brand D Lignin based WRSA)	DD (0.5% for X15, 0.4% for D17 of total cement binder weight)	S50 (50% replacement of slag)	35°C (95˚F)

Note: MWRA: mid-range water reducing admixture (Calcium lignosulfonate); WRRA: water reducing and set retarding admixture (Calcium lignosulfonate and compound carbohydrates); TD: manufacturer's typical recommended dosage, DD: double the manufacturer's typical recommended dosage

The researchers used 32 mix combinations, including 8 controls. The combination of two cements and three SCMs gives rise to eight controls. Table 5.2 shows the mixture number and code for each mix. These mixture numbers and codes will be used to explain the results of laboratory tests at Chapter 6. Since the 32 tests were repeated under three different temperature conditions, the researchers ran 96 total tests. The water to cementitious ratio (w/cm) was selected for all the controlled mixtures based on a constant flow (i.e., a pat area of 5000 mm^2 at 5 minutes after mixing) determined by mini-slump flow tests on cement / (cement +SCMs) pastes. The resulting w/cm for the mixtures with Class F ash was 0.38, whereas those with Class C fly ash and slag were 0.36 and 0.45, respectively. These w/cm are valid for the both cements C2 and C4. The w/c for both the cement pastes (C2 and C4) without SCM was found to be 0.4.

Materials were selected based on the available historical information. Some combinations in the above design of experiments are expected to show incompatibilities in the laboratory tests through the following possible mechanisms:

- In general, an overdose of chemical admixtures (e.g., double dosage in Table 5.1) commonly causes concrete incompatibilities.

- A mix with satisfactory performance at higher temperature (e.g., summer) can become an incompatible mix at lower temperature (e.g., winter) as a result of change in reaction kinetics in different temperatures.
- Complex interactions between fly ash, cement, and chemical admixtures creates chemical incompatibilities.

Table 5.2. Experimental Design Table for Laboratory Test Program.

Group	Cement	SCMs	MRWA Type	MRWA Dosage	Mix. No.	Mixture Code
Control	C2	-	-	-	1	C2
	C4	-	-	-	2	C4
Group I	C2	F35	-	-	3	C2-F35
		C35	-	-	4	C2-C35
		S50	-	-	5	C2-S50
	C4	F35	-	-	6	C4-F35
		C35	-	-	7	C4-C35
		S50	-	-	8	C4-S50
Group II	C2	F35	X15	TD	9	C2-F35-X15-TD
			D17	TD	10	C2-F35-D17-TD
		C35	X15	TD	11	C2-C35-X15-TD
			D17	TD	12	C2-C35-D17-TD
		S50	X15	TD	13	C2-S50-X15-TD
			D17	TD	14	C2-S50-D17-TD
	C4	F35	X15	TD	15	C4-F35-X15-TD
			D17	TD	16	C4-F35-D17-TD
		C35	X15	TD	17	C4-C35-X15-TD
			D17	TD	18	C4-C35-D17-TD
		S50	X15	TD	19	C4-S50-X15-TD
			D17	TD	20	C4-S50-D17-TD
Group III	C2	F35	X15	DD	21	C2-F35-X15-DD
			D17	DD	22	C2-F35-D17-DD
		C35	X15	DD	23	C2-C35-X15-DD
			D17	DD	24	C2-C35-D17-DD
		S50	X15	DD	25	C2-S50-X15-DD
			D17	DD	26	C2-S50-D17-DD
	C4	F35	X15	DD	27	C4-F35-X15-DD
			D17	DD	28	C4-F35-D17-DD
		C35	X15	DD	29	C4-C35-X15-DD
			D17	DD	30	C4-C35-D17-DD
		S50	X15	DD	31	C4-S50-X15-DD
			D17	DD	32	C4-S50-D17-DD

Past records showed that some combinations in Table 5.2 have actually manifested incompatibilities in the field because of one or more of the above mechanisms.

Test Methods

Table 5.3 summarizes the test methods used in the main experimental program (Chapter 6). These test methods except mini-slump test are already described in the preliminary test program in Chapter 3. The mini-slump cone test was included in the main test program to measure flow characteristics of the cementitious system as an alternative or supporting tool for the rheology test.

Table 5.3. Test Methods in the Experimental Program.

Test Method	Test Equipment	Measured Properties
Rheological behavior of fresh cement paste	Modified Bohlin CVO rheometer, DSR (Malvern Instrument)	Rheological parameters (yield stress and plastic viscosity)
Heat generation behavior of the cementitious system (ASTM C 186)	Isothermal conduction calorimeter (OMNICAL)	Heat of Hydration
Setting behavior (ASTM C191)	Vicat needle apparatus	Initial and Final set time
Flow characteristics	Mini-Slump cone	5, 10, 20, and 30 minutes pat area

Development of an Effective Evaporation Control Measure

It has subsequently been observed that the evaporation control measure (i.e., wet sponge method), developed during the preliminary test program (Chapter 3) was not very effective. The device may record changes due to evaporation while measuring the rheological changes due to cement hydration and any interparticle interaction (during induction period). Therefore, it would be ideal to remove the evaporation effects at the best. The research team conducted an extensive

48

study to develop a very effective evaporation control system in order to avoid evaporation effects during rheology measurements. The research team actually verified three different methods of evaporation prevention, i.e., (1) applying a thin layer of mineral oil (immiscible with the sample) especially at the periphery of the parallel plates, (2) placing a humidifier in close proximity to maintain high relative humidity (RH) in the surrounding areas, and (3) encapsulating the sample chamber by a plastic sealing cap. The sealing cap option (Figure 5.1) was found to be the most effective method and accepted as a final evaporation control measure for the main test program.
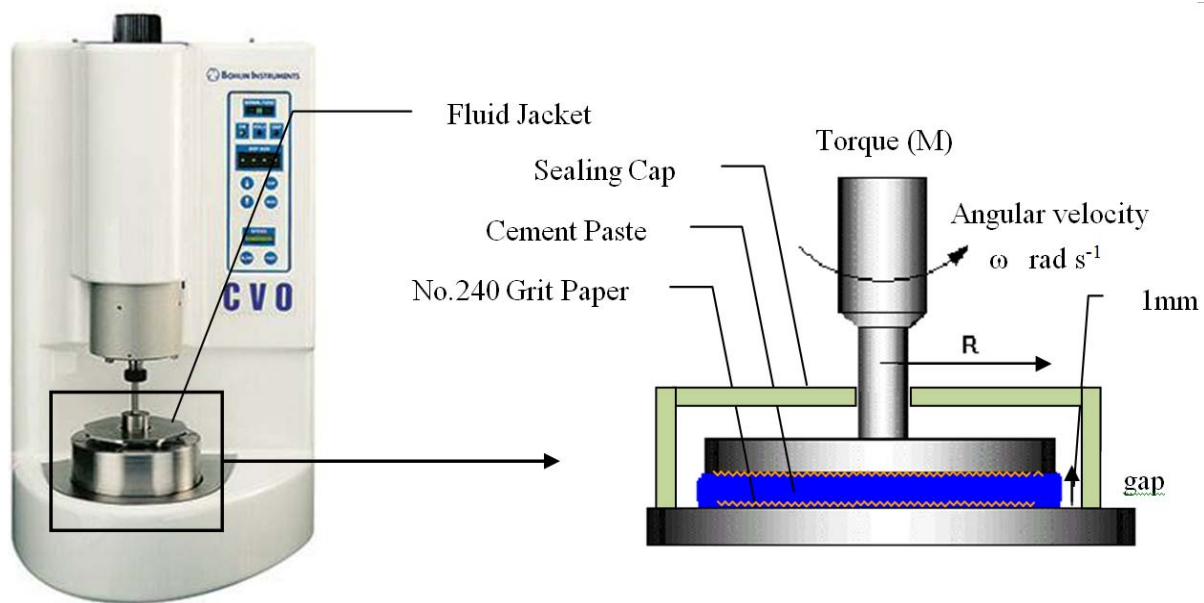
Figure 5.1. Evaporation Control on Modified DSR Using Sealing Cap.

Test Procedures

The same temperature-controlled high shear mixing developed during preliminary test program (described in Chapter 3) has been used in the main test program. However, the researchers changed the rheometer test procedure and calculation of the rheological parameters as described below. Additionally, a test procedure for mini-slump test is also provided as this procedure is included in the main test program.

Rheometer Test Procedure

 A relatively longer test duration (up to 2 hours with 10, 30, 60, 90, and 120 minutes testing intervals) was found to be sensitive to derive an effective rate of change of rheological parameters (described later) under total evaporation control situation. As a result, the rheometer test procedure was changed (in comparison with the procedure that used in the preliminary test program described in Chapter 3) as described below:

1. Take cement paste specimen from the mixing bowl using five 3-ml syringes immediately after mixing procedure.
2. All the syringes filled with cement paste were kept under the respective studied temperatures (e.g., inside an oven/refrigerator for $35°C/10°C$ and under room temperature of $24°C$). The syringes were kept in a horizontal position to minimize any segregation/sedimentation effect.
3. Five syringes corresponding to each mixture and under a particular temperature were tested one by one with the selected five time intervals, i.e., 10, 30, 60, 90, and 120 minutes. This procedure ensured not to disturb the changes in the paste due to hydration or any other structural changes (during induction period) and thereby monitoring the changes of rheological parameters as a function of time.
4. With the syringe, place the predetermined quantity of cement paste (i.e., 1.5 ml) onto the lower plate of the rheometer.
5. Sandwich the specimen between the two parallel plates with a 1 mm plate gap and shear with shear rate from 0 to 200/s representing the up curve, followed by 200 to 0/s representing the down curve. Record the shear stress as a function of the shear rate. A run with one cycle consisting of one up curve and one down curve takes approximately 3 minutes.
6. Start the first run approximately 10 minutes after adding water to the cement. Conduct another four runs using the remaining specimens in the four syringes with different time intervals of 30, 60, 90, and 120 minutes following the same procedure described above.

Calculation of Rheological Parameters

Figure 5.2 (a) presents typical data showing shear rate versus shear stress. The plastic viscosity and yield stress determined using the Bingham model are shown in Figure 5.2 (b). The plastic viscosity is calculated from the slope of the linear region of the down curve, whereas yield stress is calculated from the interception as shown in Figure 5.2 (b).
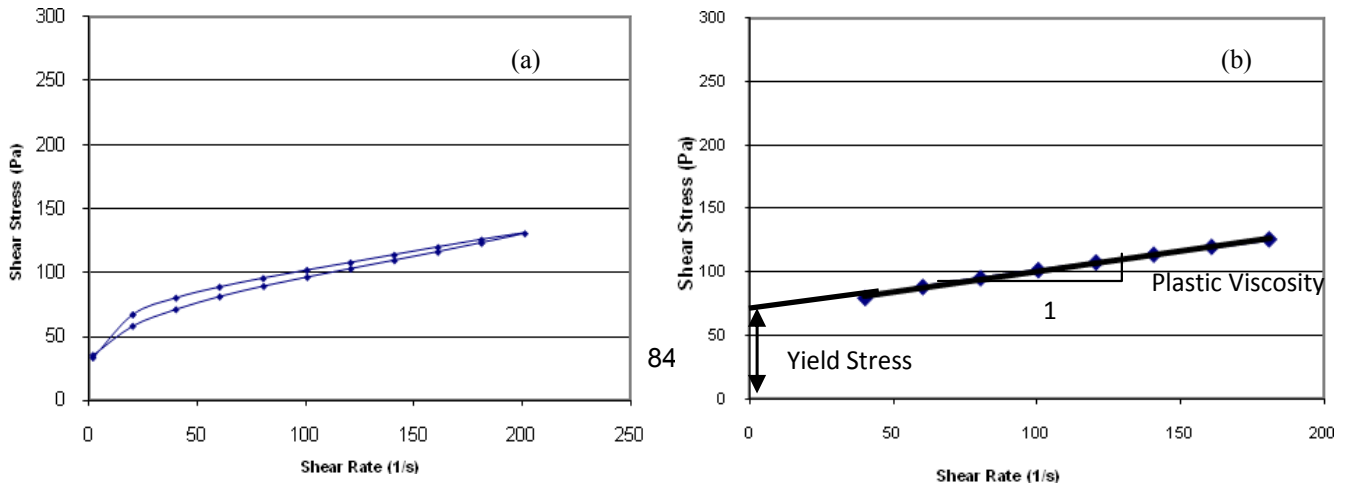
Figure 5.2. (a) Typical Plot of Shear Stress vs. Shear Rate,
(b) Calculation of Rheological Parameters.

The rheological parameters, i.e., plastic viscosity and yield stress, corresponding to five different time intervals were calculated as described above. Data was taken from five different time-interval tests and plotted in Figure 5.3 (a). Figure 5.3 (b) shows change of plastic viscosity as a function of time. The slope of the linear region in Figure 5.3 (b) represents the rate of change of plastic viscosity (RPV) within 2-hour time periods. The rate of change of yield stress (RYS) within a 2-hour time period is calculated by applying the same procedure.
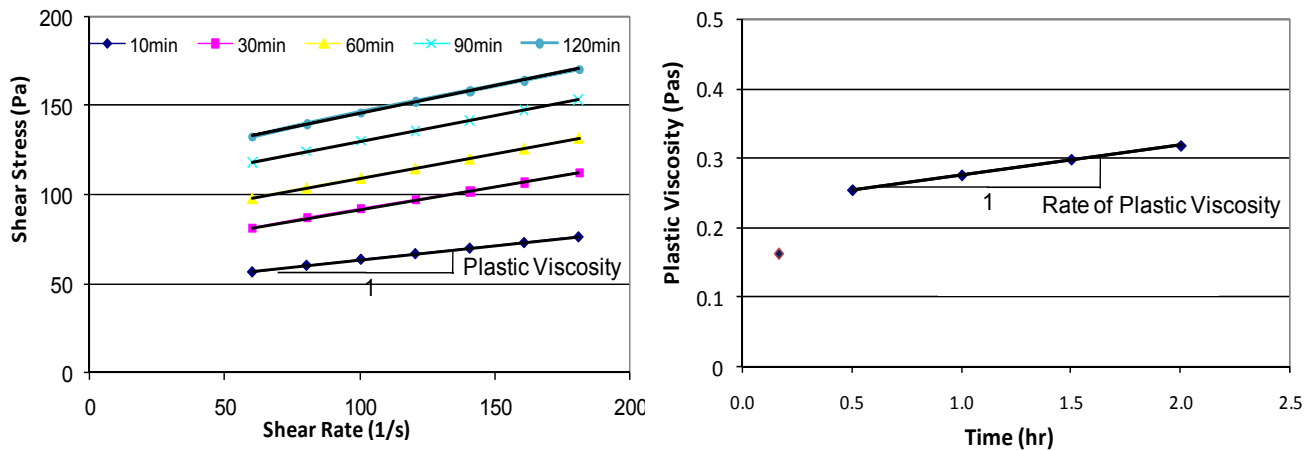
Figure 5.3. (a) Plastic Viscosities with Five Time Intervals,

(b) Calculation of Rate of Plastic Viscosity.

Mini Slump Cone Test Procedure

The research team conducted the mini slump cone test for of all the studied mixtures (according to Table 5.1). The mini slump cone used the following dimensions: 19 mm (.75 in.) as top diameter, 38 mm (1.5 in.) as bottom diameter, and 57 mm (2.25 in.) as height. The dimensions are in the same proportions as in the concrete slump test (ASTM Test C 143). Figure 5.4 shows the design details of the mini slump cone test. The mini slump test procedure is described below:

1. The mixing procedure was the same as rheology tests presented at Chapter 3 (Figure 3.7).
2. Immediately after mixing, the sample was placed in the cone resting on a Lucite (acrylic) sheet. As the cone was filled, a small spatula was moved both laterally and vertically to aid the escape of entrapped air bubbles.
3. The cone was lifted with a motion rapid enough for the cone to remain clear of the flowing paste but slow enough to avoid imparting a significant upward momentum to the paste.
4. Several diameters of the pat were measured in different directions with a caliper. An average diameter was calculated and the pat area was determined.
5. The rest of the specimen were kept under the respective studied temperatures (e.g., inside an oven / refrigerator for 35°C/10°C and under room temperature of 24°C).

52

6. The specimen corresponding to each mixture and under a particular temperature were
    tested one by one with the selected three time intervals, i.e., 10, 20, and 30 minutes. This
    procedure ensured no disturbance to the changes in the paste due to hydration or any
    other structural changes (during induction period) and thereby monitored the flow
    behavior as a function of time.
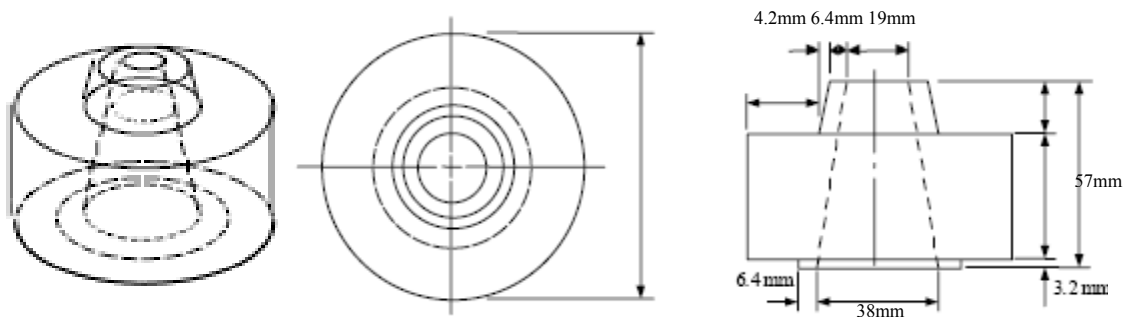
Figure 5.4. Schematic Representation of Mini Slump Cone.

The researchers measured the pat area results from the mini slump tests for C2 and C4
cement system as a function of time and temperature. The results from the mini slump cone test
were presented at Chapter 6.

CHAPTER 6

CONDUCTING LABORATORY TESTING AND DATA ANALYSIS

This chapter presents the test results and discussion of the laboratory tests that have been conducted based on the experimental design (Table 5.1) and test method (Table 5.3) given in Chapter 5. This chapter represents Task 6 in the original proposal.

Test Results and Discussion

All the test runs according to the experimental design in Table 5.1 were conducted using the DSR test procedure mentioned in Chapter 5. Tests for heat of hydration, setting time, and mini-slump were also conducted for all the combinations as supporting tools. The results are presented in the following order.

- Heat of hydration (HOH) and setting time characteristics of all the combinations–The procedure to identify incompatible mixtures based on heat of hydration and setting time characteristics is developed and discussed.
- Rheological parameters that were determined by the modified DSR tests–The method to identify incompatible mixtures based on rheological characteristics is developed and discussed.
- A comparative assessment was made to verify whether the identification of the incompatible mixtures based on rheology method is supported by HOH and setting time methods.
- Flow characteristics by the mini slump cone test–The flow behavior as a function of elapsed time was measured from the mini slump cone test. The researchers evaluated whether the mini slump test has any potential feasibility to identify the incompatible mixtures from the normal ones similar to rheology method.

Heat of Hydration by Conduction Calorimeter (OMNICAL)

The heat evolution characteristics, i.e., the amount and time of occurrence of the second peak and integrated heat evolution for all the test runs, were measured by the micro-calorimeter and are presented in Table 6.1 (a) and 6.1 (b). Appendix B contains heat of hydration graphs for

Table 6.1.(a) Heat Evolution Data with C2 Cement System at Different Temperatures.

	Experimental Design	Second Peak Value (mW/g)	Second Peak Time (hr)	Integrated Heat Evolution (J/g)	% of Heat Evolution w.r.t. Control (C2)
10°C (50°F)	3_C2+F35	0.78	20	98	56.65
	9_C2+F35+X15TD	0.89	21	96	55.49
	21_C2+F35+X15DD	0.88	31	91	52.60
	10_C2+F35+D17TD	0.67	44	52	30.06
	22_C2+F35+D17DD	N/A	N/A	19	10.98
	4_C2+C35	0.73	28	81	46.82
	11_C2+C35+X15TD	0.74	30	79	45.66
	23_C2+C35+X15DD	0.49	33	57	32.95
	12_C2+C35+D17TD	0.18	35	30	17.34
	24_C2+C35+D17DD	N/A	N/A	20	11.56
	5_C2+S50	0.63	14	79	45.66
	13_C2+S50+X15TD	0.63	16.5	79	45.66
	25_C2+S50+X15DD	0.63	21	75	43.35
	14_C2+S50+D17TD	0.62	29	64.5	37.28
	26_C2+S50+D17DD	N/A	N/A	10.5	6.07
24°C (75°F)	*1_C2	2.43	8.7	172	100.00
	3_C2+F35	1.79	12.5	135.5	78.32
	9_C2+F35+X15TD	1.78	13.2	122	70.52
	21_C2+F35+X15DD	1.80	16.2	118.5	68.50
	10_C2+F35+D17TD	1.18	34	102.5	59.25
	22_C2+F35+D17DD	N/A	N/A	25	14.45
	4_C2+C35	1.73	15.8	128.5	74.28
	11_C2+C35+X15TD	1.77	20.6	128	73.99
	23_C2+C35+X15DD	1.74	29.5	108.5	62.72
	12_C2+C35+D17TD	N/A	N/A	39	22.54
	24_C2+C35+D17DD	N/A	N/A	25	14.45
	5_C2+S50	1.5	6	129	74.57
	13_C2+S50+X15TD	1.51	9	127.5	73.70
	25_C2+S50+X15DD	1.52	10	111	64.16
	14_C2+S50+D17TD	1.68	22	107.5	62.14
	26_C2+S50+D17DD	N/A	N/A	25	14.45
35°C (95°F)	3_C2+F35	3.25	8	151.5	87.57
	9_C2+F35+X15TD	3.15	9	144	83.24
	21_C2+F35+X15DD	2.79	12.5	130	75.14
	10_C2+F35+D17TD	2.21	16	127.5	73.70
	22_C2+F35+D17DD	N/A	N/A	18	16.18
	4_C2+C35	3.25	10.5	171	98.84
	11_C2+C35+X15TD	2.95	14	160.5	92.77
	23_C2+C35+X15DD	2.49	21	136	78.61
	12_C2+C35+D17TD	N/A	N/A	35	20.23
	24_C2+C35+D17DD	N/A	N/A	29	16.76
	5_C2+S50	2.59	5.5	154	89.02
	13_C2+S50+X15TD	2.45	6.5	150.5	86.99
	25_C2+S50+X15DD	2.38	9	150.5	86.99
	14_C2+S50+D17TD	2	14.5	143	82.66
	26_C2+S50+D17DD	N/A	N/A	18	16.18

Note: ▮ *identified as incompatible mixtures*   ▮ *identified as marginal mixtures*

56

Table 6.1.(b) Heat Evolution Data with C4 Cement System at Different Temperatures.

	Experimental Design	Second Peak Value (mW/g)	Second Peak Time (hr)	Integrated Heat Evolution (J/g)	% of Heat Evolution w.r.t. Control (C4)
10°C (50°F)	6_C4+F35	0.8	16	122	73.94
	15_C4+F35+X15TD	0.92	21	121.5	73.64
	27_C4+F35+X15DD	0.92	30.5	113	68.48
	16_C4+F35+D17TD	0.73	33	89	53.94
	28_C4+F35+D17DD	N/A	N/A	25.5	15.45
	7_C4+C35	0.74	18.5	111	67.27
	17_C4+C35+X15TD	0.74	22	93.5	56.67
	29_C4+C35+X15DD	0.68	29	82	49.70
	18_C4+C35+D17TD	0.38	36.5	57.5	34.85
	30_C4+C35+D17DD	N/A	N/A	29.5	17.88
	8_4+S50	0.7	12	107	64.85
	19_C4+S50+X15TD	0.7	16	103.5	62.73
	31_C4+S50+X15DD	0.7	20	99.5	60.30
	20_C4+S50+D17TD	0.68	25.5	83	50.30
	32_C4+S50+D17DD	N/A	N/A	25	15.15
24°C (75°F)	*2_C4	2.86	7.2	165	100.00
	6_C4+F35	1.95	8.5	131	79.39
	15_C4+F35+X15TD	1.94	10.6	129.5	78.48
	27_C4+F35+X15DD	1.94	12.5	129.5	78.48
	16_C4+F35+D17TD	1.78	17.6	120.5	73.03
	28_C4+F35+D17DD	N/A	N/A	25	15.15
	7_C4+C35	1.78	10.3	136.5	82.73
	17_C4+C35+X15TD	1.75	13.2	121	73.33
	29_C4+C35+X15DD	1.78	14	118.5	71.82
	18_C4+C35+D17TD	1.74	21	115.5	70.00
	30_C4+C35+D17DD	N/A	N/A	24	14.55
	8_C4+S50	1.64	6	127	76.97
	19_C4+S50+X15TD	1.64	6.8	124.5	75.45
	31_C4+S50+X15DD	1.58	8.1	121	73.33
	20_C4+S50+D17TD	1.42	13.2	98	59.39
	32_C4+S50+D17DD	N/A	N/A	23	13.94
35°C (95°F)	6_C4+F35	3.34	5	139.5	84.55
	15_C4+F35+X15TD	3.34	7	138.5	83.94
	27_C4+F35+X15DD	3.28	8	138	83.64
	16_C4+F35+D17TD	2.71	14	132	80.00
	28_C4+F35+D17DD	2.06	38	59	35.76
	7_C4+C35	3.13	6.7	150	90.91
	17_C4+C35+X15TD	2.83	8	138.2	83.76
	29_C4+C35+X15DD	2.67	9.8	126.8	76.85
	18_C4+C35+D17TD	2.39	13.2	124.5	75.45
	30_C4+C35+D17DD	0.93	45.8	31.9	19.33
	8_C4+S50	2.81	3.4	149.8	90.79
	19_C4+S50+X15TD	2.72	4.1	140.6	85.21
	31_C4+S50+X15DD	2.7	4.9	139.8	84.73
	20_C4+S50+D17TD	2.23	11	112.1	67.94
	32_C4+S50+D17DD	0.32	42.8	51.2	32.43

Note: ▓ *identified as incompatible mixtures*   ▓ *identified as marginal mixtures*

each cement/SCM system. The results are discussed in the following sub-system in order to reflect the effect of SCMs, chemical admixtures, and temperature separately.

Control: The heat evolution of cement only (C2 and C4) was used as a control. The second peak of C2 cement (Type I/II) occurs at approximately 8.7 hours after the addition of water with a value of 2.43 mW/g ,whereas for C4 cement (Type V), it occurs at 7.2 hours with a value of 2.86 m W/g. The integrated heat evolution of control mixtures after 48 hours is 172 J/g for C2 and 165 J/g for C4 [marked * in Table 6.1 (a) and (b)] and are considered to be equal to 100 percent. The percentages of heat evolution for the other mixtures are then calculated with respect to cement-water heat evolution as 100 percent and are presented in the last column of Table 6.1 (a) and 6.1 (b). Based on the amount of heat generated and time of occurrence of the second peak (Appendix B), the possible incompatible and marginal mixes are identified and marked on Table 6.1 (a) and (b) by a yellow and green color. A perusal of Table 6.1 shows that a criterion of below 30 percent of integrated heat evolution is considered to be appropriate to distinguish between incompatible and normal mixtures.

Effects of SCMs: The addition of fly ash to cement (both C2 and C4) generally results in the reduction of the second peak intensity and the delay of the occurrence of the second peak (i.e., retardation),whereas the addition of slag results in the reduction of the second peak intensity but the acceleration of the occurrence of the second peak. The mixtures with Class F fly ash showed less retarding effect compared to the mixtures with Class C fly ash.

Effects of Chemical Admixtures: An overall effect of reduction in heat evolution is evident for the mixtures with chemical admixture X15 (a mid-range water reducing admixture) at both normal and high dosages regardless of SCM types. The degree of reduction was higher in the mixtures with double dosages (0.5 percent of total cement weight) than the mixtures with normal dosages. However, the higher dose addition of admixture X15 had no detrimental effect on the hydration process since the second peak of the hydration was clearly observed, and the percentage of integrated heat evolution after 48 hours for all the mixtures with X15 admixture remained above the 30 percent criteria.

On the other hand, the chemical admixture D17 (a water reducing and set retarding admixture) showed a significant reduction even with the typical dosage (as expected) for all mixtures with D17 admixture. This admixture not only reduces water demand but also retards the setting time. At the typical dosage of D17 admixture, the class C ash with C2 cement showed a significant reduction in heat evolution manifested by the absence of the second peak after 48 hours of testing period. This seems to be an example of chemical incompatibility that arises due to complex interaction between cement, class C ash, and D17 chemical admixture. The percent heat evolution for this mixture is below the 30 percent limit for all three temperatures. Therefore, mixture number 12 (C2+C35+D17TD) was identified as an incompatible mixture at all three temperatures (Table 6.1a). The addition of admixture D17 with double dose (0.4 percent of cement weight) resulted in heat evolution abnormalities (i.e., the second peak did not appear even after 48 hours of testing) for all the tested mixtures regardless of the cement and SCMs types. As a result, mixtures 22, 24, and 26 with cement 2 (yellow marked mixtures in Table 6.1a) and mixtures 28, 30, and 32 with cement 4 (Table 6.1b) were identified as incompatible mixtures due to an overdose of D17 admixture.

Effects of Ambient Temperature: The effect of temperature was investigated at 10°C (50°F) and 35°C (95°F) to grossly simulate winter and summer time concrete paving. As expected all mixtures tested at low temperature condition had less integrated heat evolution as well as second peak intensity than those tested at intermediate temperature (i.e., 24°C/75°F). Conversely, all the mixtures tested under high temperature condition had more integrated heat evolution as well as second peak intensity than those tested under intermediate temperature. Therefore, the effect of low temperature resulted in the retardation of cement hydration process, whereas the high temperature caused the acceleration of the cement hydration process on all tested mixtures. As a result, some of the normal mixes at both 35 and 24°C (mixture No. 10 and 23 in Table 6.1a) became marginal (close to incompatible criteria of 30 percent, marked as green) at low temperatures (10°C). Similarly, the mixture 28 (Table 6.1b) behaved as marginal at higher temperature (35°C) but become incompatible at both low and intermediate temperatures.

Setting Time by Vicat Apparatus

Setting time was measured using the vicat apparatus equipment (ASTM C 191) for all the studied mixtures under intermediate temperature condition (24°C/75°F) and are presented in Table 6.2 (a) and 6.2 (b). Table 6.2 shows that both the initial and final setting time is retarded more or less with the addition of chemical admixtures.

The usage of chemical admixture X15 resulted in a 2 to 5-hour delay of setting time (depending on the type of SCMs) at both typical and double dose. In the case of admixture D17, the setting time was delayed significantly (5–11 hours for the fly ash mixtures and around 2 hours for the slag mixtures with typical dosage level and 11–19 hours for class C ash, 21-29 hours for class F ash and around 8 hours for slag mixtures at double dosage) compared with those of the mixtures tested without chemical admixtures.

The delay of setting time for the mixtures with class C ash and typical dosage of D17 is higher (9–11 hours) than the other mixtures (5–8 hours with class F ash and around 2 hours with slag). It is interesting to note that the same mixtures (i.e., with class C ash and D17TD) are also identified as incompatible based on integrated heat evolution criteria (Table 6.1a). This is an indication that, in general, setting time and heat evolution results support each other. It seems the delay of setting time by 2–8 hours with the D17 admixture (as with F ash/slag and D17TD) is within the normal range (as D17 admixture is a set retarder as well as a water reducer).

The addition of admixture D17 with double dose (i.e., 0.4 percent of cement weight) detrimentally affected the cement set behavior (delayed by 8–30 hours) for all the tested specimens regardless of the cement and SCMs types. These abnormalities of setting behavior with a double dose of admixture D17 are in general agreement with the integrated heat evolution results (mixtures with yellow marks in Table 6.1a and 6.1b).

With the C4 cement, the initial and final setting time tend to occur 1 to 5 hours earlier than those of the C2 cement system. This phenomenon is also in agreement with the heat of hydration results.

The researchers identified mixtures with slag and D17DD as incompatible based on integrated heat evolution criteria, although, the setting time delay is only around 7-8 hours. Either this setting time delay for slag mixtures is still abnormal or setting time determination based on the vicat apparatus is not sensitive enough to identify all kind of incompatible mixtures because of some inherent limitations in the procedure. The criteria based on integrated heat

evolution is more sensitive than setting time and considered an efficient supporting tool for the rheological results. Therefore, the determination of setting time at the other two studied temperatures (10°C/50°F and 35°C/90°F) for the studied mixtures was not performed.

Table 6.2.(a) Setting Time Data with C2 Cement System at 24°C.

Experimental Design	Initial Set (Hours)	Final Set (Hours)
1_C2	4.17	5.34
3_C2+F35	6.83	8.25
9_C2+F35+X15TD	8	9.33
21_C2+F35+X15DD	9.5	11.17
10_C2+F35+D17TD	14.67	16.33
22_C2+F35+D17DD	35	37
4_C2+C35	9	10.34
11_C2+C35+X15TD	12.17	13.67
23_C2+C35+X15DD	14	15.5
12_C2+C35+D17TD	18.67	21
24_C2+C35+D17DD	20.17	23.17
5_C2+S50	3.75	5.34
13_C2+S50+X15TD	4.5	6
25_C2+S50+X15DD	5.33	6.83
14_C2+S50+D17TD	5.92	7.75
26_C2+S50+D17DD	11.83	13.5

Note: The mixtures with yellow marks are identified as incompatible mixtures based on heat evolution criteria (as in Table 6.1a).

Rheological Parameters Using the Modified DSR

Table 5.1 shows the plastic viscosity and yield stress of all the studied mixtures measured using the modified DSR. Five measurements at five different time intervals (10, 30, 60, 90, and 120 minutes) for each mixture and at each temperature were conducted. The rate of plastic viscosity (RPV) and rate of yield stress (RYS) were then calculated based on these five measurements as described in the test method earlier (Chapter 5). Tables 6.3 and 6.4 present the absolute values of plastic viscosity (PV) and yield stress (YS) with the first measurement at 10 minutes after water is added to the cement, and Tables 6.5 and 6.6 show RPV and RYS. The bar graphs for PV, YS, RPV, and RYS as a function of admixture type/dosage and temperature for C2 cement + F35 (Class F fly ash 35 percent replacement) are presented in Figure 6.1 as an example. The bar graphs for C2 + C35, C2 + S50, C4 + F35, C4 + C35, and C4 + S50 systems are presented in Appendix C.

Table 6.2.(b) Setting Time Data with C4 Cement System at 24°C.

Experimental Design	Initial Set (Hours)	Final Set (Hours)
2_C4	3.17	4.17
6_C4+F35	4.1	5.58
15_C4+F35+X15TD	6.17	7.67
27_C4+F35+X15DD	7.33	8.83
16_C4+F35+D17TD	9.67	11.17
28_C4+F35+D17DD	25.83	27
7_C4+C35	5.67	7.17
17_C4+C35+X15TD	8.17	9.67
29_C4+C35+X15DD	9.83	11.33
18_C4+C35+D17TD	13.25	14.75
30_C4+C35+D17DD	23	26.5
8_C4+S50	2.67	4.17
19_C4+S50+X15TD	3.67	5.17
31_C4+S50+X15DD	4.42	5.83
20_C4+S50+D17TD	4.67	6.25
32_C4+S50+D17DD	9.33	11.17

Note: The mixtures with yellow marks are identified as incompatible mixtures based on heat evolution criteria (as in Table 6.1b)

Absolute Values of Rheology Parameters (Plastic Viscosity and Yield Stress): The researchers made the following key observations based on the plastic viscosity and yield stress results.

- Both plastic viscosity and yield stress decrease with the addition of the chemical admixtures to the control mixtures (mixtures with only SCMs) where the admixture D17 showed relatively higher reduction in both PV and YS than the admixture X15 (Tables 6.3 and 6.4; Figure 6.1). The similar decreasing trend of PV and YS is also noticed with the increasing dosage (i.e., from typical dosage to double dosage) of the individual chemical admixture.

- Both plastic viscosity and yield stress increased slightly with increasing temperature for all the mixtures with class F ash and slag (Tables 6.3 and 6.4; Figure 6.1). The PV showed decreasing trend or negligible change with increasing temperature for some mixtures with class C ash, although the YS showed the same behavior as in the mixtures with F ash and slag.

Table 6.3. Plastic Viscosity of All the Studied Mixtures.

SCM Type	Exp. No. C2	Exp. No. C4	Admix Type and Dosage	C2 (Type I/II Cement) 10°C	C2 (Type I/II Cement) 24°C	C2 (Type I/II Cement) 35°C	C4 (Type V Cement) 10°C	C4 (Type V Cement) 24°C	C4 (Type V Cement) 35°C
Class F (35%)	3	6	No Admix	0.2221	0.2295	0.2658	0.2249	0.2359	0.2551
	9	15	X15TD	0.1995	0.2356	0.2425	0.1995	0.2092	0.2225
	21	27	X15DD	0.1573	0.1954	0.2581	0.1598	0.1638	0.2181
	10	16	D17TD	0.1390	0.1652	0.2309	0.1689	0.1962	0.2442
	22	28	D17DD	0.1241	0.1351	0.1548	0.124	0.1437	0.1536
Class C (35%)	4	7	No Admix	0.1498	0.1589	0.1651	0.1712	0.1798	0.1789
	11	17	X15TD	0.1413	0.1478	0.1329	0.1687	0.1612	0.1581
	23	29	X15DD	0.1240	0.1221	0.1124	0.1354	0.1314	0.1322
	12	18	D17TD	0.1057	0.1011	0.1068	0.1259	0.1211	0.1231
	24	30	D17DD	0.0845	0.0824	0.0804	0.1195	0.1154	0.1157
Slag (50%)	5	8	No Admix	0.2316	0.2413	0.2896	0.2039	0.2113	0.2413
	13	19	X15TD	0.1763	0.1961	0.2411	0.1856	0.1874	0.2169
	25	31	X15DD	0.1423	0.1523	0.1856	0.1487	0.1501	0.1748
	14	20	D17TD	0.1584	0.1853	0.2633	0.1552	0.1652	0.2164
	26	32	D17DD	0.1233	0.1359	0.1406	0.1156	0.1256	0.1342

Note: Incompatible (yellow) and marginal (green) mixtures based on heat evolution criteria (Table 6.1a and 6.1b) are superimposed.

- The change of yield stress with increasing dosage of chemical admixtures (Table 6.4) is greater than the change of plastic viscosity (Table 6.3). The difference in YS between the incompatible (the mixture with double dosage of D17 identified based on heat evolution criteria earlier) and normal mixtures is greater than the difference in PV for those mixtures. However, the level of difference for both PV and YS is not good enough to clearly differentiate between the incompatible and normal mixtures. For example, the difference in YS and PV between the incompatible mixture of No.12 (C2 cement with class C ash and typical dose of D17) and the normal mixture of No. 23 (C2 cement with class C ash and double dose of X15) is not considerable (Tables 6.3 and 6.4; Appendix C). The incompatible/marginal mixtures, identified by heat evolution criteria (Tables 6.1a and 6.1b), show abnormal/marginal PV/YS (Tables 6.3 and 6.4) values as expected. However, more normal mixtures (based on heat evolution criteria) show PV and YS

values in somewhat abnormal or marginal range (the sky-blue marked mixtures in Tables 6.3 and 6.4). These are considered as mismatch between absolute values of rheological parameters and heat evolution characteristics. Interestingly, the number of mismatches is higher with yield stress (Table 6.4) than plastic viscosity (Table 6.3). Therefore, criteria based on absolute values of PV and YS to identify incompatible mixtures was inconclusive.

Table 6.4. Yield Stress of All the Studied Mixtures.

SCM Type	Exp. No. C2	Exp. No. C4	Admix Type and Dosage	C2 (Type I/II Cement) 10°C	C2 (Type I/II Cement) 24°C	C2 (Type I/II Cement) 35°C	C4 (Type V Cement) 10°C	C4 (Type V Cement) 24°C	C4 (Type V Cement) 35°C
Class F (35%)	3	6	No Admix	71.37	80.79	123.51	71.375	81.97	121.97
	9	15	X15TD	44.28	62.25	91.04	59.56	68.72	91.04
	21	27	X15DD	25.26	43.54	74.22	42.1	46.92	69.89
	10	16	D17TD	19.06	39.56	61.87	40.23	45.59	83.045
	22	28	D17DD	4.57	16.59	31.88	14.57	23	47.587
Class C (35%)	4	7	No Admix	45.97	78.21	129.53	55.29	80.11	112.38
	11	17	X15TD	30.75	58.29	110.25	37.86	57.21	84.14
	23	29	X15DD	23.47	38.23	74.5	26.52	39.66	64.54
	12	18	D17TD	14.28	32.87	77.88	21.57	35.25	65.21
	24	30	D17DD	3.78	13.58	27.05	9.59	16.39	37.24
Slag (50%)	5	8	No Admix	53.5	79.23	94.25	62.33	80.87	118.29
	13	19	X15TD	35.51	51.74	83.64	44.28	55.45	89.54
	25	31	X15DD	15.2	29.32	53.18	24.58	31.23	58.67
	14	20	D17TD	19.94	31.08	51.48	27.98	33.52	52.81
	26	32	D17DD	4.98	12.45	29.41	13.23	15.82	35.23

Note: Incompatible (yellow) and marginal (green) mixtures based on heat evolution criteria (Table 6.1a and 6.1b) are superimposed.

Table 6.5. Rate of Change of Plastic Viscosity (RPV) of All Studied Mixtures.

SCM Type	Exp. No. C2	Exp. No. C4	Admix Type and Dosage	C2 (Type I/II Cement) 10°C	C2 (Type I/II Cement) 24°C	C2 (Type I/II Cement) 35°C	C4 (Type V Cement) 10°C	C4 (Type V Cement) 24°C	C4 (Type V Cement) 35°C
Class F (35%)	3	6	No Admix	0.0852	0.1058	0.1787	0.0789	0.0924	0.1459
	9	15	X15TD	0.0702	0.0924	0.1321	0.0687	0.0807	0.1136
	21	27	X15DD	0.0389	0.0486	0.0658	0.0356	0.0436	0.0517
	10	16	D17TD	0.0211	0.0325	0.0402	0.0214	0.0318	0.0388
	22	28	D17DD	0.0018	0.0102	0.0143	0.0016	0.0115	0.0204
Class C (35%)	4	7	No Admix	0.0891	0.1254	0.2153	0.0857	0.1158	0.1587
	11	17	X15TD	0.0852	0.1135	0.1852	0.0849	0.1042	0.1459
	23	29	X15DD	0.0402	0.0831	0.1023	0.0428	0.0612	0.0923
	12	18	D17TD	0.0112	0.0145	0.0167	0.0254	0.0512	0.0873
	24	30	D17DD	0.0032	0.0057	0.0129	0.0085	0.0138	0.0198
Slag (50%)	5	8	No Admix	0.1138	0.1659	0.2345	0.1278	0.1586	0.2114
	13	19	X15TD	0.1069	0.1589	0.2068	0.1151	0.1411	0.1951
	25	31	X15DD	0.0723	0.1023	0.1357	0.0659	0.0953	0.1312
	14	20	D17TD	0.0521	0.0753	0.0987	0.0585	0.0847	0.1185
	26	32	D17DD	0.0175	0.0185	0.0176	0.0168	0.0191	0.0228

Time Functioned Rheology Parameters (Rate of Change of Plastic Viscosity and Rate of Change of Yield Stress): The rates of change of the rheological parameters were calculated based on the plastic viscosity and yield stress data at five different time intervals during a 2-hour testing period and are presented in Tables 6.5 and 6.6 and Figure 6.1. A perusal of these tables and figures showed the following observations:

- Both the value of the rate of change of plastic viscosity and the rate of change of yield stress tend to decrease when the dosage of the chemical admixture increases (Tables 6.5 and 6.6; Figure 6.1).

- Both RPV and RYS show an increasing trend with increasing temperature for all the studied mixtures (Tables 6.5 and 6.6; Figure 6.1). This trend agrees with the fact that the rate of change of rheological parameters becomes faster at higher temperature due to higher reaction kinetics than that at lower temperature. In general, the rate of increase is greater at higher temperature range (i.e., 24-35°C) and slower at lower temperature range (10-24°C) for the normal mixtures (Figure 6.1 and Appendix D).

Table 6.6. Rate of Change of Yield Stress (RYS) of All Studied Mixtures.

SCM Type	Exp. No. C2	Exp. No. C4	Admix Type and Dosage	C2 (Type I/II Cement) 10°C	C2 (Type I/II Cement) 24°C	C2 (Type I/II Cement) 35°C	C4 (Type V Cement) 10°C	C4 (Type V Cement) 24°C	C4 (Type V Cement) 35°C
Class F (35%)	3	6	No Admix	42.51	45.26	59.87	35.69	39.469	49.469
	9	15	X15TD	35.32	36.53	45.29	31.78	33.294	39.87
	21	27	X15DD	25.41	26.49	32.14	21.59	24.75	29.56
	10	16	D17TD	15.39	15.87	24.58	11.26	14.81	22.98
	22	28	D17DD	8.98	9.87	11.21	6.969	8.14	14.72
Class C (35%)	4	7	No Admix	41.29	49.65	52.46	34.54	37.54	45.23
	11	17	X15TD	33.26	39.52	43.21	33.52	32.58	39.25
	23	29	X15DD	23.12	28.57	35.92	20.58	23.58	27.21
	12	18	D17TD	8.35	11.29	12.89	13.52	16.56	18.56
	24	30	D17DD	4.52	6.59	9.54	7.59	9.87	13.58
Slag (50%)	5	8	No Admix	48.97	55.87	65.32	48.95	56.89	68.24
	13	19	X15TD	39.65	47.52	56.89	41.54	49.58	57.27
	25	31	X15DD	29.89	39.56	49.59	30.54	37.41	48.54
	14	20	D17TD	16.89	23.48	31.58	19.52	28.45	35.23
	26	32	D17DD	9.63	11.21	12.56	10.58	12.34	18.59

- It is important to note that a significant difference between RPV and RYS of the normal and incompatible mixtures exists regardless of the ambient temperature effects. This phenomenon matches well with the heat evolution characteristics from the isothermal conduction calorimetry and set behavior form vicat apparatus test.

- Almost all the incompatible and marginal mixtures, identified based on heat evolution criteria (Table 6.1a and 6.1b), show abnormal (yellow) and marginal (green) ranges of RPV and RYS (Tables 6.5 and 6.6). The number of mismatches (sky-blue marked mixtures in Tables 6.5 and 6.6) is greatly reduced. Therefore, criteria based on rate of change of rheological parameters are more sensitive than that based on absolute values to identify incompatible mixtures.

- Both RPV and RYS are acceptable for criteria of incompatibilities; however, RPV is more sensitive to distinguish between normal and incompatible mixtures. Interestingly, the mismatches are more with RYS (Table 6.6) than RPV (Table 6.5). The details are described in the next section on establishing acceptance criteria.
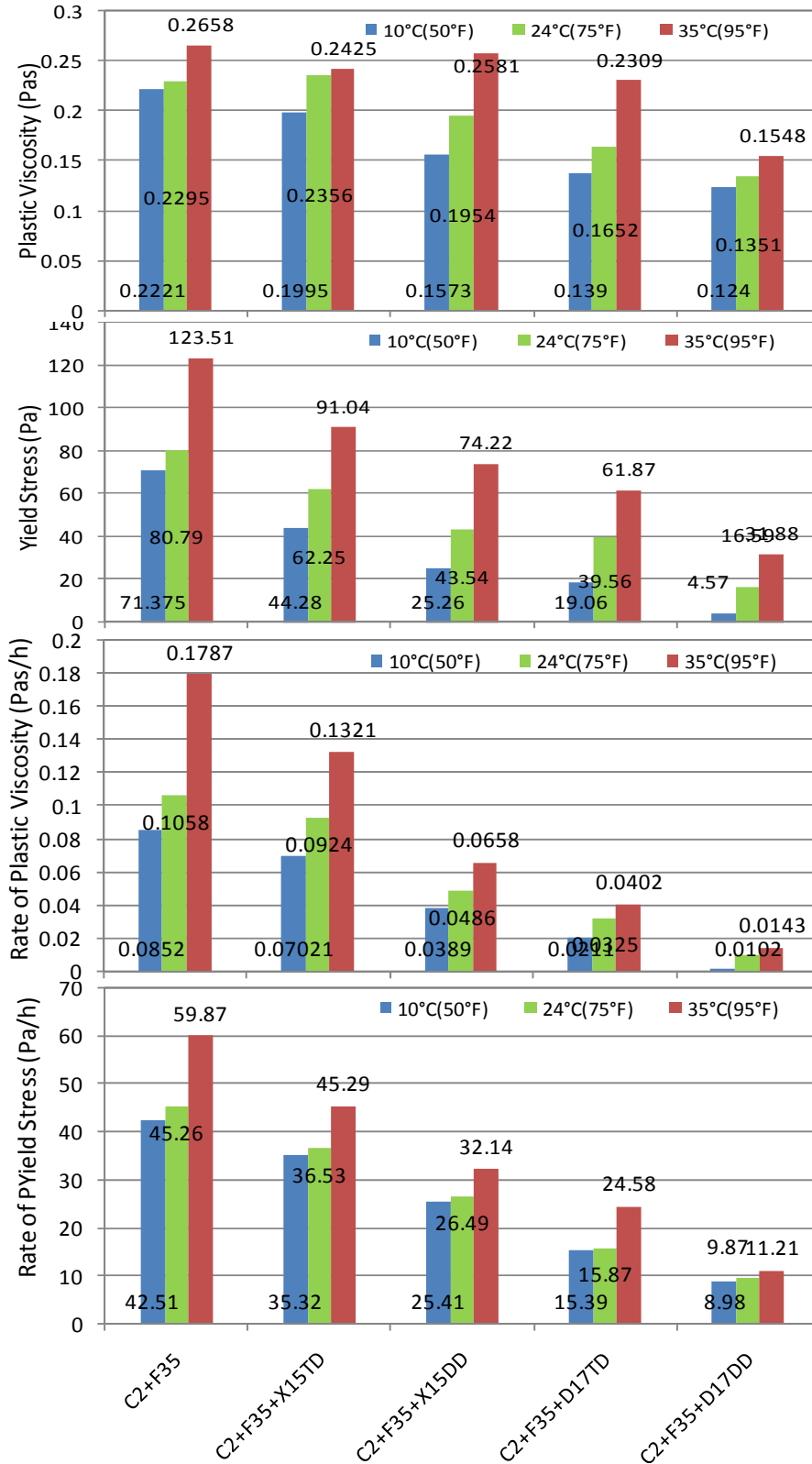
Figure 6.1. PV, YS, RPV, and RYS for C2+F35 System as a Function of Temperature, Admixture Type, and Dosages.

Mini Slump Cone Test

        The researchers used a mini slump cone to conduct a mini slump test on all the studied mixtures (according to Table 5.1). The pat area results from mini slump tests for C2 and C4 cement system as a function of time and temperature are presented in Table 6.7 (a) and (b), respectively. In general, researchers consider that the higher the pat area the higher is the flowability. Table 6.7 shows the following.

Effects of Chemical Admixtures: The effect of chemical admixture on the mini-slump flow behavior is described below.

- The addition of both the chemical admixtures, i.e., X15 and D17, makes the cement paste more flowable (i.e., increase of pat areas) than the paste without admixtures. The higher admixture dosage (i.e., from typical dosage to double dosage) always makes pat areas bigger, i.e., increase of flowability, irrespective of type of admixture.
- The cement pastes with admixture D17 always show larger pat areas (i.e., higher flowability) than those with admixture X15 irrespective of SCMs types and temperature.

Effects of Ambient Temperature: The mini slump tests were carried out at all three selected temperatures—10°C (50°F), 24°C (75°F), and 35°C (95°F)—to verify the temperature effects on the flow properties of cement pastes (Table 6.7).

- The pat areas for all the tested mixtures irrespective of SCMs and admixture types generally show a decreasing trend with increasing temperature. This is an indication of a decrease in flowability with increasing temperature as expected.
- As observed from the foregoing discussion, the mini slump cone test can detect the changes in terms of measuring different pat areas as a result of (i) adding different types of SCMs and chemical admixtures and (ii) temperature changes. It would be interesting to see how the mini slump results compare with the rheological parameters determined earlier. The plots of 5 minute pat areas vs. the absolute rheological parameters (i.e., plastic viscosity and yield stress) are presented in Figures 6.2 (a) and 6.2 (b) respectively. The graphs of the rate of pat area loss (equivalent to slump loss) vs. the rate

of change of rheological parameters (i.e., RPV and RYS) are plotted at Figure 6.3 (a) and 6.3 (b) respectively. Rate of pat area loss was calculated by dividing elapsed time of 25 minutes to the difference in pat area between 5 and 30 minutes. Some important observations are listed below.

- The mini slump pat area and the yield stress data from the rheology test at 5 minutes after water is added to cement has a good relationship by showing the high R^2 of 0.80 as plotted at Figure 6.2 (b). Figure 6.2 (b) indicates that paste mixtures with higher pat areas have lower yield stresses and vice versa irrespective of SCMs and admixtures types and temperature. These results confirm the observation by earlier researchers (28), i.e., the mini slump pat areas increase proportionally as the yield stresses decrease.

- As the ambient temperature increases, the slope of the pat area vs. yield stress changes more steeply, as shown in Figure 6.2 (b). Based on this result it can be concluded that the mini slump pat area has higher sensitivity to represent yield stress of a corresponding cement paste at higher temperature.

- A poor correlation ($R^2 = 0.53$) exists between 5 minute pat areas and plastic viscosity (Figure 6.2a). The correction, however, improves ($R^2 = 0.68$) by comparing 5 minute pat areas and RPV (Figure 6.2c).

- Pat area measurement shows a good correlation with yield stress (Figure 6.2b) but poor correlation with plastic viscosity (Figure 6.2a). Therefore, the pat area provides partial information pertaining to flowability whereas rheology measurement provides a complete characterization of flowability. Therefore, criteria based on mini slump to identify incompatible mixtures will have the same limitations as with yield stress (discussed earlier).

- The rate of pat area loss shows poor correlation with both RPV and RYS (considered best parameters for acceptance criteria of incompatibility) by showing low R^2 of 0.53 and 0.61, respectively, as presented in Figure 6.3 (a) and 6.3 (b). This indicates that the rate of pat area loss cannot serve as an effective criterion.

Table 6.7.(a) Mini Slump Test Data for C2 Cement System under Different Temperatures.

	Exp. #	5min mm^2	10min mm^2	20min mm^2	30min mm^2	Rate of Pat Area Loss 5 to 30 min
C (50°F)	3_C2+F35	5153.0	4536.5	4185.4	4071.5	43.3
	9_C2+F35+X15TD	6939.8	5741.5	5410.6	4778.4	86.5
	21_C2+F35+X15DD	8741.7	7238.2	6013.2	5410.6	133.2
	10_C2+F35+D17TD	9331.3	7088.2	6647.6	6291.2	121.6
	22_C2+F35+D17DD	12568.1	11785.9	10659.6	9589.9	119.1
	4_C2+C35	5026.5	4071.5	3631.7	3318.3	68.3
	11_C2+C35+X15TD	9245.9	7620.1	4901.7	4656.6	183.6
	23_C2+C35+X15DD	11309.7	8908.2	7238.2	5876.5	217.3
	12_C2+C35+D17TD	12767.6	9589.9	8741.7	7543.0	209.0
	24_C2+C35+D17DD	15614.5	14313.9	12469.0	11499.0	164.6
	5_C2+S50	5026.5	4477.0	4417.9	3959.2	42.7
	13_C2+S50+X15TD	7389.8	6221.1	6151.4	5607.9	71.3
	25_C2+S50+X15DD	9503.3	7088.2	6866.1	6361.7	125.7
	14_C2+S50+D17TD	8992.0	7932.7	7088.2	7013.8	79.1
	26_C2+S50+D17DD	12568.1	11785.9	9852.0	9076.3	139.7
24°C (75°F)	*1_C2	5085.7	3655.8	2642.1	2623.9	98.4
	3_C2+F35	5345.6	4839.8	4596.3	4015.2	53.2
	9_C2+F35+X15TD	6647.6	5741.5	4963.9	4185.4	98.5
	21_C2+F35+X15DD	8332.3	7620.1	5808.8	5153.0	127.2
	10_C2+F35+D17TD	9160.9	7313.8	6221.1	6221.1	117.6
	22_C2+F35+D17DD	12667.7	11309.7	8824.7	7543.0	205.0
	4_C2+C35	5541.8	4242.9	3369.6	3068.0	99.0
	11_C2+C35+X15TD	7466.2	5674.5	4901.7	4185.4	131.2
	23_C2+C35+X15DD	9331.3	6792.9	5410.6	4778.4	182.1
	12_C2+C35+D17TD	11028.8	8171.3	6792.9	6013.2	200.6
	24_C2+C35+D17DD	15174.7	12667.7	9503.3	8171.3	280.1
	5_C2+S50	4901.7	4242.9	4071.5	4071.5	33.2
	13_C2+S50+X15TD	6720.1	5808.8	4778.4	4901.7	72.7
	25_C2+S50+X15DD	8576.7	7088.2	6866.1	6221.1	94.2
	14_C2+S50+D17TD	9331.3	7932.7	6939.8	6647.6	107.3
	26_C2+S50+D17DD	11785.9	10659.6	8908.2	8091.4	147.8
35°C (95°F)	3_C2+F35	3631.7	3217.0	2922.5	2687.8	37.8
	9_C2+F35+X15TD	4417.9	3631.7	3318.3	3019.1	56.0
	21_C2+F35+X15DD	6647.6	4477.0	3793.7	3421.2	129.1
	10_C2+F35+D17TD	6647.6	4359.2	3685.3	3318.3	133.2
	22_C2+F35+D17DD	10568.3	8659.0	5808.8	3793.7	271.0
	4_C2+C35	3685.3	2780.5	2419.2	1847.5	73.5
	11_C2+C35+X15TD	4359.2	3267.5	2507.2	2123.7	89.4
	23_C2+C35+X15DD	6647.6	3631.7	2551.8	2123.7	181.0
	12_C2+C35+D17TD	7088.2	3959.2	2734.0	2290.2	191.9
	24_C2+C35+D17DD	11979.1	8494.9	4778.4	2970.6	360.3
	5_C2+S50	3631.7	3318.3	3166.9	2922.5	28.4
	13_C2+S50+X15TD	4963.9	4128.2	3739.3	3473.2	59.6
	25_C2+S50+X15DD	6792.9	6013.2	5476.0	5026.5	70.7
	14_C2+S50+D17TD	7466.2	6013.2	4656.6	4656.6	112.4
	26_C2+S50+D17DD	10117.7	7854.0	6720.1	5876.5	169.6

Note: ▓ *identified as incompatible mixtures*   ▓ *identified as marginal mixtures*

70

Table 6.7.(b) Mini Slump Test Data for C4 Cement System under Different Temperatures.

	Exp. #	5min	10min	20min	30min	Rate of Pat Area Loss
		mm^2	mm^2	mm^2	mm^2	5 to 30 min
10°C (50°F)	6_C4+F35	5541.8	4656.6	4071.5	3848.5	67.7
	15_C4+F35+X15TD	7543.0	5876.5	5153.0	4417.9	125.0
	27_C4+F35+X15DD	10751.3	8171.3	6221.1	5216.8	221.4
	16_C4+F35+D17TD	11689.9	8659.0	6647.6	5741.5	237.9
	28_C4+F35+D17DD	15065.7	11309.7	9940.2	7775.6	291.6
	7_C4+C35	5674.5	4536.5	4071.5	3525.7	86.0
	17_C4+C35+X15TD	9940.2	6720.1	5741.5	4359.2	223.2
	29_C4+C35+X15DD	11979.1	8659.0	6866.1	5607.9	254.8
	18_C4+C35+D17TD	13684.8	9676.9	7620.1	5876.5	312.3
	30_C4+C35+D17DD	15948.5	13069.8	11028.8	8741.7	288.3
	8_4+S50	5410.6	4536.5	4128.2	3848.5	62.5
	19_C4+S50+X15TD	8091.4	6013.2	5476.0	4963.9	125.1
	31_C4+S50+X15DD	10386.9	8413.4	6866.1	6151.4	169.4
	20_C4+S50+D17TD	10028.7	8576.7	7088.2	6291.2	149.5
	32_C4+S505+D17DD	13788.6	11404.2	9245.9	7466.2	252.9
24°C (75°F)	*2_C4	3731.2	3252.3	3117.2	2922.5	32.3
	6_C4+F35	4128.2	3848.5	3848.5	3631.7	19.9
	15_C4+F35+X15TD	6647.6	5026.5	4717.3	4300.8	93.9
	27_C4+F35+X15DD	8659.0	6082.1	5476.0	4901.7	150.3
	16_C4+F35+D17TD	9245.9	7543.0	5345.6	5281.0	158.6
	28_C4+F35+D17DD	11979.1	10751.3	8824.7	5741.5	249.5
	7_C4+C35	4596.3	4185.4	3793.7	3369.6	49.1
	17_C4+C35+X15TD	7088.2	5476.0	4839.8	4071.5	120.7
	29_C4+C35+X15DD	8992.0	7088.2	6082.1	5153.0	153.6
	18_C4+C35+D17TD	10028.7	6647.6	4717.3	3369.6	266.4
	30_C4+C35+D17DD	13581.3	8659.0	6082.1	4015.2	382.6
	8_C4+S50	4778.4	4071.5	3959.2	3739.3	41.6
	19_C4+S50+X15TD	7163.0	5674.5	4901.7	4417.9	109.8
	31_C4+S50+X15DD	9589.9	8171.3	6575.5	5944.7	145.8
	20_C4+S50+D17TD	9503.3	7620.1	5944.7	5674.5	153.2
	32_C4+S50+D17DD	12370.2	10659.6	8251.6	6503.9	234.7
35°C (95°F)	6_C4+F35	3473.2	3166.9	2922.5	2780.5	27.7
	15_C4+F35+X15TD	4242.9	3793.7	3525.7	3267.5	39.0
	27_C4+F35+X15DD	6503.9	4778.4	4128.2	3525.7	119.1
	16_C4+F35+D17TD	6792.9	5089.6	4300.8	3421.2	134.9
	28_C4+F35+D17DD	9852.0	7697.7	5281.0	3578.5	250.9
	7_C4+C35	3525.7	2874.8	2463.0	2164.8	54.4
	17_C4+C35+X15TD	4300.8	3369.6	2734.0	2290.2	80.4
	29_C4+C35+X15DD	6432.6	4477.0	3217.0	2463.0	158.8
	18_C4+C35+D17TD	6866.1	4656.6	3318.3	2332.8	181.3
	30_C4+C35+D17DD	11499.0	5674.5	3959.2	3166.9	333.3
	8_4+S50	3631.7	3318.3	3166.9	2642.1	39.6
	19_C4+S50+X15TD	4778.4	4242.9	3848.5	3019.1	70.4
	31_C4+S50+X15DD	6575.5	5808.8	5410.6	4417.9	86.3
	20_C4+S50+D17TD	7088.2	6221.1	5410.6	4071.5	120.7
	32_C4+S50+D17DD	9676.9	7620.1	7088.2	4417.9	210.4

Note: ▯ identified as incompatible mixtures   ▯ identified as marginal mixtures

71
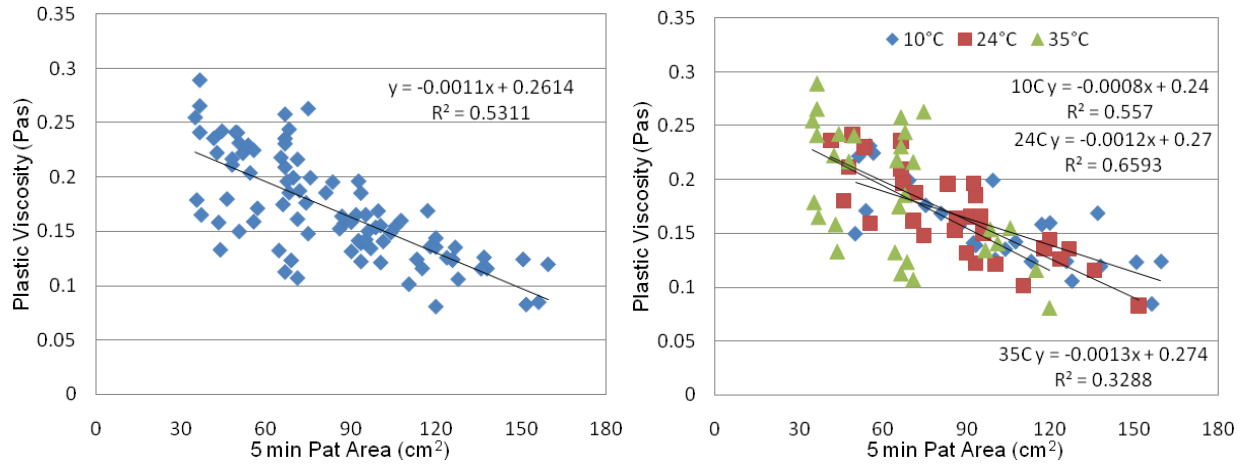
Figure 6.2.(a) Plastic Viscosity vs. Mini Slump Pat Area at 5 minutes after Water Added.
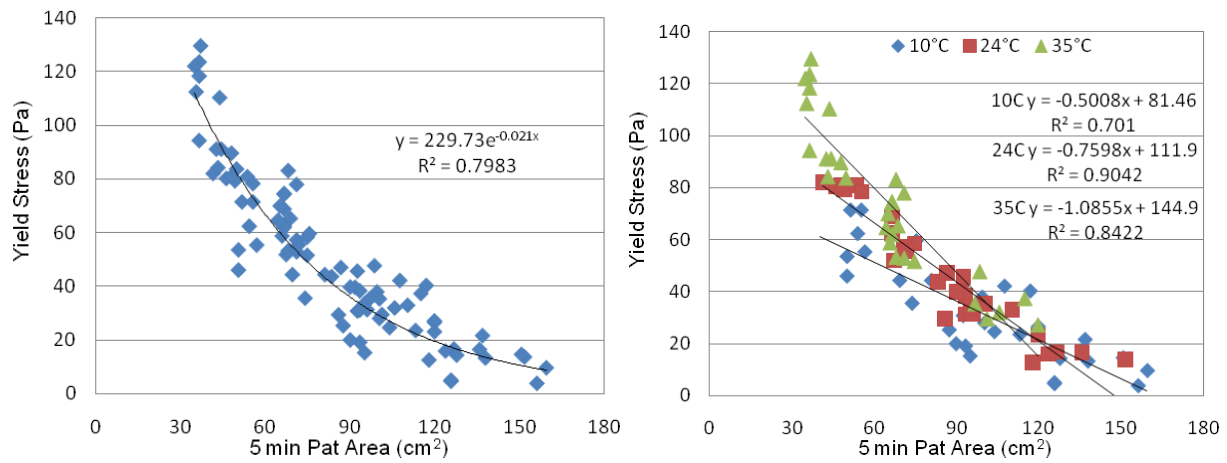
Figure 6.2.(b) Yield Stress vs. Mini Slump Pat Area at 5 minutes after Water Added.
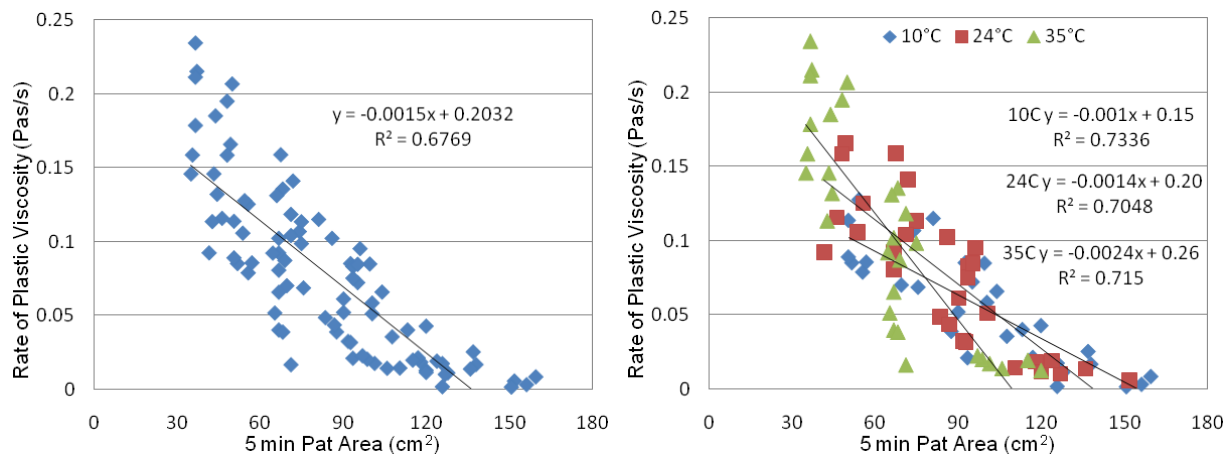
Figure 6.2.(c) RPV vs. Mini Slump Pat Area at 5 minutes after Water Added.

72
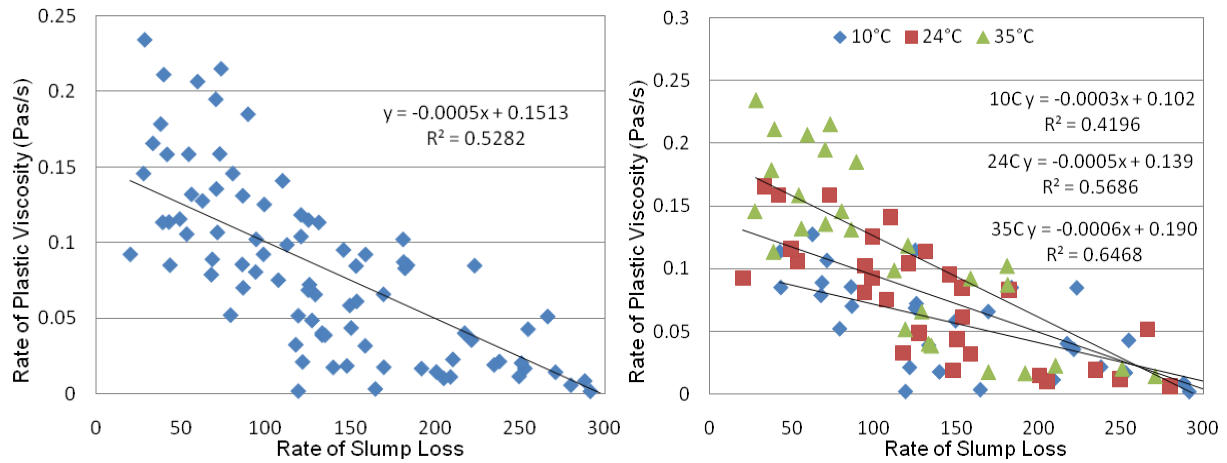
Figure 6.3.(a) RPV vs. Rate of Pat Area Loss from 5 to 30 minutes.
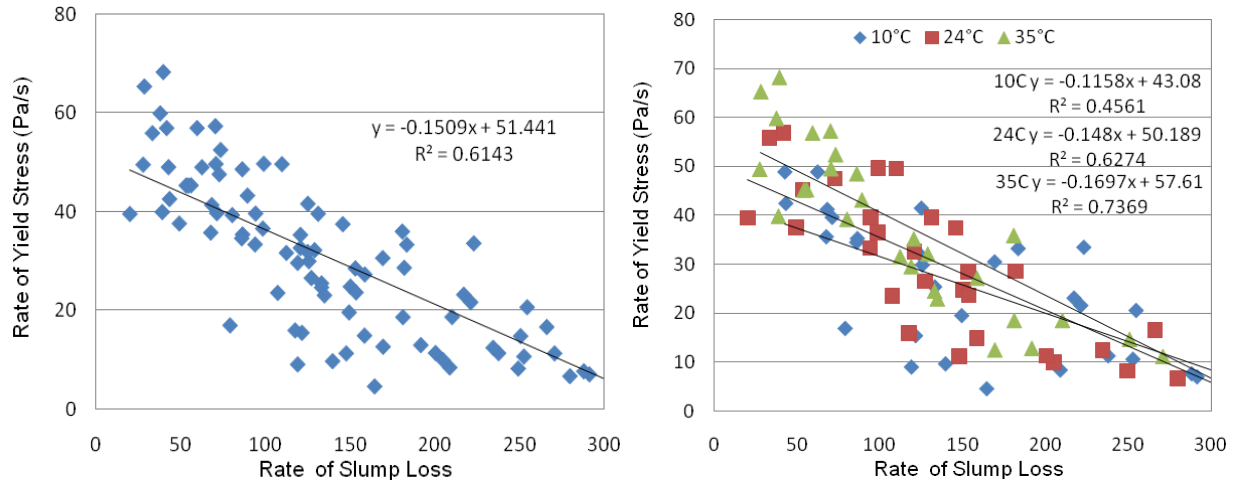
Figure 6.3.(b) RYS vs. Rate of Pat Area Loss from 5 to 30 minutes.

Mini Slump Test vs. Possible Incompatible Criteria

The researchers attempted to identify the incompatible mixtures using the data from mini slump tests. Table 6.8 lists the possible criteria based on mini slump test parameters. The 5 minute pat area (best out of four pat area measurements at four different time intervals) and rate of pat area loss are considered as potential candidates to develop some possible criteria. A comparative assessment of the mixture categorization (normal, marginal, and incompatible) by both heat evolution and mini slump criteria has been made, and observations are listed in Table 6.8. Table 6.8 shows the following observations:

- A large number of normal and marginal mixtures (based on heat evolution criteria in Table 6.1) are identified as incompatible mixtures based on rate of pat area loss criteria. In addition to that, one incompatible mix (Mix No. 26) is identified as normal/ marginal at both 24 and 35°C. Therefore, a large number of mismatches is evident.
- Additionally, the criteria change with the change of cement type and temperature as opposed to rheology-based (RPV and RYS) criteria.

Therefore, the rate of part area loss did not appear to be an effective criterion as pointed out earlier. However, the 5 minute pat area seems to be a relatively better criterion than the rate of pat area loss for the following reasons:

- Limited number of mixtures identified as mismatches–For example, one incompatible mixture with cement 2 (No. 12), another incompatible mixture with cement 4 (No. 32), and one normal mix with cement 2 (No. 14) became marginal.
- A common criterion for both the cement can be applied.

However, a tendency of both false positives and negatives are observed with the criteria based on 5 minute pat area. It is interesting to note that large numbers of normal mixes are identified as marginal on yield stress-based criteria (Table 6.4), which is an indication of false negative. However, mixture 12 was not identified as marginal in Table 6.4 and therefore, a false positive was not observed based on yield stress-based criteria. Therefore, it can be concluded that the 5 minute pat area cannot be accepted as an effective criteria, although it appeared to be

promising. However, researchers must generate a greater number of data including different types of fly ashes, cement, and chemical admixtures as a function of temperature in order to confirm this conclusion. The rate of rheological parameters is the best parameter to establish the criteria to identify the incompatible mixtures. The next chapter discusses establishing acceptance criteria based on RPV and RYS.

Table 6.8. Possible Criteria Based on Pat Area, Rate of Pate Area Loss, and Related Issues.

Temperature		10°C		24°C		35°C		Issues
Status		**Incom.**	**Marg.**	**Incom.**	**Marg.**	**Incom.**	**Marg.**	
5 min. Pat Area	C2	≥ 12568	11309-9331	≥ 11028		≥10177	10117-7088	IM (16) and NM (18) identified as marginal at 35^{0}C
	C4	≥ 13788	13788-13684	≥11979		≥ 9852	9852-9676	IM (42) identified as marginal at 35^{0}C
Rate of Pat Area Loss (5-30 min)	C2	≥ 119 (1) NM (31,15,35) and MM (33, 14) based on HEC (Table 6.4) identified as IM (2) IM (32) identified as MM		≥ 200 (1) IM (36) identified as NM / MM; (2) NM (33) identified as MM		≥ 192 (1) IM (36) identified as NM / MM; (2) NM (33) identified as MM		Mostly normal (31, 15, 35) and marginal (33,14) mixtures based on HEC identified as incompatible mixtures
	C4	≥ 253 NM 39 and MM 22 became IM		≥ 234 NM 22 became IM		≥ 333	250-210	Normal (39) and marginal (22) mixtures identified as incompatible

Note: NM – Normal Mixture(s), MM – Marginal Mixture(s), IM – Incompatible Mixture(s),   HEC – Heat Evolution Criteria.

CHAPTER 7

ESTABLISHING ACCEPTANCE CRITERIA

In this project, the researchers attempted to develop rheology-based acceptance criteria based on the test results generated from the laboratory investigation (Chapter 6) and discussed below. In Chapter 6, the rate of rheological parameters is the most effective parameter to establish acceptance criteria for identifying incompatible mixtures.

Procedure to Develop Rheology-Based Acceptance Criteria

Tables 7.1a and 7.1b list the incompatible mixtures identified based on integrated heat evolution criteria. The mixture numbers 12, 22, 24, and 26 with C2 cement and 30, 32 with C4 cement were identified as incompatible mixtures at all three temperature conditions. Mixture number 28 with C4 cement is identified as incompatible mixture both at low (10°C) and intermediate temperatures (24°C) but becomes compatible at high temperature (35°C). The rheological parameters, i.e., rate of change of plastic viscosity and rate of change of yield stress corresponding to the identified incompatible mixtures, are then compared with the percent of heat evolution after 48 hours (Table 7.1a and 7.1b) to see whether identification of incompatible mixtures based on the two methods supports each other. The following observations are important in this connection.

- An incompatible mix should show a very low value of RPV and RYS. It is interesting to see that all the incompatible mixtures identified by heat evolution criteria (12, 22, 24, 26 with C2 cement and 30, 32 with C4 cements) showed the lowest RPV and RYS values (Tables 7.1a and 7.1b). This is in good agreement between heat evolution and rheology-based criteria.
- Table 7.1c lists the possible marginal mixtures based on combined criteria of percent heat evolution, RPV, and RYS. Based on percent of heat evolution criteria, the mixtures having percent heat evolution between 30–37 percent are considered as marginal mixes. Therefore, the mixture numbers 10, 23, 14 with cement 2 at 10°C; 22 with cement 4 at 10°C and 28 and 32 with cement 4 at 35°C (Table 7.1c) are identified as marginal mixtures based on heat evolution criteria alone. Out of these 6 possible marginal

mixtures, mixture numbers 23 and 14 show higher RPV and RYS and are therefore, not ultimately considered as marginal mixtures. The mixture no. 16 (C4+F35+D17TD) at 10°C has both lower RPV and RYS but slightly higher percent of heat evolution (53.94) and is therefore, considered as marginal mixture. The mixtures 10 (C2+F35+D17TD) at 24°C, 16 (C4+F35+D17TD) at 24°C, and 18 (C4+C35+D17TD) at both 24 and 35°C show lower yield stress values but all having higher RPV and percent heat evolution. Therefore, these mixtures are also not considered finally as marginal mixtures.

- Table 7.1d lists the final confirmed marginal mixtures. The values of the confirmed marginal mixtures have served to fix the upper limit for the acceptance criteria.

- Based on the values of RPV and RYS for the confirmed incompatible mixtures (Tables 7.1a and 7.1b) and marginal mixtures (Table 7.1d), the possible acceptance criteria is formulated and given in Table 7.2.

Table 7.1.(a) Incompatible Mixtures with C2 Cement under Different Temperatures.

	Mixture Combinations	Heat Evolution w.r.t. Control after 48 hrs (%)	RPV	RYS
10°C (50°F)	22_C2+F35+D17DD	10.98	0.0018	8.98
	12_C2+C35+D17TD	17.34	0.0112	8.35
	24_C2+C35+D17DD	11.56	0.0032	4.52
	26_C2+S50+D17DD	6.07	0.0175	9.63
24°C (75°F)	22_C2+F35+D17DD	14.45	0.0102	9.87
	12_C2+C35+D17TD	22.54	0.0145	11.29
	24_C2+C35+D17DD	14.45	0.0057	6.59
	26_C2+S50+D17DD	14.45	0.0185	11.21
35°C (95°F)	22_C2+F35+D17DD	16.18	0.0143	11.21
	12_C2+C35+D17TD	20.23	0.0167	12.89
	24_C2+C35+D17DD	16.76	0.0129	9.54
	26_C2+S50+D17DD	16.18	0.0176	12.56

Table 7.1.(b) Incompatible Mixtures with C4 Cement under Different Temperatures.

	Mixture Combinations	Heat Evolution w.r.t. Control after 48 hrs (%)	RPV	RYS
10°C (50°F)	28_C4+F35+D17DD	15.45	0.0016	6.96
	30_C4+C35+D17DD	17.88	0.0085	7.59
	32_C4+S50+D17DD	15.15	0.0168	10.58
24°C (75°F)	28_C4+F35+D17DD	15.15	0.0115	8.14
	30_C4+C35+D17DD	14.55	0.0138	9.87
	32_C4+S50+D17DD	13.94	0.0191	12.34
35°C (95°F)	30_C4+C35+D17DD	19.33	0.0198	13.58
	32_C4+S50+D17DD	32.43	0.0228	18.59

Table 7.1.(c) All Possible Marginal Mixtures under Different Temperatures.

	Mixture Combinations	Heat Evolution w.r.t. Control after 48 hrs (%)	RPV	RYS
10°C (50°F)	10_C2+F35+D17TD	30.06	0.0211	15.39
	23_C2+C35+X15DD	32.95	0.0402	23.12
	18_C4+C35+D17TD	34.85	0.0254	13.52
	14_C2+S50+D17TD	37.28	0.0521	16.89
	16_C4+F35+D17TD	53.94	0.0214	11.26
24°C (75°F)	10_C2+F35+D17TD	59.25	0.0325	15.87
	16_C4+F35+D17TD	73.03	0.0318	14.81
	18_C4+C35+D17TD	70.00	0.0512	16.56
35°C (95°F)	28_C4+F35+D17DD	35.76	0.0204	14.72
	18_C4+C35+D17TD	75.45	0.0873	18.56
	32_C4+S50+D17DD	32.43	0.0228	18.59

Table 7.1.(d) Confirmed Marginal Mixtures under Different Temperatures.

	Mixture Combinations	Heat Evolution w.r.t. Control after 48 hrs (%)	RPV	RYS
10°C (50°F)	10_C2+F35+D17TD	30.06	0.0211	15.39
	18_C4+C35+D17TD	34.85	0.0254	13.52
	16_C4+F35+D17TD	53.94	0.0214	11.26
35°C (95°F)	28_C4+F35+D17DD	35.76	0.0204	14.72
	32_C4+S50+D17DD	32.43	0.0228	18.59

Table 7.2. Criteria of Incompatibilities Based on RPV and RYS.

Criteria	RPV	RYS
Incompatible Mixtures	≤ 0.0198	4.52-13.58
Marginal Mixtures	0.0198-0.0254	13.58-18.59
Normal Mixtures	> 0.0254	> 18.59

Table 7.2 shows the following observations:

- As described earlier, the normal and incompatible mixtures can be clearly distinguished based on rate of change of plastic viscosity and rate of change of yield stress. Both RPV and RYS can be used to identify incompatible mixtures. However, RPV is more sensitive than RYS. In addition, the reproducibility of RPV is generally better than that of RYS as manifested by lower coefficient of variation (COV) [Tables 6.3 (a) and 6.3(b)].
- A generalized criterion irrespective of SCM type and temperature is obtained based on the limited data. It is anticipated that separate criteria for low temperature (winter) and high temperature (summer) as a minimum may be needed. A generalized criterion irrespective of SCMs type is a good indication of robustness and user-friendliness of the use of DSR-based rheology method to identify incompatible mixtures. However, a large volume of data needs to be generated in order to verify the applicability of the approach.

Further refinement of these acceptance criteria based on more specific work covering wide range of incompatibilities and field laboratory validation through implementation efforts are beyond the scope of the present research. This research will ultimately help material suppliers, concrete producers, and other users to detect problematic combination of concrete ingredients during the mixture design process thereby avoiding concrete cracking and other durability issues due to incompatibilities.

CHAPTER 8
CONDUCT FIELD DEMONSTRATION

The research team has conducted a demonstration program in front of TxDOT personnel as a part of field demonstration of the DSR-based test method (Task 8). The reproducibility tests of the rheological parameters using the modified DSR were conducted in this demonstration program and are described below.

Reproducibility of the Rheological Parameters

Tables 8.1 and 8.2 present the reproducibility of the rheological parameters (both absolute values and rates) based on the two mixes at three different temperatures with three replicas. The ingredients corresponding to each mixture at the selected temperature were mixed and tested separately three times in order to generate three replicas. Average of rheological parameters (i.e., plastic viscosity, yield stress, rate of plastic viscosity, and rate of yield stress) based on three replicas and their respective coefficient of variation (COV) were calculated for the studied mixture combinations and are presented in Table 8.1 for PV and YS, and Table 8.2 for RPV and RYS. The plastic viscosity and yield stress data in Table 8.1 represents data from the first run, i.e., 10 minutes after adding water to the cement, for the selected mixtures. Note that the mixture with C4 + F35 + X15DD was identified as normal mixture, and the mixture with C4 + F35 + D17DD was identified as incompatible mixture (Chapters 6 and 7) based on both the rheological parameters and heat of hydration data.

Table 8.1. Reproducibility of Plastic Viscosity (PV) and Yield Stress (YS).

Mixture Combination			PV	PV Average	COV%	YS	YS Average	COV%
C4+F35+X 15DD	10°C	1	0.1598			42.1		
		2	0.1524	0.1553	2.54	41.51	41.06	3.21
		3	0.1537			39.58		
	24°C	1	0.1638			46.92		
		2	0.1594	0.1616	1.36	33.62	39.70	16.93
		3	0.1617			38.56		
	35°C	1	0.2181			69.89		
		2	0.2019	0.2099	3.86	63.84	65.53	5.80
		3	0.2096			62.87		
C4+F35+ D17DD	10°C	1	0.124			14.57		
		2	0.1215	0.1221	1.35	16.59	15.54	6.51
		3	0.1209			15.47		
	24°C	1	0.1437			23.00		
		2	0.1348	0.1381	3.55	16.72	20.03	15.75
		3	0.1357			20.37		
	35°C	1	0.1536			47.587		
		2	0.1602	0.1538	4.10	56.32	51.25	8.84
		3	0.1476			49.85		

Table 8.2. Reproducibility of Rate of Plastic Viscosity (RPV) and Rate of Yield Stress (RYS).

Mixture Combination			RPV	RPV Average	COV%	RYS	RYS Average	COV%
C4+F35+X 15DD	10°C	1	0.0356			21.59		
		2	0.0381	0.0370	3.48	26.34	24.17	9.93
		3	0.0374			24.57		
	24°C	1	0.0436			24.75		
		2	0.0459	0.0437	4.81	28.12	26.80	6.72
		3	0.0417			27.54		
	35°C	1	0.0517			29.56		
		2	0.0534	0.0548	7.38	31.58	32.78	12.09
		3	0.0594			37.21		
C4+F35+ D17DD	10°C	1	0.0016			6.969		
		2	0.0014	0.0015	6.67	5.23	6.49	17.02
		3	0.0015			7.28		
	24°C	1	0.0115			8.14		
		2	0.0119	0.0120	4.21	9.21	9.07	9.58
		3	0.0125			9.86		
	35°C	1	0.0204			14.72		
		2	0.0249	0.0227	9.92	15.65	16.20	11.26
		3	0.0228			18.24		

Tables 8.1 and 8.2b indicate that the coefficient of variation (COV) of both absolute values of PV and RPV is below 10. The COV of the YS and RYS is also under 10 for 60 percent of the cases. The COV of the YS and RYS for the remaining 40 percent cases is under 17. It was also demonstrated that both RPV and RYS were more sensitive to differentiate the two studied mixtures than absolute values of PV and YS (as manifested in Tables 8.1 and 8.2).

CHAPTER 9

CONCLUSIONS AND RECOMMENDATIONS

Conclusions

The research team performed an extensive literature search to collect information on (i) theoretical background of rheology in connection with cement paste and concrete, (ii) cement paste rheology as a good indicator in identifying mineral admixtures/chemical admixtures/ sulfate incompatibilities in concrete, and (iii) possible areas of modifications in DSR to make it suitable for measuring cement paste rheology. The existing information on the applicability of parallel plate fluid rheometer to measure cement paste rheology by NIST along with the suggestions provided by the DSR manufacturer, were the main sources of information for item (iii). From this information, the suitable areas of modifications in DSR were identified and adopted for upgrading the DSR. Preliminary investigation was conducted using the modified DSR to optimize the DSR test conditions and develop a DSR-based rheology test procedure. A special temperature-controlled, high-shear (up to 6000 rpm) cement paste mixing procedure was developed to simulate the shearing effects that cement paste experiences in actual concrete due to aggregates. The researchers employed temperature-controlled mixing in addition to temperature control in the DSR device during rheology measurement in order to investigate the temperature effect more accurately. Another advanced rheometer (AR 2000) was used in the preliminary program to validate the applicability of DSR to measure cement paste rheology with permissible reproducibility and sensitivity. The heat of hydration test by isothermal micro-calorimeter and setting time test by Vicat apparatus were used as supporting tools to verify the DSR test results.

An extensive laboratory investigation was conducted subsequently using the modified and optimized DSR based rheology test procedure with varieties of cements, supplementary cementitious materials (SCMs), and different types and dosages of commonly used chemical admixtures under different temperature conditions. The materials and experimental factors were selected based on the available historical information in such a way that some combinations in the experimental design are expected to manifest incompatibilities in the laboratory. The heat of hydration and setting time tests were also performed as supporting tools in the main test program. The researchers subsequently developed a procedure to formulate rheology-based acceptance criteria based on the available test results from the main laboratory investigation. A

85

field demonstration program was conducted to show the repeatability and sensitivity of the DSR based rheology test method to measuring cement paste rheology as well as identifying incompatibilities. A mini-slump test was included in the main test program to measure flow characteristics of the cementitious system as an alternative or supporting tool for the rheology test.

The researchers drew the following conclusions from this project:

1. The modifications that are made to the DSR to make it suitable for measuring cement paste rheology are (i) both upper and lower plates were covered by 240 grit paper to prevent slippage, (ii) a closed water circulation-based fluid jacket system was installed for temperature controlling, which ensured avoiding direct specimen contact with water during rheology measurements, and (iii) a sealing cap was developed and installed to prevent water evaporation from the cement paste specimen during DSR test—free rotation of the upper plates without any interference from the sealing cap was ensured.

2. The DSR test conditions were optimized in order to satisfy both repeatability and sensitivity in monitoring the rheological changes of the cement paste at very early ages. The optimized test conditions are (i) 1 mm gap between two plates was found to be optimum to generate data with the best reproducibility and sensitivity, (ii) a longer test duration (up to 2 hours with 10, 30, 60, 90, and 120 minute testing intervals) was needed in order to derive an effective rate of change of rheological parameters under controlled evaporation control condition, and (iii) the shear rate range from 0 to 200/s yielded the most reproducible rheological parameters, although, DSR normally operates with shear rates 0 to 300/s.

3. In the preliminary test program, both the DSR and AR 2000 rheometers in modified form were capable of measuring cement paste rheology with permissible reproducibility and sensitivity with a 1 mm plate gap. Both the rheometers were able to distinguish between normal and incompatible mixtures in the similar manner, although the absolute values were not exactly the same. This validated the applicability of DSR to measure cement paste rheology as well as identifying incompatible mixtures. The heat of hydration data from isothermal calorimeter test and setting time behaviors from vicat needle test have strongly supported the rheology-based observations.

4. An experimental design has been formulated by considering two types of cements, three types of SCMs, two types of lignin-based chemical admixtures with two different dosages, and three temperatures for the main laboratory investigation. Absolute values of plastic viscosity and yield stress were determined corresponding to five time intervals (10, 30, 60, 90, and 120 minutes) for all the selected mixtures. The slope of the linear region from time vs. PV/YS plots represented the rate of change of plastic viscosity and yield stress within a 2-hour time period. Almost all the incompatible mixtures identified by heat evolution criteria are identified with abnormal ranges of RPV and RYS. Therefore, the heat evolution and setting time results strongly supported the rheology-based test results.

5. The rate of change of rheological parameters was found to be more sensitive than the absolute values of rheological parameters to identify the studied incompatible mixtures. Both RPV and RYS are acceptable to formulate criteria of incompatibilities, however, RPV is more sensitive to distinguish between normal and incompatible mixtures. A generalized acceptance criterion, i.e., ≤ 0.0198 for PRV and ≤ 13.58 for RYS irrespective of SCM type and temperature, is obtained based on the available data from this project.

6. Reproducibility of the rheological parameters (both absolute values and rates) based on the two mixes at three different temperatures with three replicas are verified as a part of a field demonstration program. Coefficient of variation (COV) of both absolute values of PV and RPV is below 10. The COV of the YS and RYS is also under 10 for the 60 percent of the cases. The COV of the YS and RYS for the remaining 40 percent cases is under 17.

7. In the mini slump cone test, 5 minute pat area was found to be a relatively better criterion than the other parameters (e.g., rate of change of pat area). However, the researchers observed both false positive and negatives after applying this criterion, and therefore, it did not appear to be an effective criteria.

Recommendations

The following recommendations can be made based on the data generated and knowledge and experience gained in the present research work:

1. A field laboratory validation program through implementation efforts is warranted. Two to three district laboratories should participate in the implementation program. The existing DSR in the respective laboratory needs to be modified in accordance with the modifications performed in the present research. Each laboratory should test some common mixtures (a combination of both normal and incompatible mixtures) to verify (i) the reproducibility of the device and (ii) identification of the incompatible mixtures based on some common criteria. This will ultimately validate the applicability of modified DSR to measure cement paste rheology with permissible reproducibility on one hand and to predict potential concrete mixture incompatibilities such as those between the sulfate system and mineral and chemical admixtures through the direct measurement of cement paste rheology on the other.

2. The numbers of tests that were conducted in the present research were not adequate to assign threshold numbers for establishing acceptance criteria. However an attempt has been made to develop a procedure to formulate acceptance criteria based on the available data. Therefore, further refinement of these acceptance criteria based on more detailed work covering a wide range of incompatibilities is highly necessary. The present research mainly covered incompatibilities due to overdose of chemical admixtures with less coverage on incompatibilities arises from complex interaction between SCMs, cement and chemical/mineral admixtures. More coverage on incompatibilities due to complex chemical interaction needs to be performed either by (i) testing a higher number of problematic SCMs, cement, and chemical admixtures—evaluation of large number of field data on the occurrence of this kind of incompatibilities can help to select wide range of problematic materials and related design of experiments—and/or (ii) testing artificially created incompatible mixtures, which may be formulated by adding different proportions of sulfate-bearing phases (e.g., hemi-hydrates) and/or changing the proportions of C3A contents along with varieties of suspected chemical admixtures.

3. The large volume of data covering a wide range of incompatibilities under different temperature conditions (see item 2 above) will ultimately help to verify whether a generalized criterion (irrespective of SCMs type and temperature) can still be made to identify incompatible mixtures. It is anticipated that a separate criteria for low temperature (winter) and high temperature (summer) as a minimum may be needed.

4. Apply a modeling approach using the large volume of data to improve the procedure for establishing acceptance criteria and to provide a better definition of setting time.

5. Mortar rheology measurement as parallel efforts can be made to establish a correlation between paste and mortar rheology. TTI has the vane type rheometer to measure mortar rheology. The direct mortar rheology measurements will ultimately help material suppliers, concrete producers, and other users to detect problematic combination of concrete ingredients during the mixture design process thereby avoiding concrete cracking and other durability issues due to incompatibilities.

6. Based on the available test results, the mini-slump test did not appear to be effective to distinguish all the studied normal and incompatible mixtures. However, it needs large volume of data covering wide range of material combinations in order to confirm this. It is recommended to conduct mini slump test along with the main rheology tests proposed in item 2 and generate large volume of data. The large volume of data on a comparative basis will ultimately explore the feasibility of the mini-slump test to identify cement-admixtures incompatibilities.

REFERENCES

1. Wong, G.S., A.M. Alexander, R. Haskins, T.S. Poole, P.G. Malone, and L. Wakeley. *Portland-Cement Concrete Rheology and Workability: Final report*, FHWA-RD-00-025, Federal Highway Administration, McLean, Virginia, April 2001.

2. Kosmatka, S.H., B. Kerkhoff and W.C. Panarese. *Design and Control of Concrete Mixtures*, 14th Edition, EB001.14T, Portland Cement Association, Skokie, Illinois, 2002, pp. 355.

3. Bartos, P. *Fresh Concrete: Properties and Tests*, Elsevier, New York, 1992.

4. Metha, P.K. *Concrete: Structure, Properties, and Materials*, Prentice-Hall, Inc, Englewood Cliff, New Jersey, 1986, pp. 449.

5. Tattersall, G.H., and P.F.G. Banfill. *The Rheology of Fresh Concrete*, Pitman, (1983) pp. 356.

6. Banfill, P.F.G. *The Rheology of Fresh Cement and Concrete-a Review*, Proceeding 11th International Cement Chemistry Congress, Durban, May 2003.

7. Ramachandran,V.S. and J.J. Beaudoin. *Handbook of Analytical Techniques in Concrete Science and Technology: Principles, Techniques, and Applications*, Book 2001.

8. Ghio, V.A., P.J. MMonteiro and L.A. Demsetz. *The Rheology of Fresh Cement Paste Containing Polysaccharide Gums*, Cement Concrete Research Vol. 24, No. 2, pp. 243-249

9. Taylor, P.C. *Identifying Incompatible Combinations of Concrete Materials*, FHWA HRT-06-080 Technical report, 2006.

10. Prince, W., M. Edwards-Lajnef, and P.C. Aitcin. *Interaction between Ettringite and a Polynaphthalene Sulfonate Superplasticizer in a Cementitious Paste*, Cement Concrete Research, Vol. 32, No. 1, 2002, pp.79-85

11. Hansen, W.C. *False Set in Portland Cement*, Proceedings of the 4th International Symposium on the Chemistry of Cement, Washington D.C, 1960, pp. 387-428.

12. Helmuth, R., L.M. Hills, D.A. Whiting, and S. Bhattacharja. *Abnormal Concrete Performance in the Presence of Admixtures*, PCA, RP333, pp. 25-26.

13. Flatt, R.J., N.S. Martys, and L. Bergstrom. *The Rheology of Cement Materials*, Material Research Society, Vol. 29, No. 5, pp. 314-318.

14. Zhang, H. *Using Dynamic Rheology to Explore the Microstructure and Stiffening of Cementitious Materials*, Ph.D. Thesis, University of Illinois at Urbana-Champaign, 2001.

15. C. Chen, L.J. Struble, and H. Zhang. *Using Dynamic Rheology to Measure Cement-Admixture Interactions,* Vol. 3, Journal of ASTM International, March 2006.

16. C.F. Ferraris. *Measurements of Rheological Properties of High Performance Concrete: State of the Art Report*, Journal of Research of the National Institute of Standards and Technology, Vol. 104, No. 5, 1996, pp. 461-478.

17. C.F. Ferraris, and K.H. Obla. *The Influence of Mineral Admixtures on the Rheology of Cement Paste and Concrete*, Cement Concrete Research, Vol. 31, No. 2, 2001, pp.245-255.

18. Struble, L.J., and X. Ji. *Rheology*, Handbook of Analytical Techniques in Concrete Science and Technology, Noyes Publications, New Jersey, 2001, pp. 333-367.

19. Struble, L.J., R. Szecsy, W.G. Lei, and G.K. Sun. *Rheology of Cement Paste and Concrete*, Cement Concrete Aggregates, Vol. 20, No. 2, 1998, pp. 269-277.

20. Schultz, M.A., and L.J. Struble. *Use of Oscillatory Shear to Study Flow Behavior of Cement Paste*, Cement Concrete Research, Vol. 23, No. 2, 1993, pp. 273-283.

21. Struble, L.J. and W.G. Lei. *Rheological Changes Associated with Setting of Cement Paste*, Advance Cement Based Material, Vol. 22, No. 6, 1995, pp. 224-230.

22. Hackley, V.A. and C.F. Ferraris. *Guide to Rheological Nomenclature: Measurements in Ceramic Particle Systems*, NIST special publication 946.

23. Bhattacharja, S., and F.J. Tang. *Rheology of Cement Paste in Concrete with Different Mix Designs and Interlaboratory Evaluation of the Mini-Slump Cone Test*, PCA R&D, Serial No. 2412, Portland Cement Association, Skokie, Illinois, 2000.

24. Chiara F. Ferraris. *Connection between the Rheology of Concrete and Rheology of Cement Paste,* 89-M43, ACI Materials (1992) pp. 388-393.

25. C.F. Ferraris. *Measurement of the Rheological Properties of Cement Paste: A New Approach, Role of Admixture in High Performance Concrete*, RILEM International Symposium.

26. Saak, A.W., H.M. Jennings, and S.P. Shah. *The Influence of Wall Slip on Yield Stress and Viscoelastic Measurements of Cement Paste*, Cement Concrete Research 2001, pp. 205-212.

27. Nehdi, M., and M.-A. Rahman. *Effect of Geometry and Surface Friction of Test Accessory on Oscillatory Rheological Properties of Cement Pastes*, ACI Materials (2004), No. 101-M47.

28. Kantro, D.L. *Influence of Water-Reducing Admixtures on Properties of Cement Paste-A Miniature Slump Test*, Cement Concrete Aggregates, Vol. 2, 1980, pp. 95-102.

29. Williams, D.A., A.W. Saak, and H.M. Jennings. *The Influence of Mixing on the Rheology of Fresh Cement Paste*, Cement Concrete Research June 1999.

30. Helmuth, R.A. *Fly Ash in Cement and Concrete*, Portland Cement Association, Skokie, Illinois, 1987.

31. Yang, M., and H.M. Jennings. *Influence of Mixing Methods on the Microstructure and Rheological Behavior of Cement Paste*, Advance Cement Based Material 2, 1995, pp. 70-78.

32. ASTM C 191. *Standard Test Method For Time of Setting of Hydraulic Cement by Vicat Needle*, ASTM International, West Conshohocken, Pennsylvania, 2004, pp.181-187.

33. ASTM C 494. *Standard Specification for Chemical Admixtures for Concrete*, ASTM International, West Conshohocken, Pennsylvania, 2005, pp. 277-286.

34. Havard, J., and O.E. Gjoerv. *Effect of Gypsum-Hemihydrate Ratio in Cement on Rheological Properties of Fresh Concrete*, ACI Materials, Vol. 94, I2, 1997.

APPENDIX A:

CEMENT PASTE RHEOLOGY DATA

FROM PRELIMINARY TESTS

Table A.1. Rheological Parameters and Coefficient of Variation from DSR (Bohlin).

Experimental Design #	Test No.	Plastic Viscosity	Plastic Viscosity Average	CV(%)	Yield Stress	Yield Stress Average	CV(%)
(P1) 0.2%D17 Gap:0.2mm	1	0.541			168.85		
	2	0.9593	0.8879	35.73	273.4	264.88	34.76
	3	1.1633			352.38		
(P2) 0.5%D17 Gap:0.2mm	1	0.6402			141.17		
	2	0.8029	0.6901	14.18	138.84	124.27	21.96
	3	0.6273			92.79		
(P3) 1%D17 Gap:0.2mm	1	0.6608			100.94		
	2	0.6888	0.6401	9.65	104.96	90.44	24.06
	3	0.5706			65.423		
(P1) 0.2%D17 Gap:0.5mm	1	0.5694			396.22		
	2	0.6367	0.5002	36.26	358.21	398.78	10.51
	3	0.2944			441.91		
(P2) 0.5%D17 Gap:0.5mm	1	0.3478			88.832		
	2	0.2963	0.3221	8.00	52.838	71.59	25.21
	3	0.3221			73.085		
(P3) 1%D17 Gap:0.5mm	1	0.2112			24.505		
	2	0.2106	0.2186	6.13	22.595	24.61	8.39
	3	0.2341			26.72		
(P1) 0.2%D17 Gap:1mm	1	0.3432			289.4		
	2	0.409	0.3640	10.72	350.44	324.13	9.68
	3	0.3398			332.54		
(P2) 0.5%D17 Gap:1mm	1	0.1931			58.476		
	2	0.1857	0.1925	3.36	56.227	58.29	3.39
	3	0.1986			60.163		
(P3) 1%D17 Gap:1mm	1	0.0853			17.13		
	2	0.0821	0.0845	2.50	16.402	18.79	18.77
	3	0.0861			22.844		
(P1) 0.2%D17 Gap:1.2mm	1	0.1489			47.106		
	2	0.2079	0.1767	16.78	62.284	52.56	16.07
	3	0.1732			48.277		
(P2) 0.5%D17 Gap:1.2mm	1	0.1486			47.142		
	2	0.1367	0.1496	8.98	32.37	42.79	21.18
	3	0.1635			48.857		
(P3) 1%D17 Gap:1.2mm	1	0.0978			2.2917		
	2	0.1202	0.1255	24.42	2.9786	3.15	30.36
	3	0.1584			4.1811		
(P1) 0.2%D17 Gap:1.5mm	1	0.1383			16.65		
	2	0.1584	0.1454	7.77	14.181	15.50	8.02
	3	0.1394			15.679		
(P2) 0.5%D17 Gap:1.5mm	1	0.1145			11.821		
	2	0.1202	0.1139	5.81	12.978	11.82	9.85
	3	0.107			10.651		
(P3) 1%D17 Gap:1.5mm	1	0.089			4.19		
	2	0.0978	0.0902	7.90	2.2917	3.47	29.70
	3	0.0837			3.942		

Table A.2. Rheological Parameters and Coefficient of Variation from AR 2000.

Experimental Design #	Test No.	Plastic Viscosity	Plastic Viscosity Average	CV(%)	Yield Stress	Yield Stress Average	CV(%)
(P1) 0.2%D17 G:0.2mm	1	1.2573	1.1724	17.76	399.88	355.64	33.20
	2	0.9352			221.85		
	3	1.3247			445.2		
(P2) 0.5%D17 G:0.2mm	1	0.9311	0.8690	22.30	155.88	135.49	50.55
	2	1.0242			191.47		
	3	0.6518			59.12		
(P3) 1%D17 G:0.2mm	1	0.9227	0.7947	16.26	110.03	80.93	32.24
	2	0.7971			73.143		
	3	0.6643			59.619		
(P1) 0.2%D17 G:0.5mm	1	0.9352	0.9743	20.34	271.85	280.65	18.08
	2	1.1891			335.21		
	3	0.7985			234.89		
(P2) 0.5%D17 G:0.5mm	1	0.683	0.8001	13.59	87.809	117.11	21.88
	2	0.8196			135.37		
	3	0.8978			128.14		
(P3) 1%D17 G:0.5mm	1	0.5978	0.5367	12.49	54.875	46.69	16.71
	2	0.465			39.334		
	3	0.5474			45.87		
(P1) 0.2%D17 G:1mm	1	0.4667	0.4780	2.61	159.22	162.77	2.30
	2	0.476			162.41		
	3	0.4914			166.69		
(P2) 0.5%D17 G:1mm	1	0.2545	0.2470	3.21	48.914	46.09	5.44
	2	0.2478			45.25		
	3	0.2387			44.12		
(P3) 1%D17 G:1mm	1	0.1798	0.1732	3.39	12.519	12.32	6.28
	2	0.1685			11.47		
	3	0.1714			12.98		
(P1) 0.2%D17 G:1.2mm	1	0.3543	0.3784	5.66	27.184	30.37	9.40
	2	0.3854			31.25		
	3	0.3954			32.69		
(P2) 0.5%D17 G:1.2mm	1	0.1921	0.1802	6.50	11.073	9.97	10.63
	2	0.1798			9.871		
	3	0.1687			8.96		
(P3) 1%D17 G:1.2mm	1	0.0925	0.0963	3.44	1.8743	1.53	25.11
	2	0.0976			1.1156		
	3	0.0987			1.589		
(P1) 0.2%D17 G:1.5mm	1	0.3188	0.3327	4.41	24.465	27.72	12.37
	2	0.348			27.404		
	3	0.3312			31.3		
(P2) 0.5%D17 G:1.5mm	1	0.1404	0.1432	1.99	14.957	14.94	1.01
	2	0.1461			15.076		
	3	0.1432			14.775		
(P3) 1%D17 G:1.5mm	1	0.0878	0.0877	0.75	1.0041	1.09	15.37
	2	0.087			1.2878		
	3	0.0883			0.9896		

APPENDIX B:

XRD PATTERNS FOR THE STUDIED

CEMENTS AND SCMS
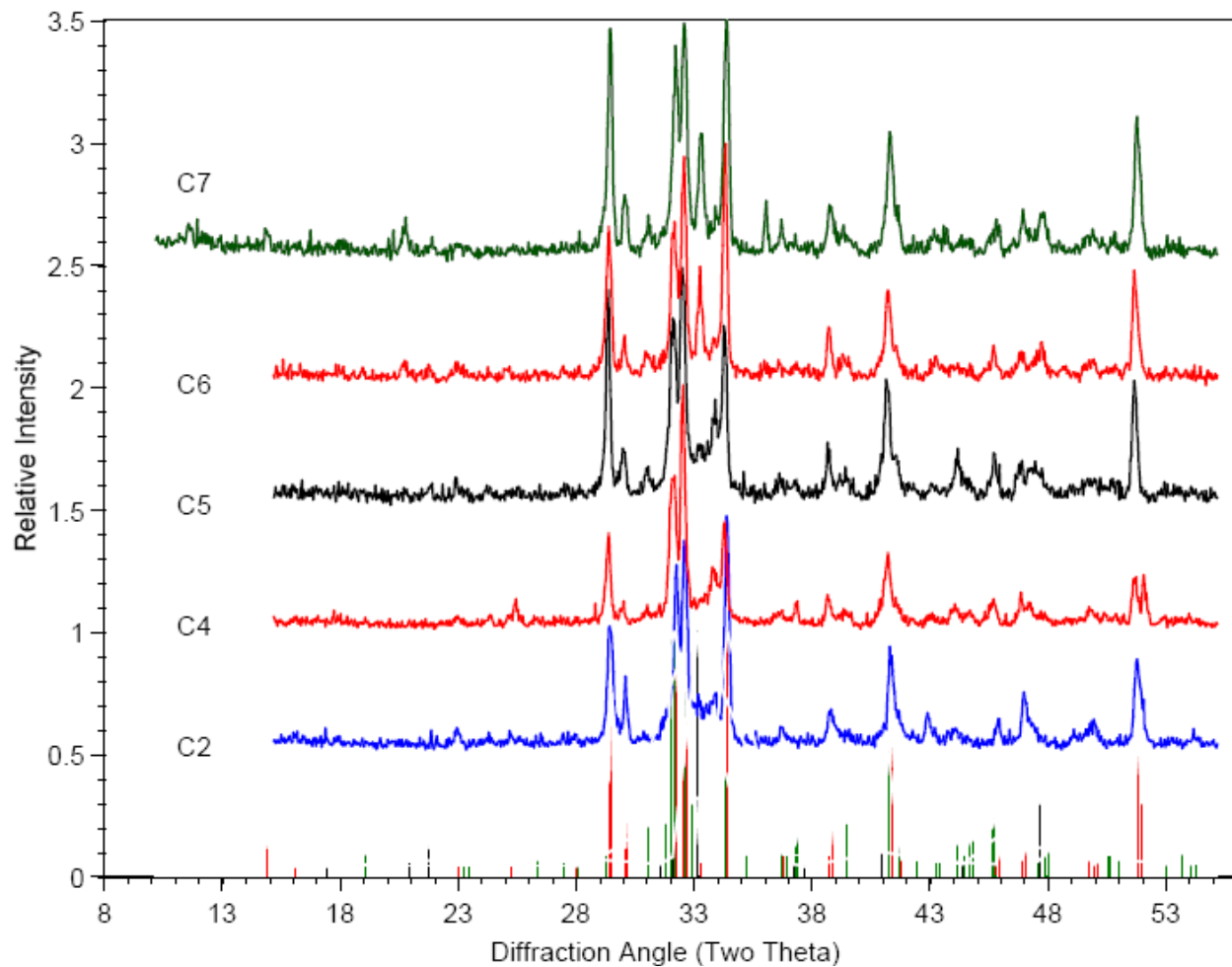
Figure B.1. XRD Patterns for Cement Samples with Stick Patterns for C_3S (red), C_2S (green), and C_3A (black).
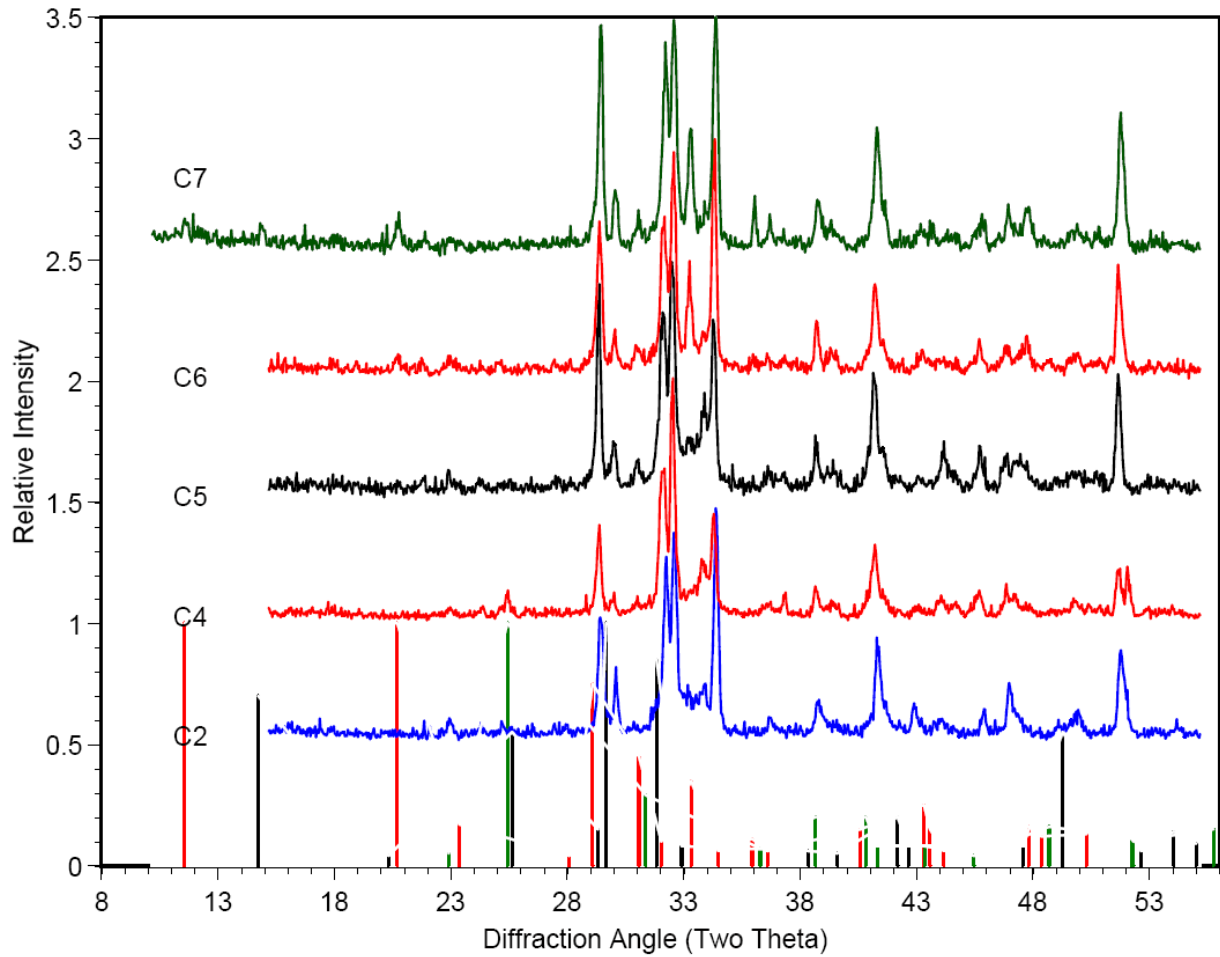
Figure B.2. XRD Patterns for Cement Samples with Stick Patterns for Gypsum (red), Anhydrite (green), and Bassanite (black).
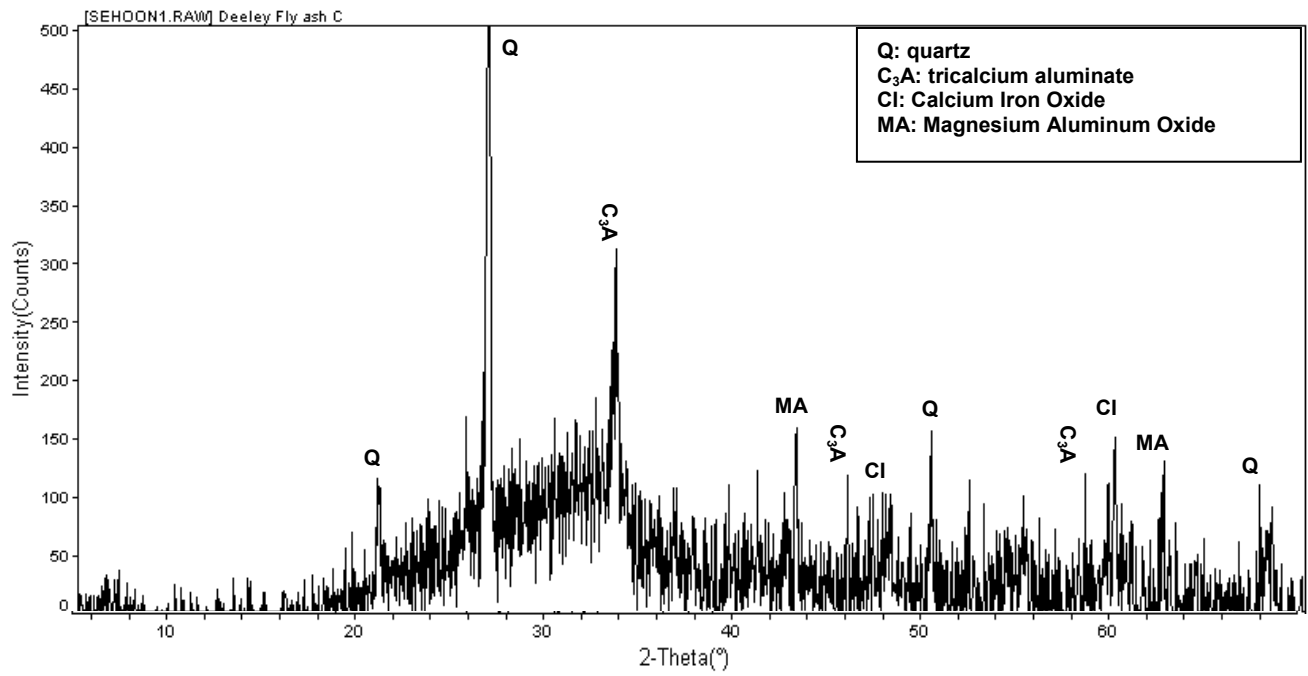
Figure B.3. XRD Pattern of Class C Fly Ash.
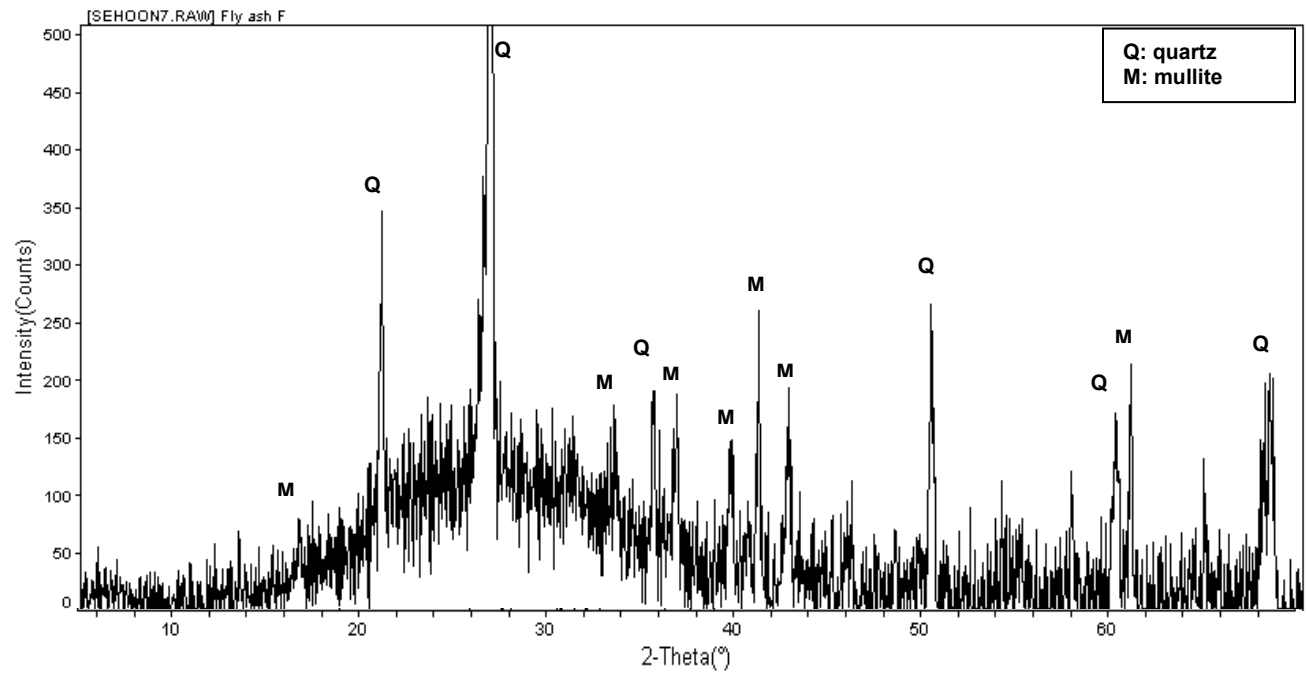
Figure B.4. XRD Pattern of Class F Fly Ash.

103
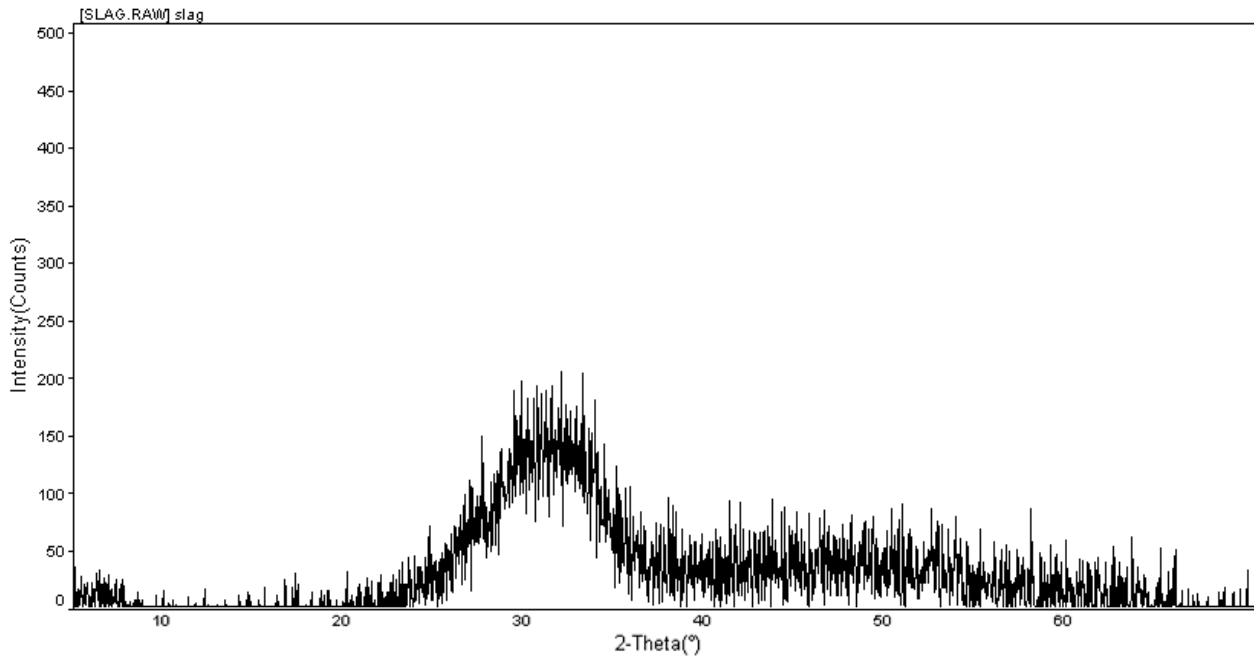
Figure B.5. XRD Pattern of Granulated Slag.

APPENDIX C:

HEAT OF HYDRATION FOR

THE STUDIED CEMENT PASTES
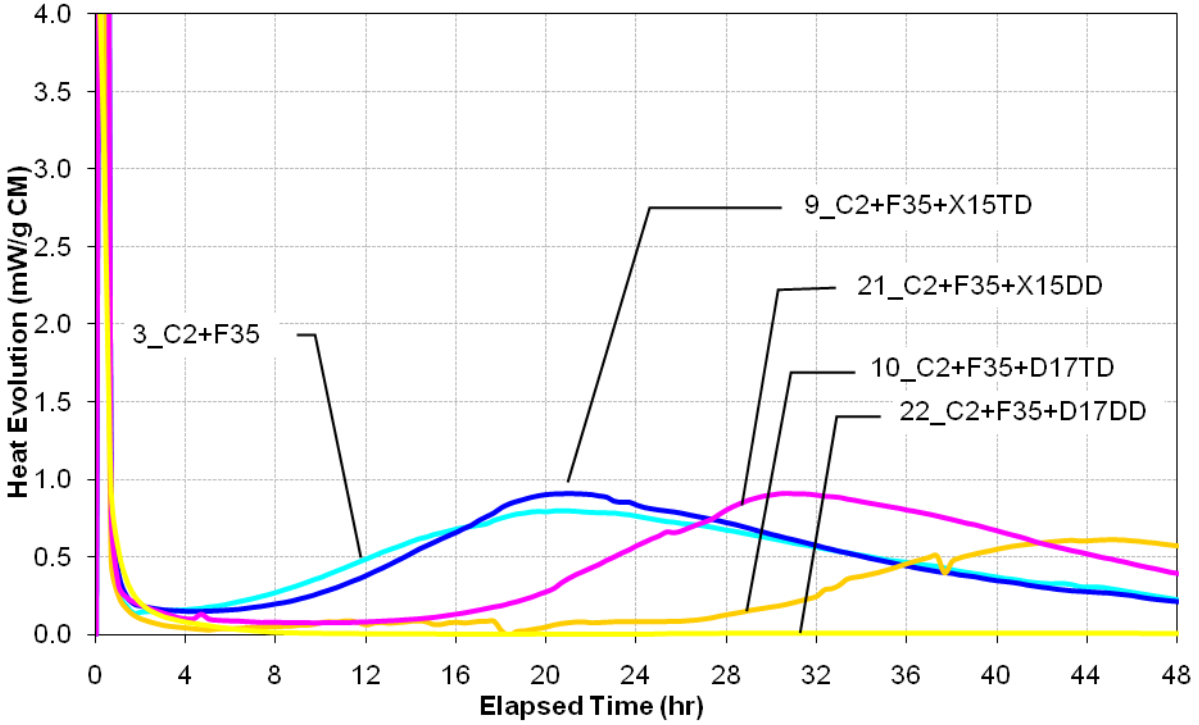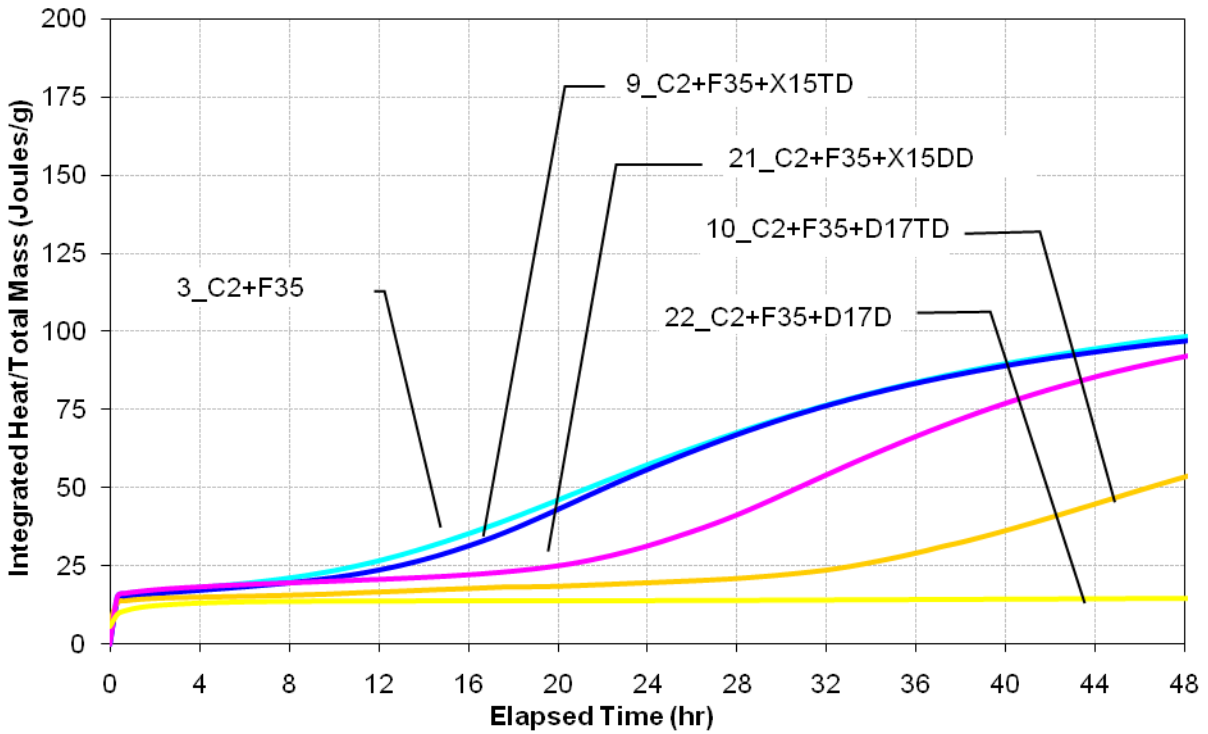
Figure C.1. Heat Evolution (Top) and Integrated Heat Evolution (Bottom) for Cement 2 with Class F Fly Ash System at 10°C.

107
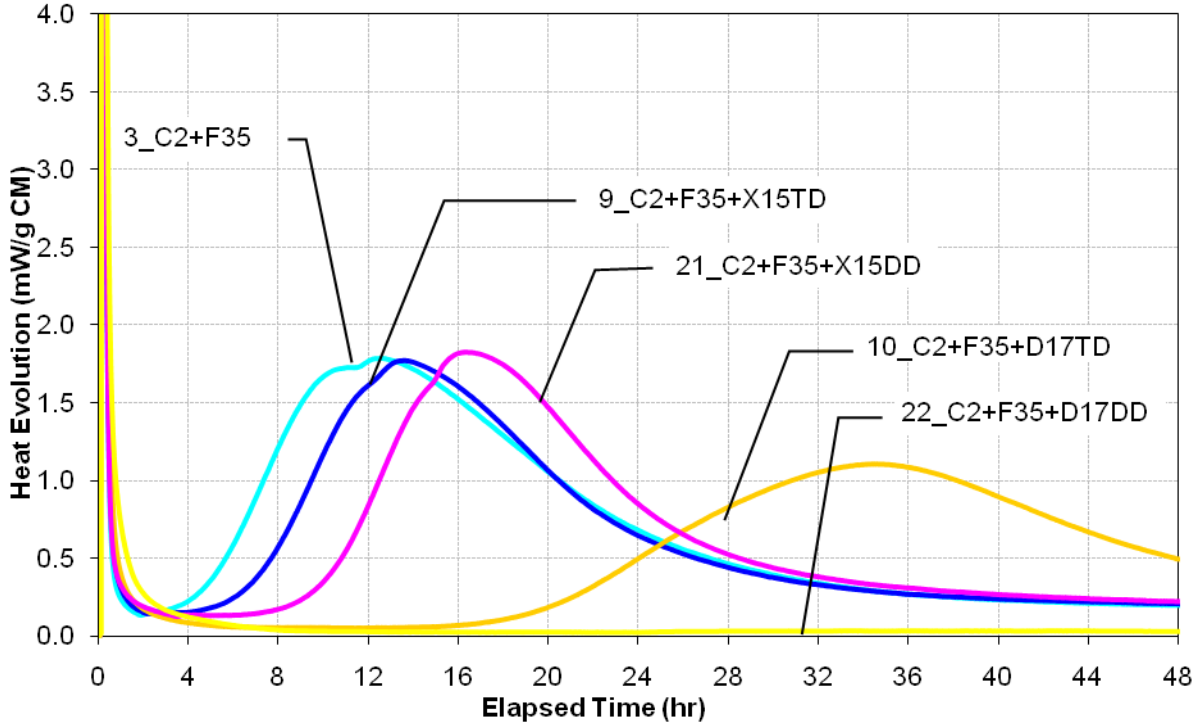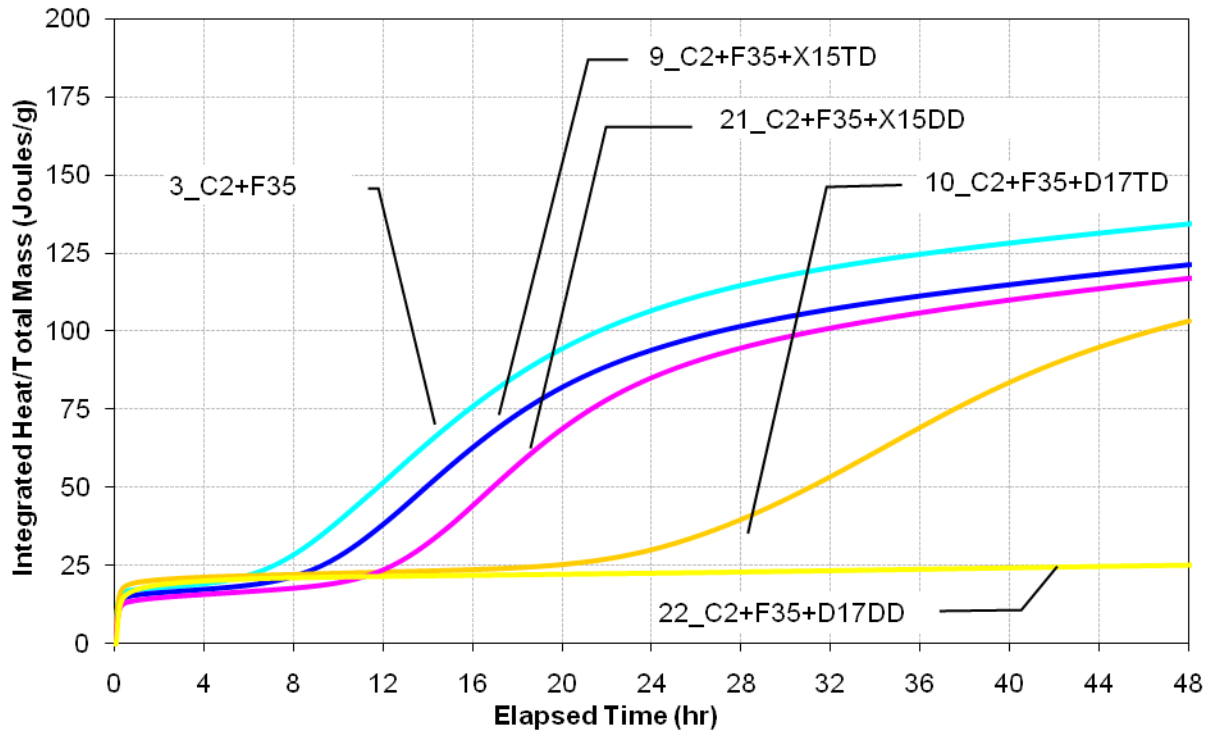
Figure C.2. Heat Evolution (Top) and Integrated Heat Evolution (Bottom) for Cement 2 with Class F Fly Ash System at 24°C.
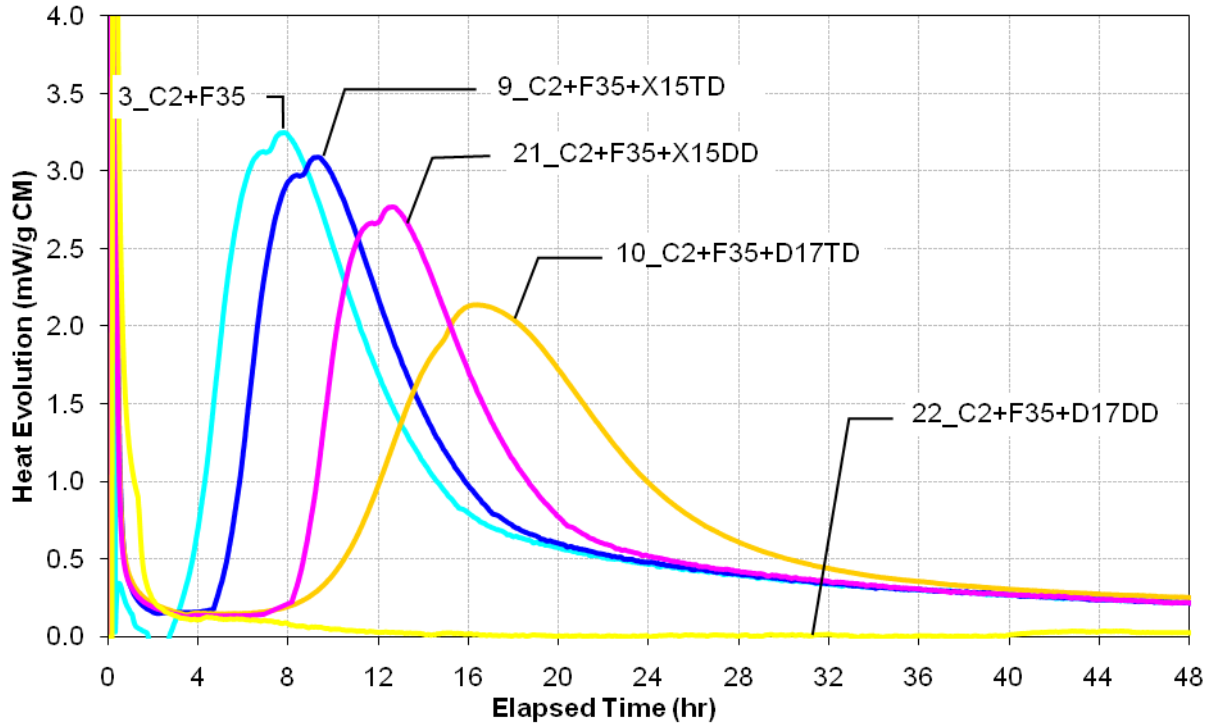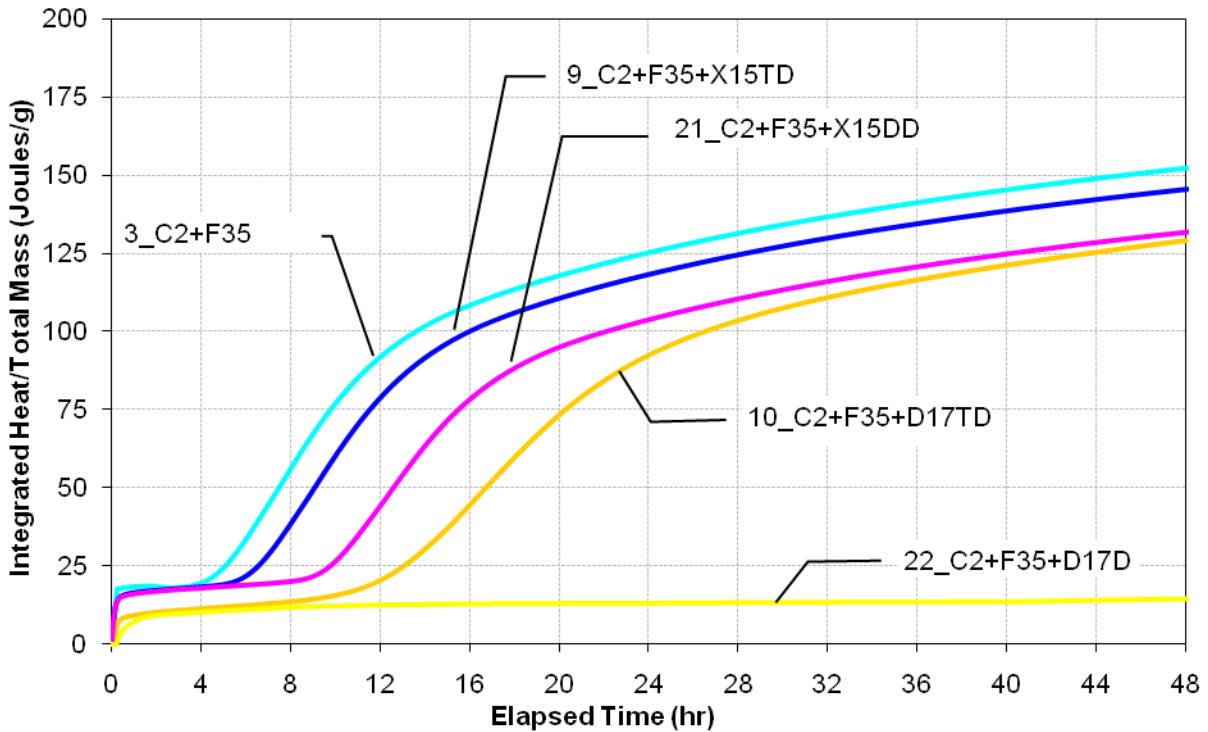
Figure C.3. Heat Evolution (Top) and Integrated Heat Evolution (Bottom) for Cement 2 with Class F Fly Ash System at 35°C.

109
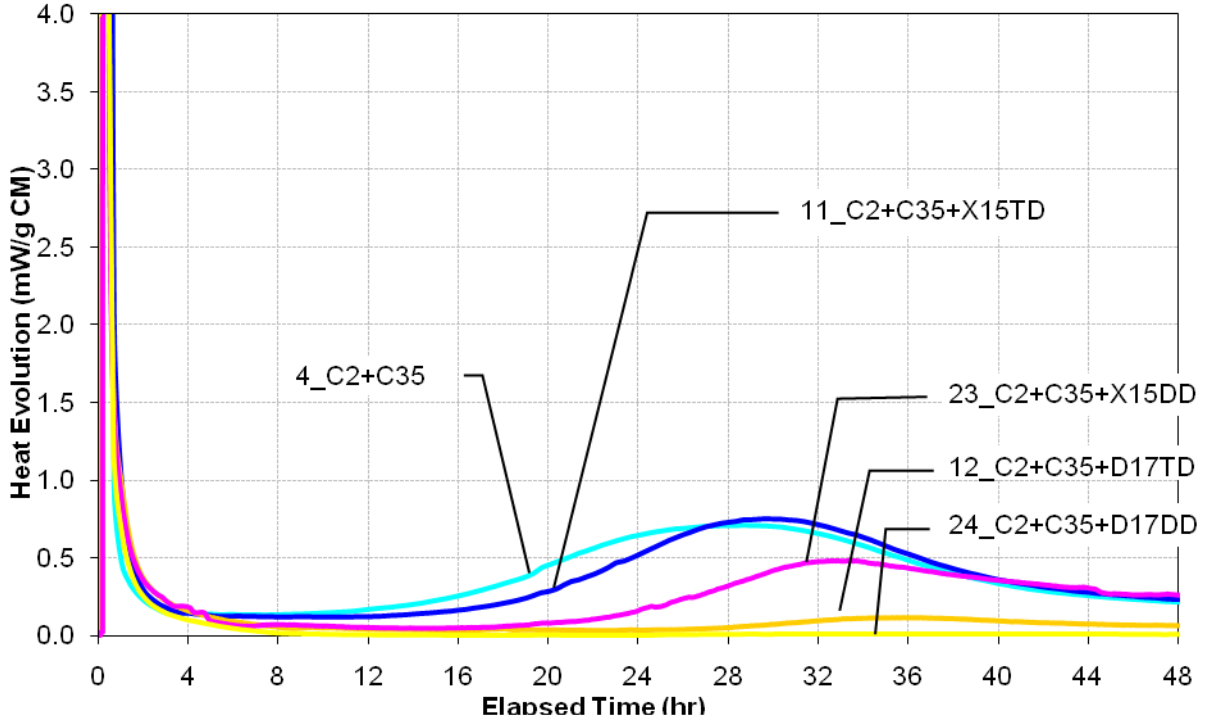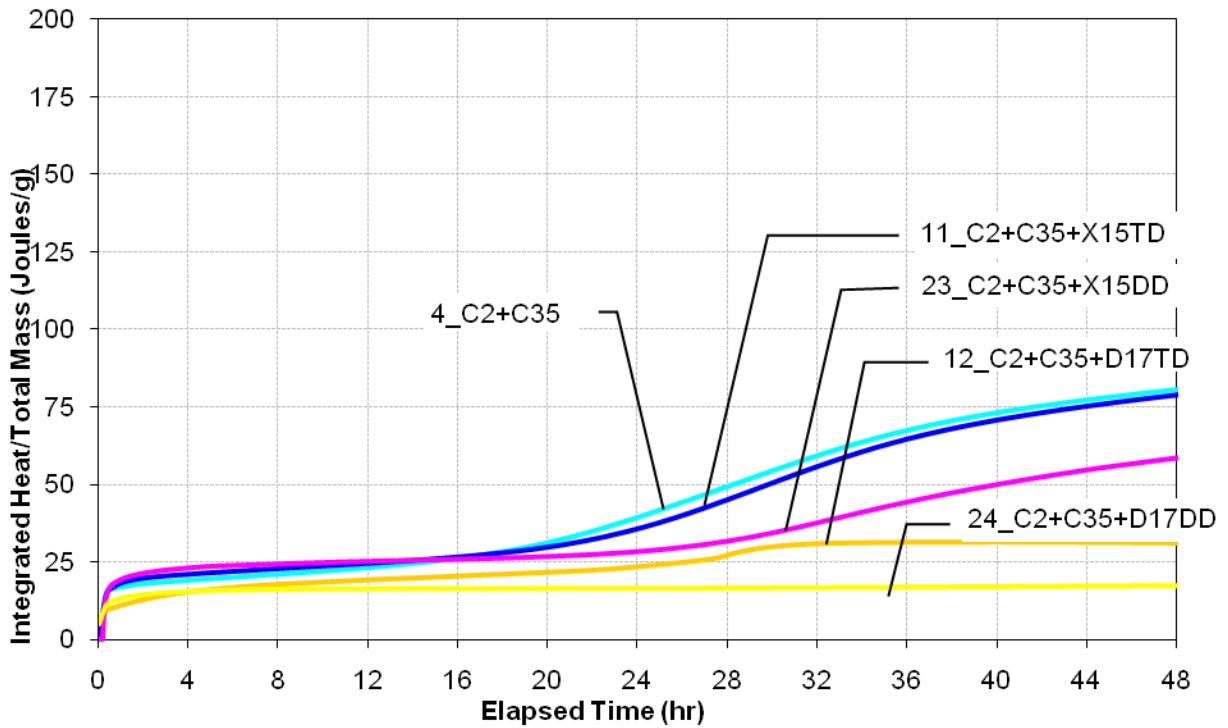
Figure C.4. Heat Evolution (Top) and Integrated Heat Evolution (Bottom) for Cement 2 with Class C Fly Ash System at 10°C.

110
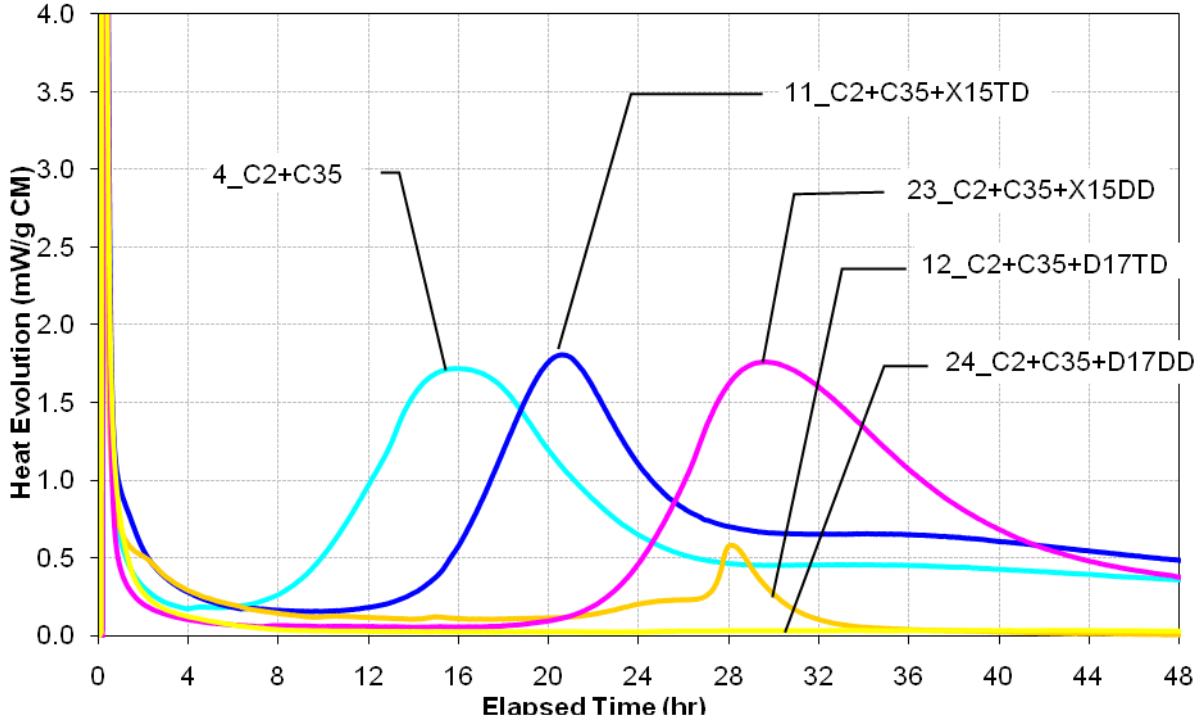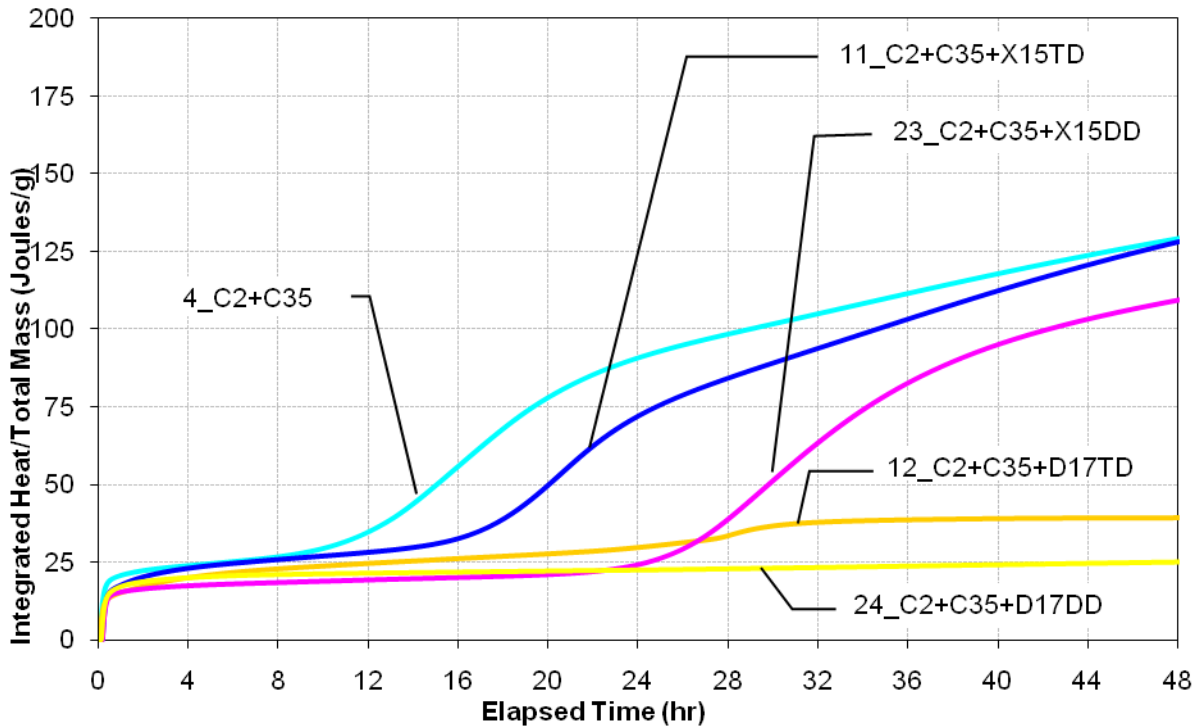
Figure C.5. Heat Evolution (Top) and Integrated Heat Evolution (Bottom) for Cement 2 with Class C Fly Ash System at 24°C.
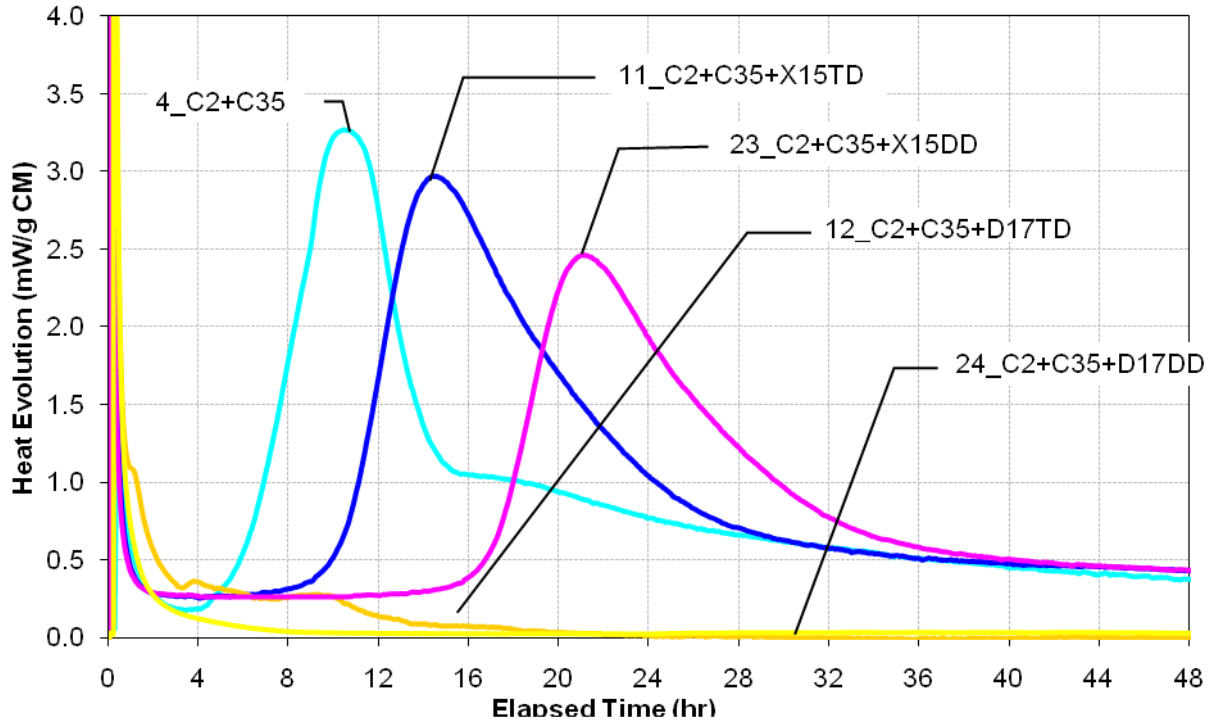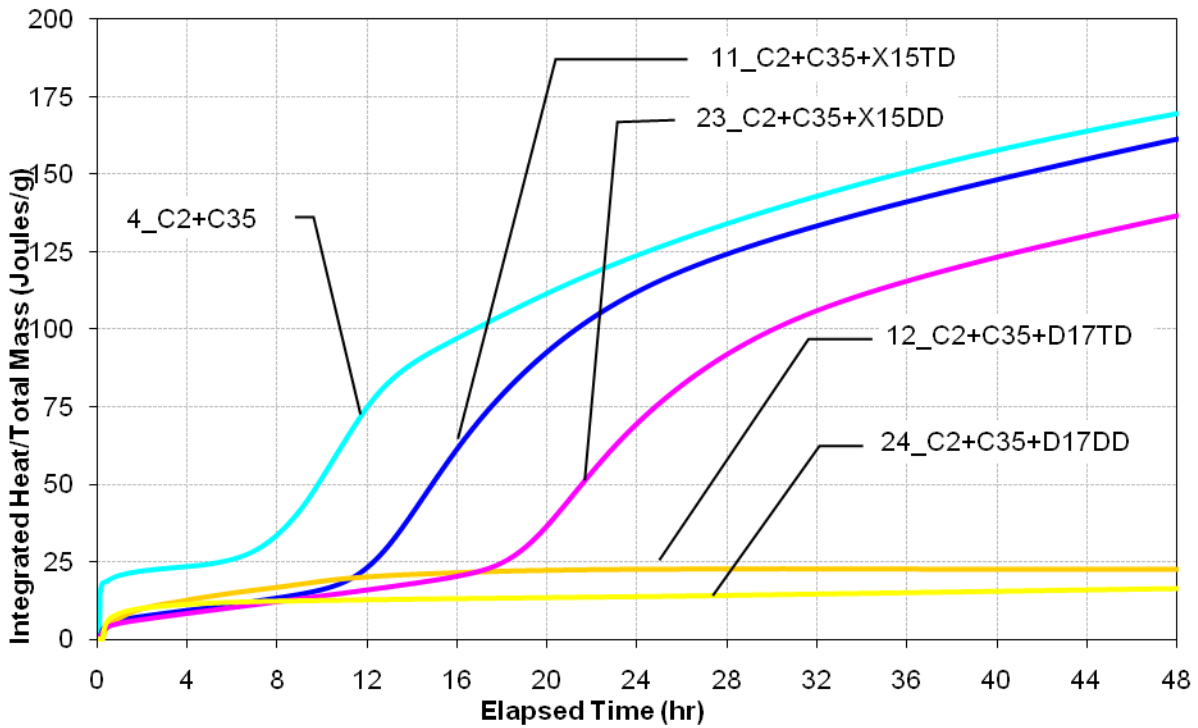
Figure C.6. Heat Evolution (Top) and Integrated Heat Evolution (Bottom) for Cement 2 with Class C Fly Ash System at 35°C.

112
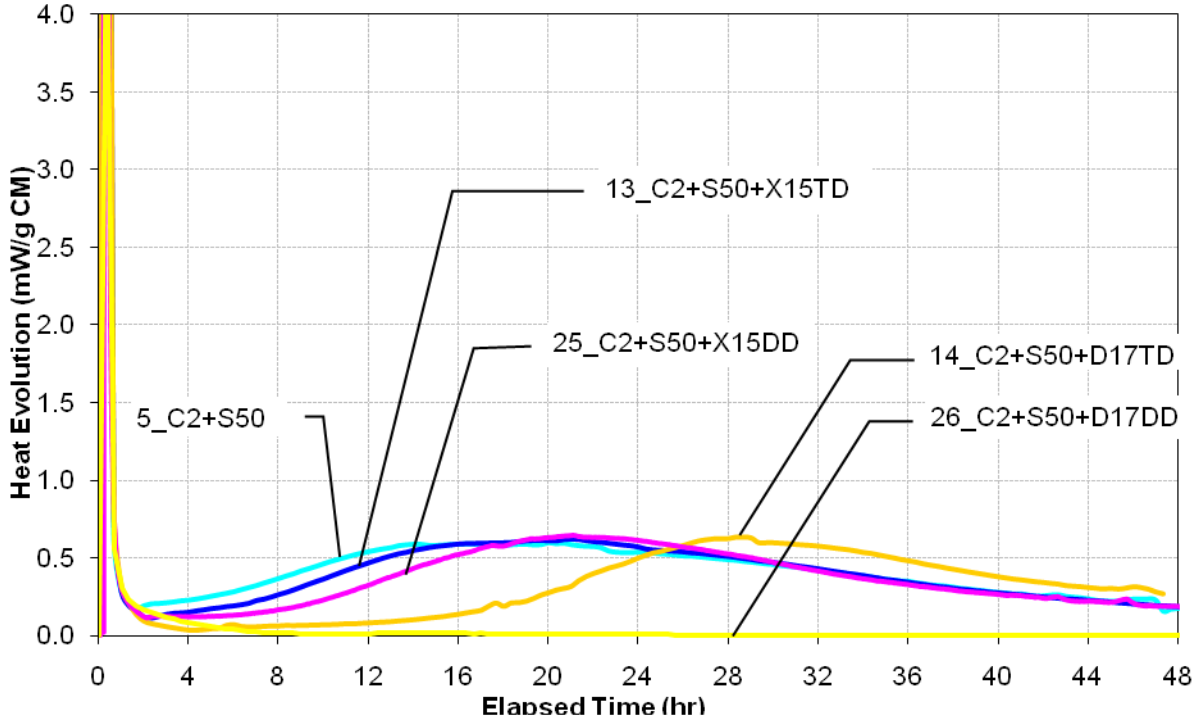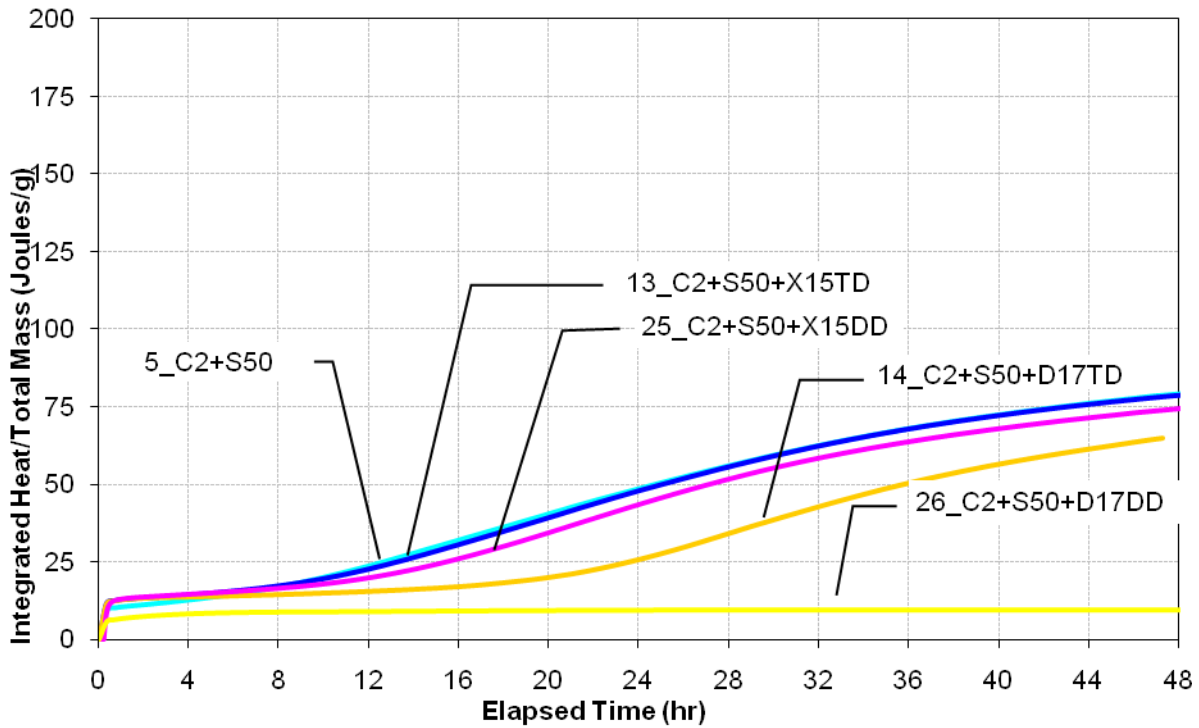
Figure C.7. Heat Evolution (Top) and Integrated Heat Evolution (Bottom) for Cement 2 with Slag System at 10°C.

113
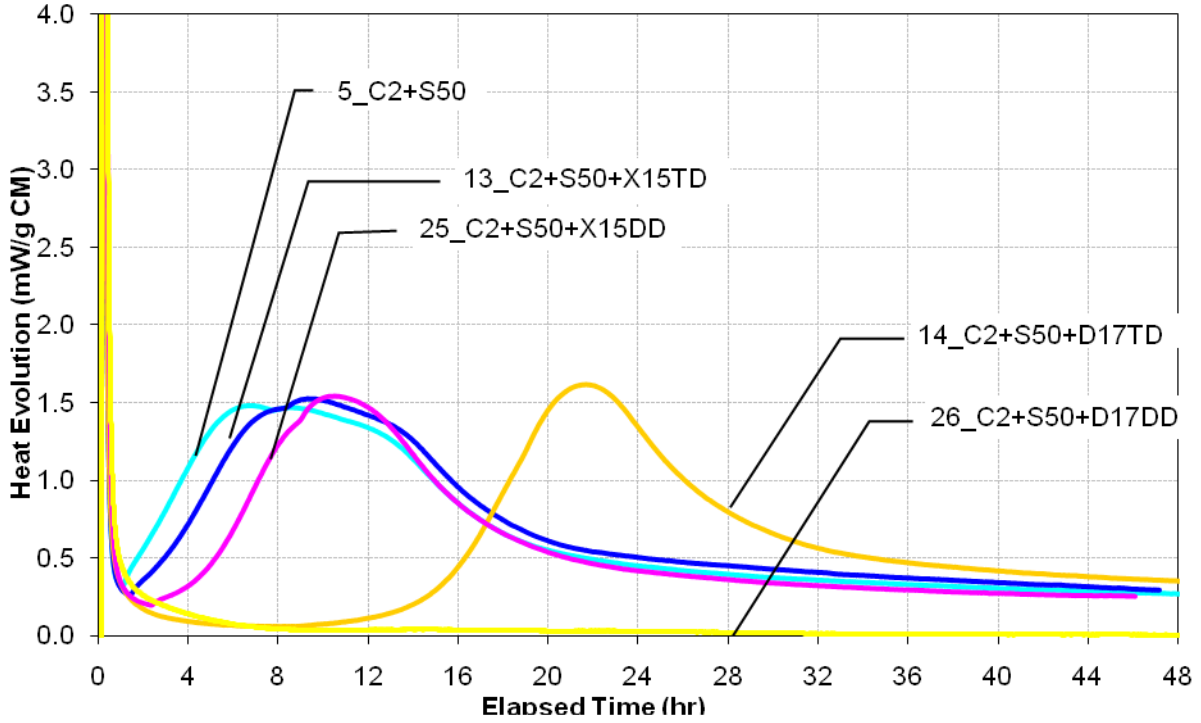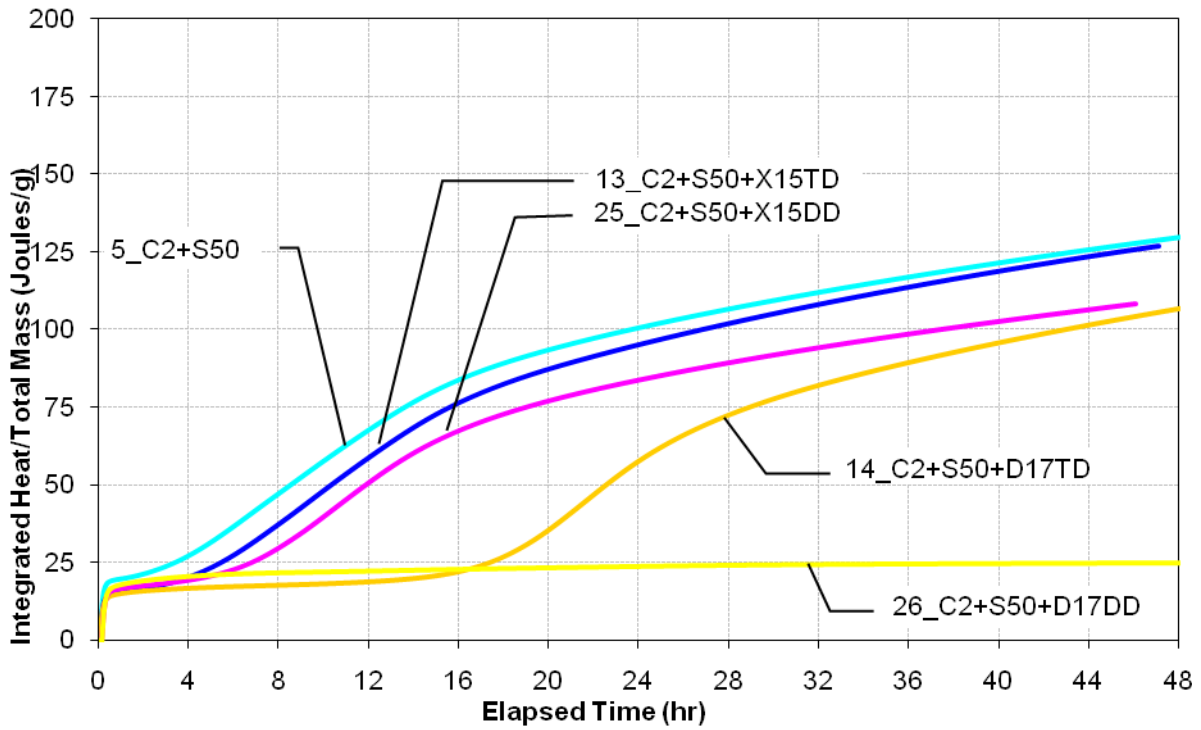
Figure C.8. Heat Evolution (Top) and Integrated Heat Evolution (Bottom) for Cement 2 with Slag System at 24°C.

114
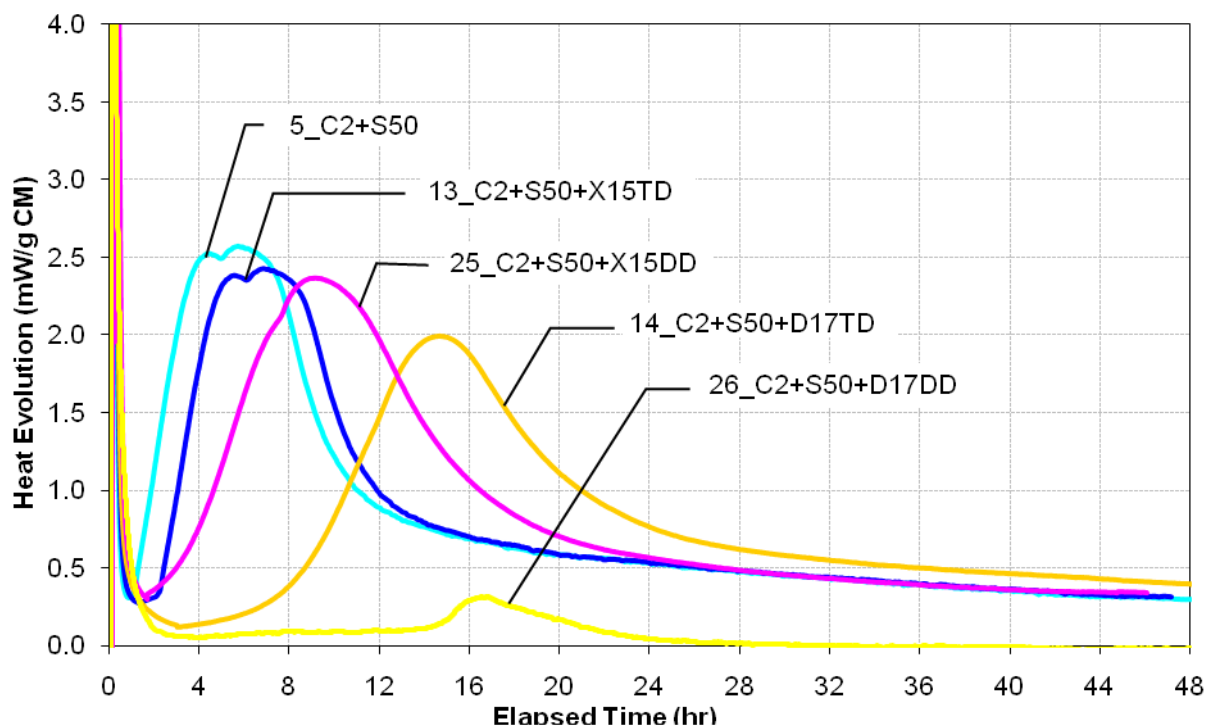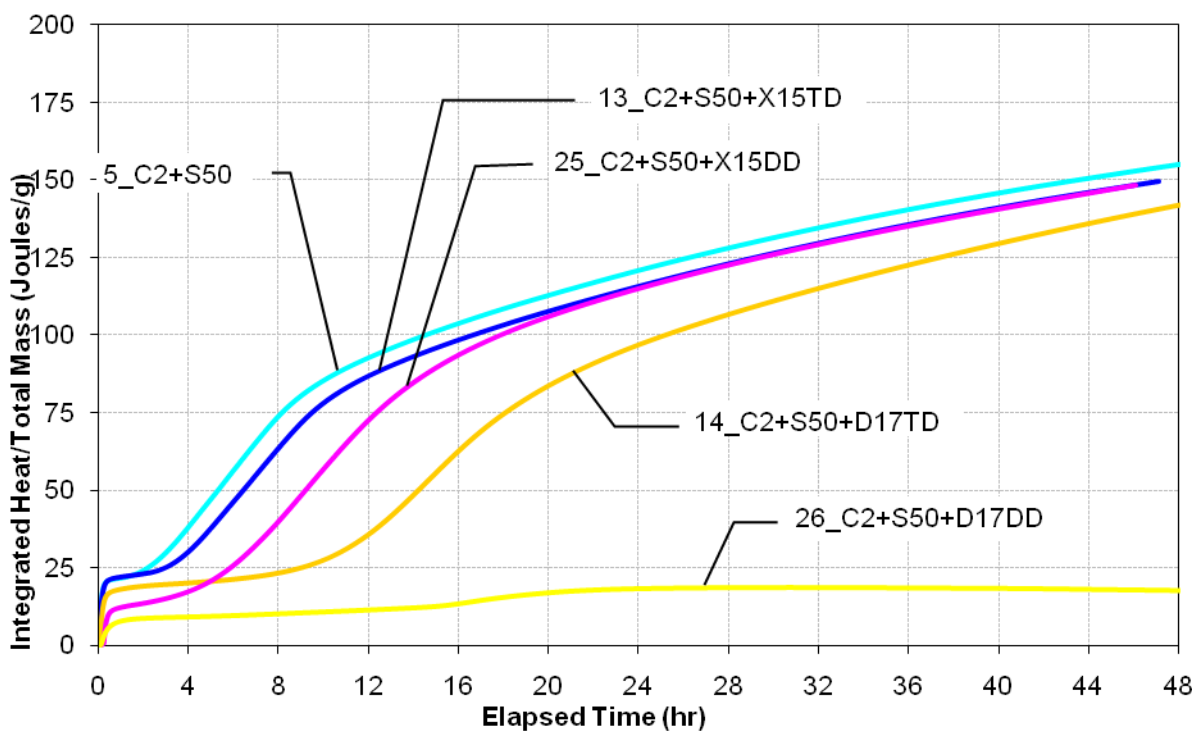
Figure C.9. Heat Evolution (Top) and Integrated Heat Evolution (Bottom) for Cement 2 with Slag System at 35°C.
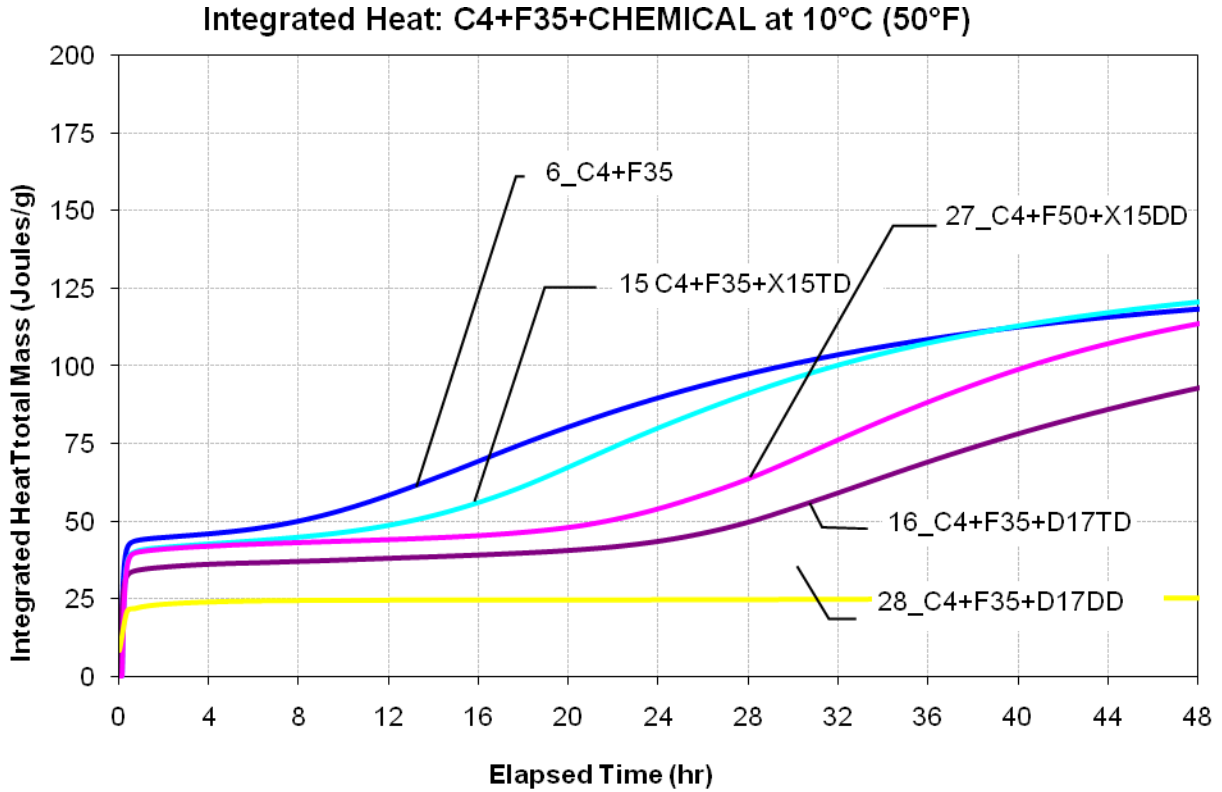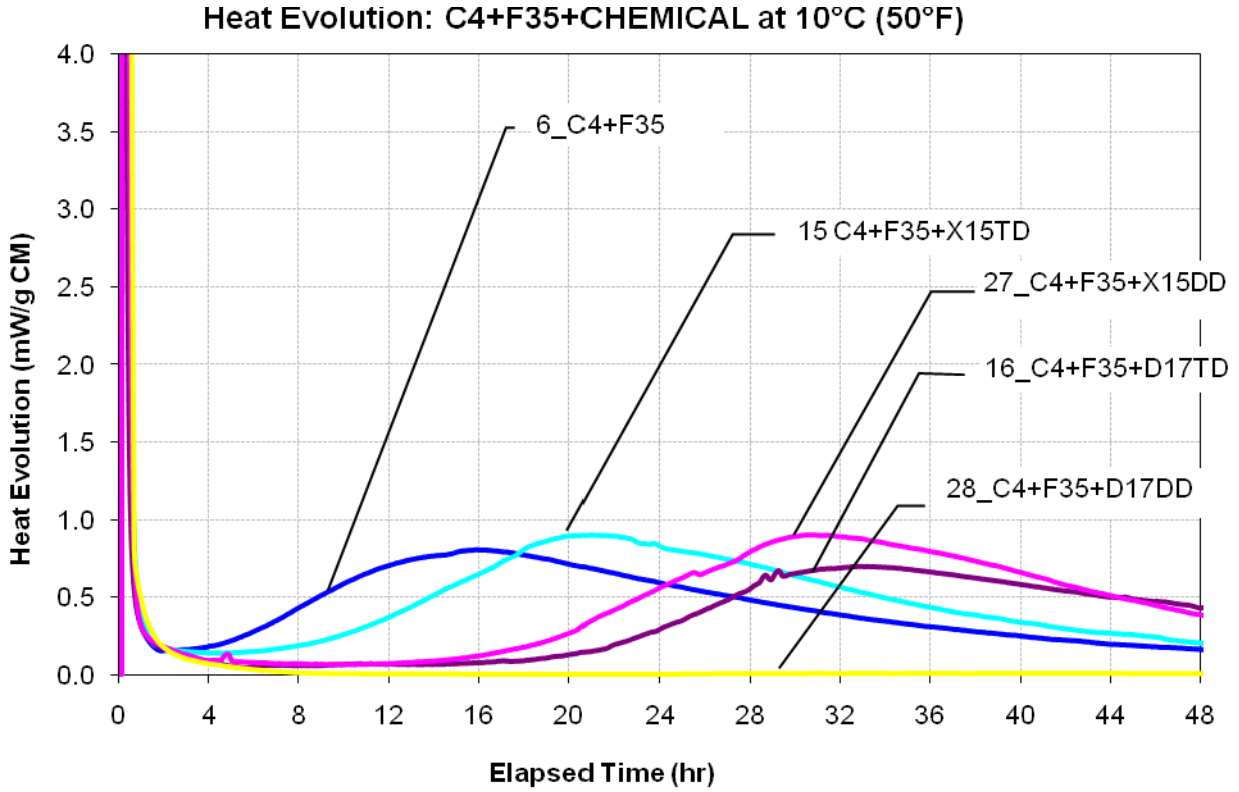
Figure C.10. Heat Evolution (Top) and Integrated Heat Evolution (Bottom) for Cement 4 with Class F Fly Ash System at 10°C.
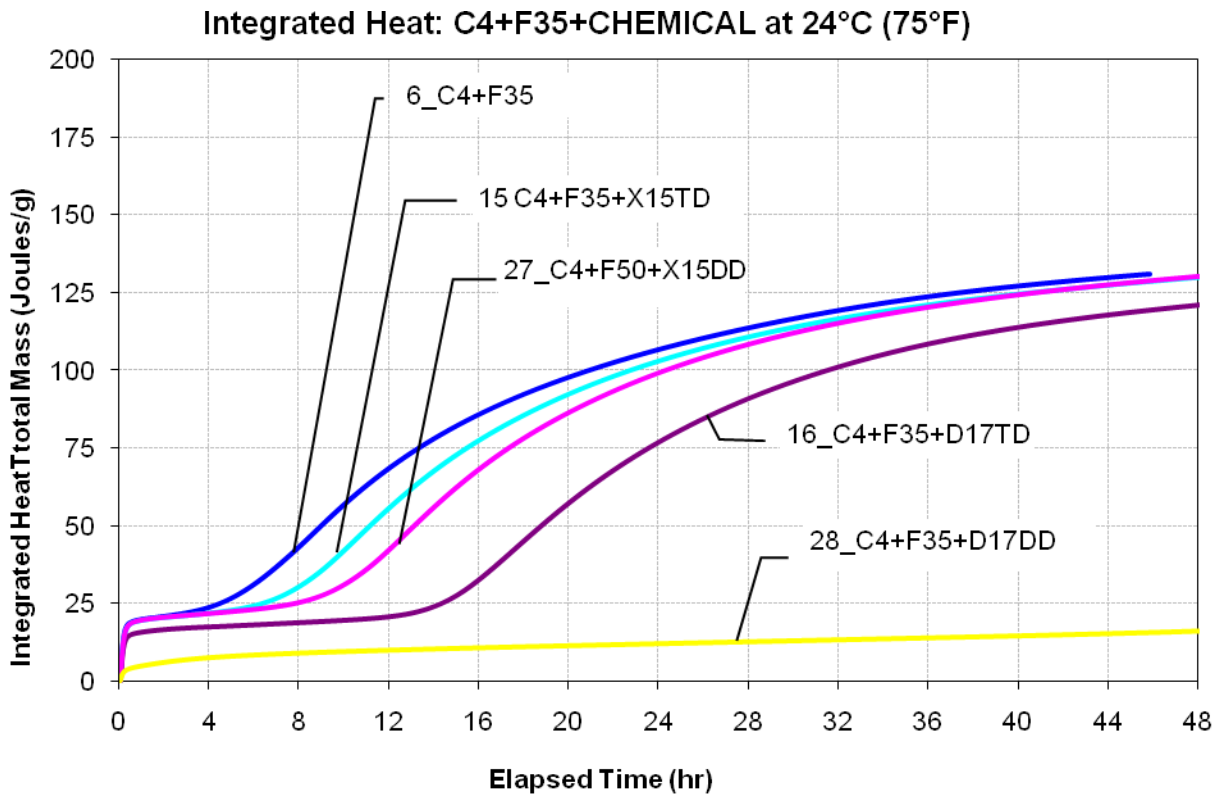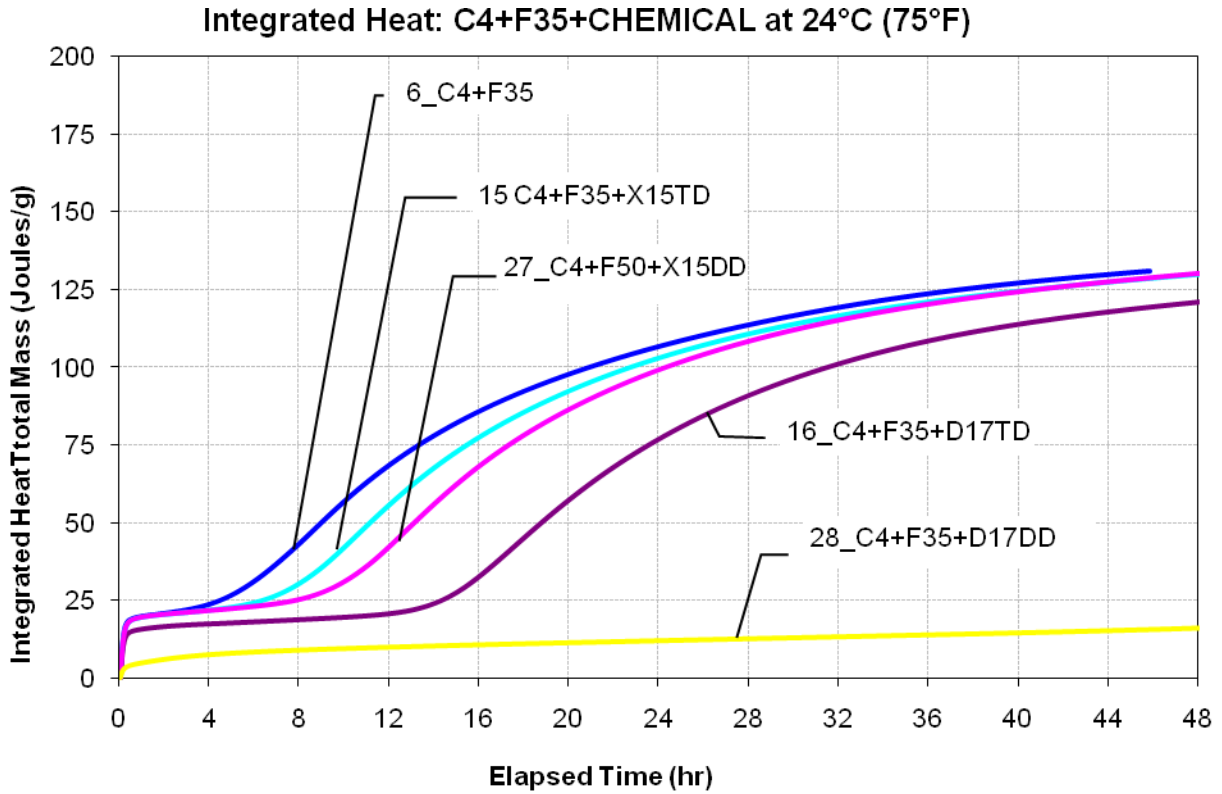
Figure C.11. Heat Evolution (Top) and Integrated Heat Evolution (Bottom) for Cement 4 with Class F Fly Ash System at 24°C.
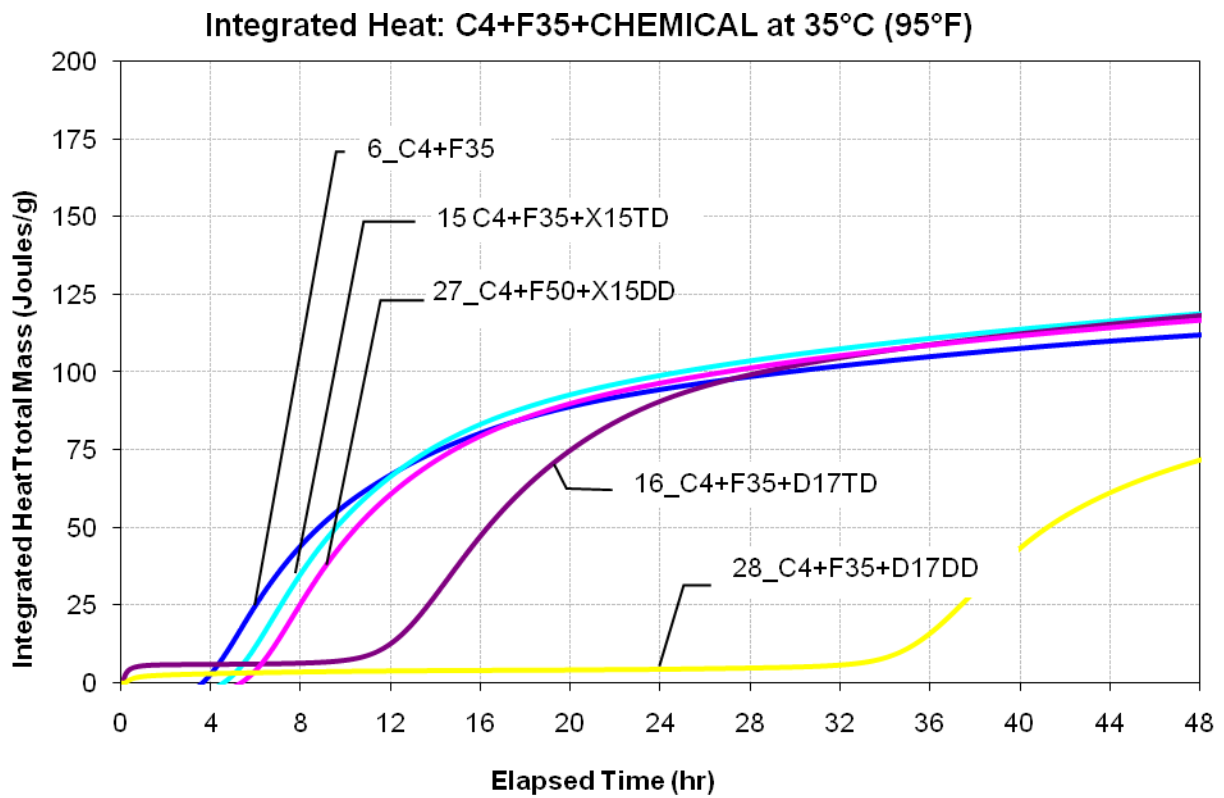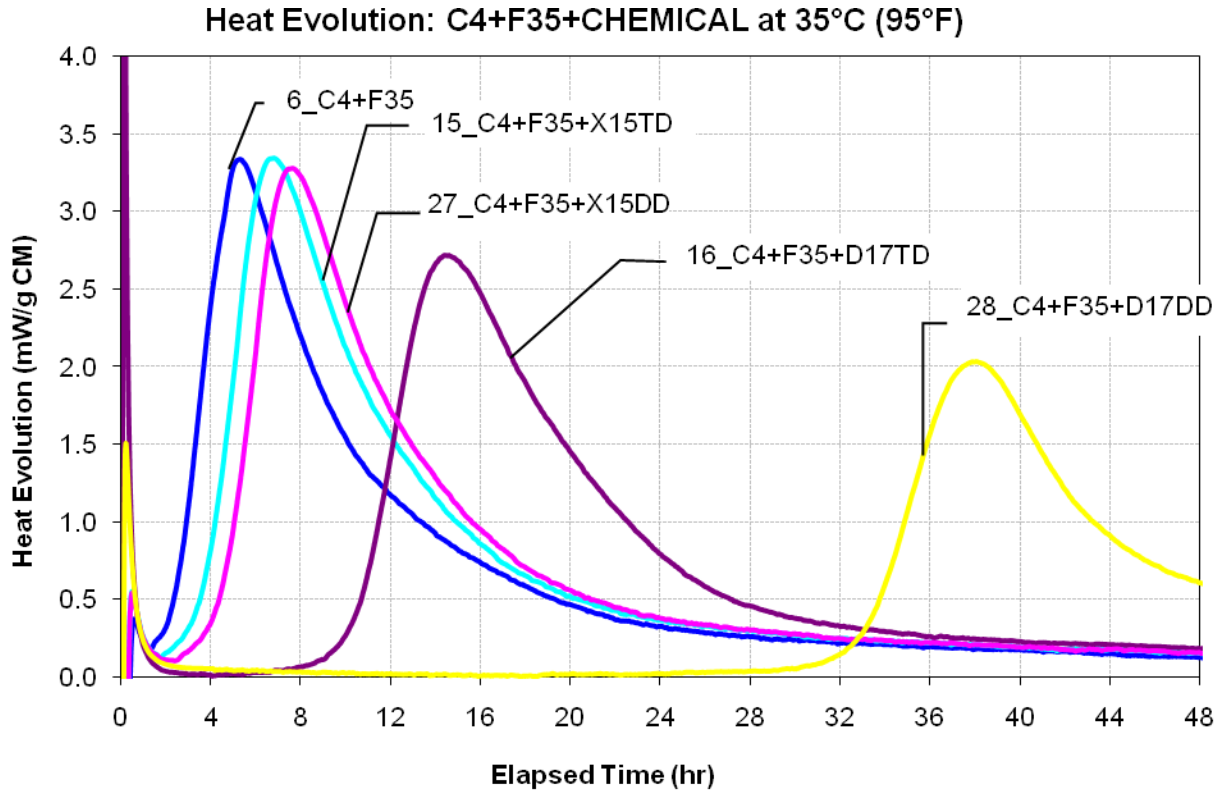
Figure C.12. Heat Evolution (Top) and Integrated Heat Evolution (Bottom) for Cement 4 with Class F Fly Ash System at 35°C.
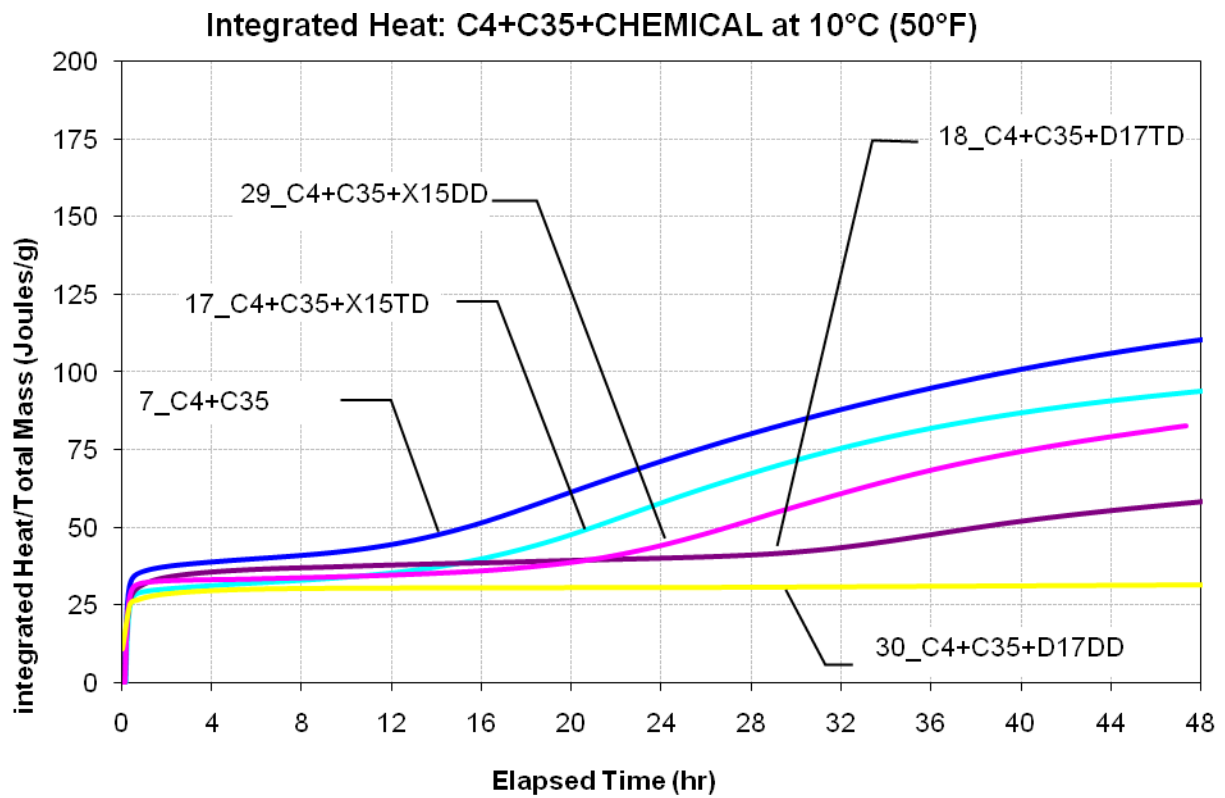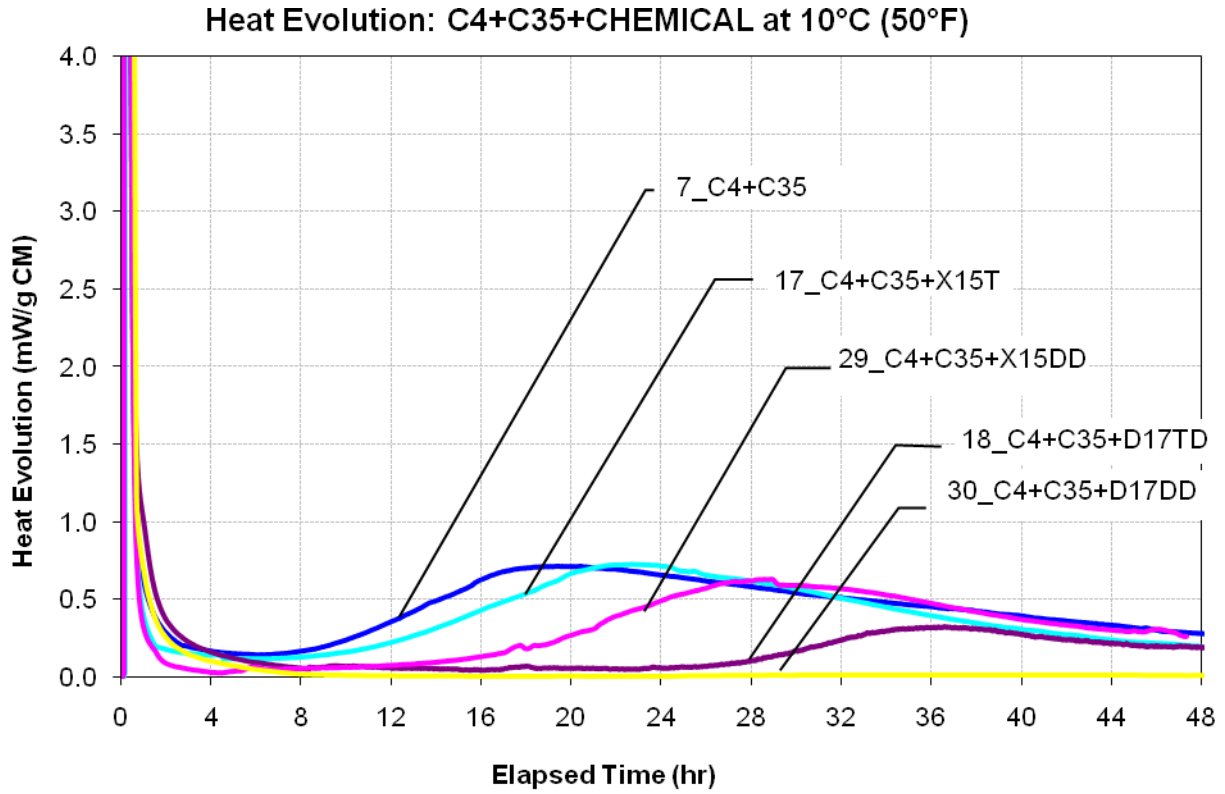
Figure C.13. Heat Evolution (Top) and Integrated Heat Evolution (Bottom) for Cement 4 with Class C Fly Ash System at 10°C.

119
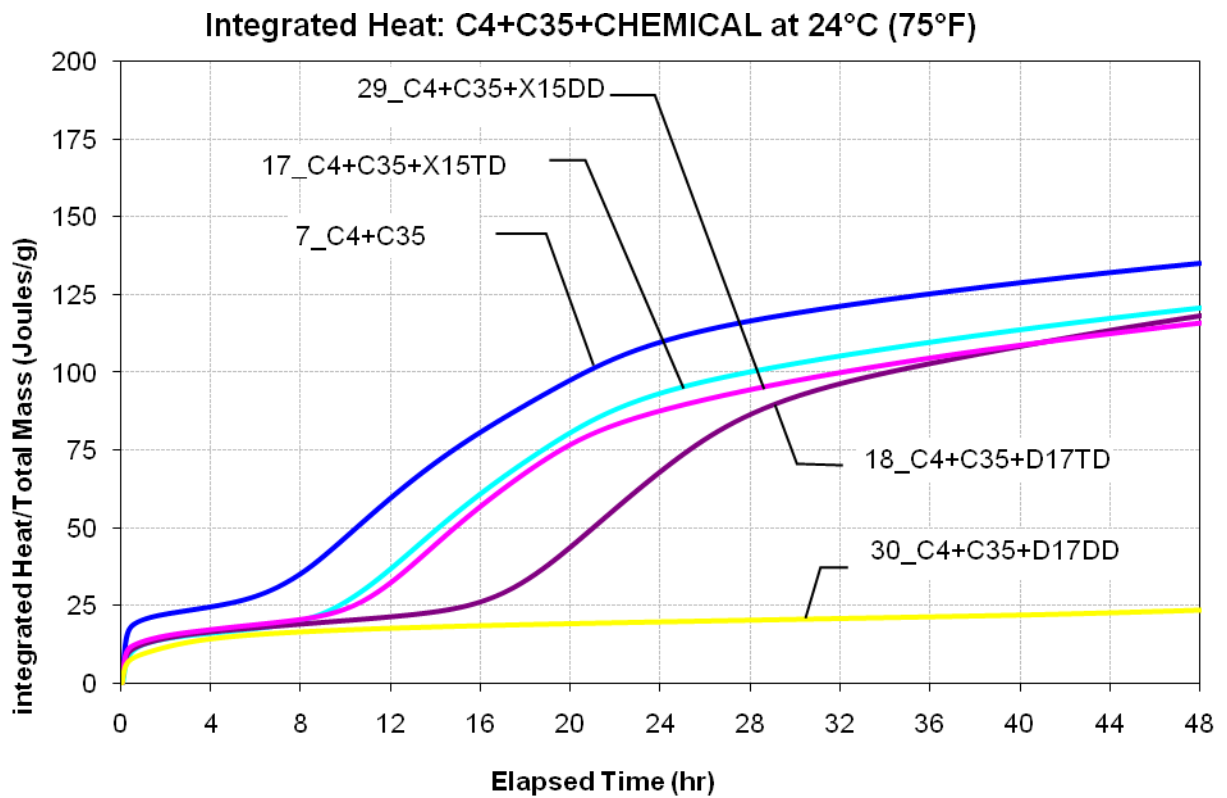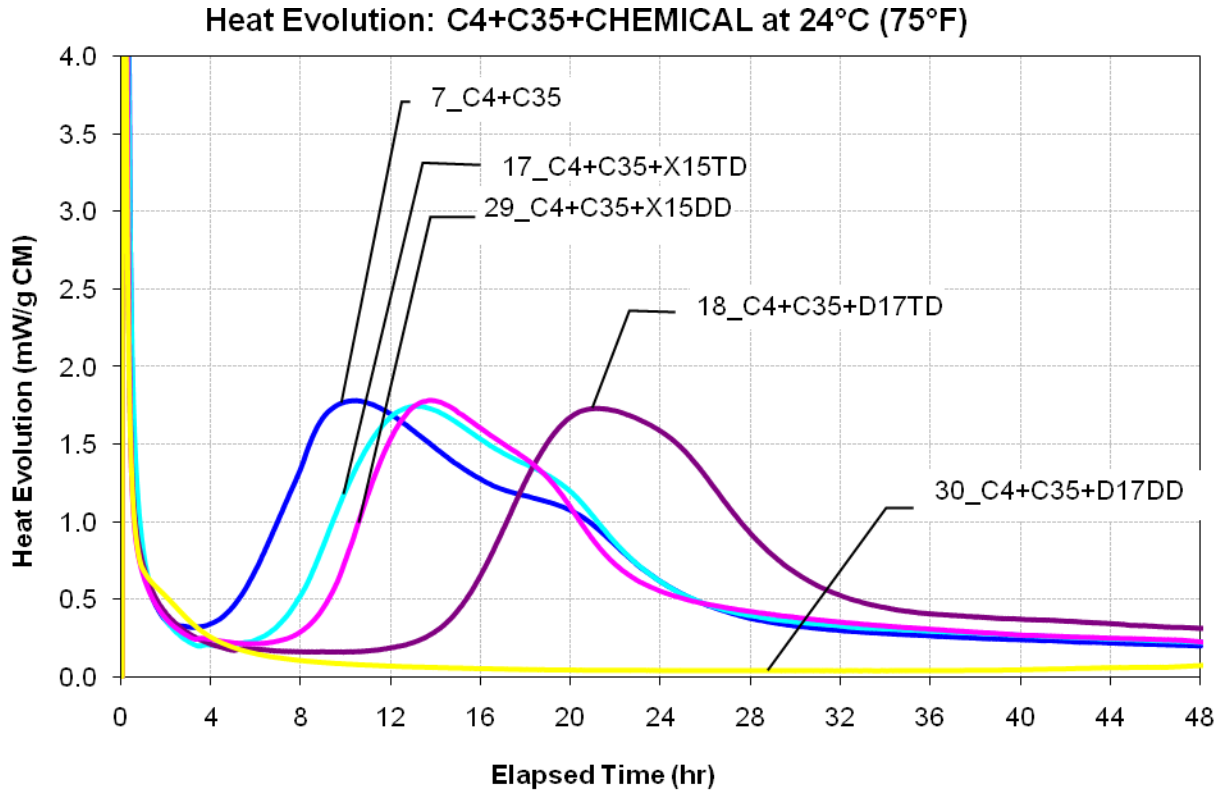
Figure C.14. Heat Evolution (Top) and Integrated Heat Evolution (Bottom) for Cement 4 with Class C Fly Ash System at 24°C.
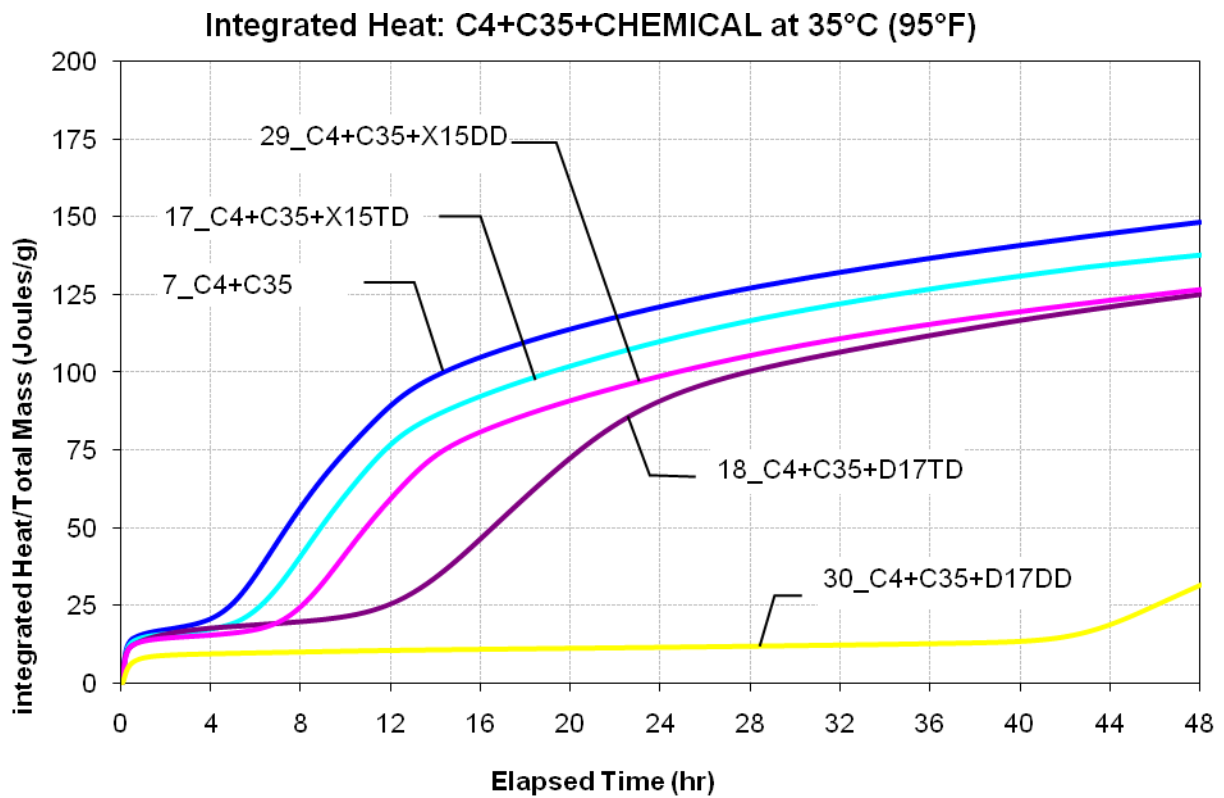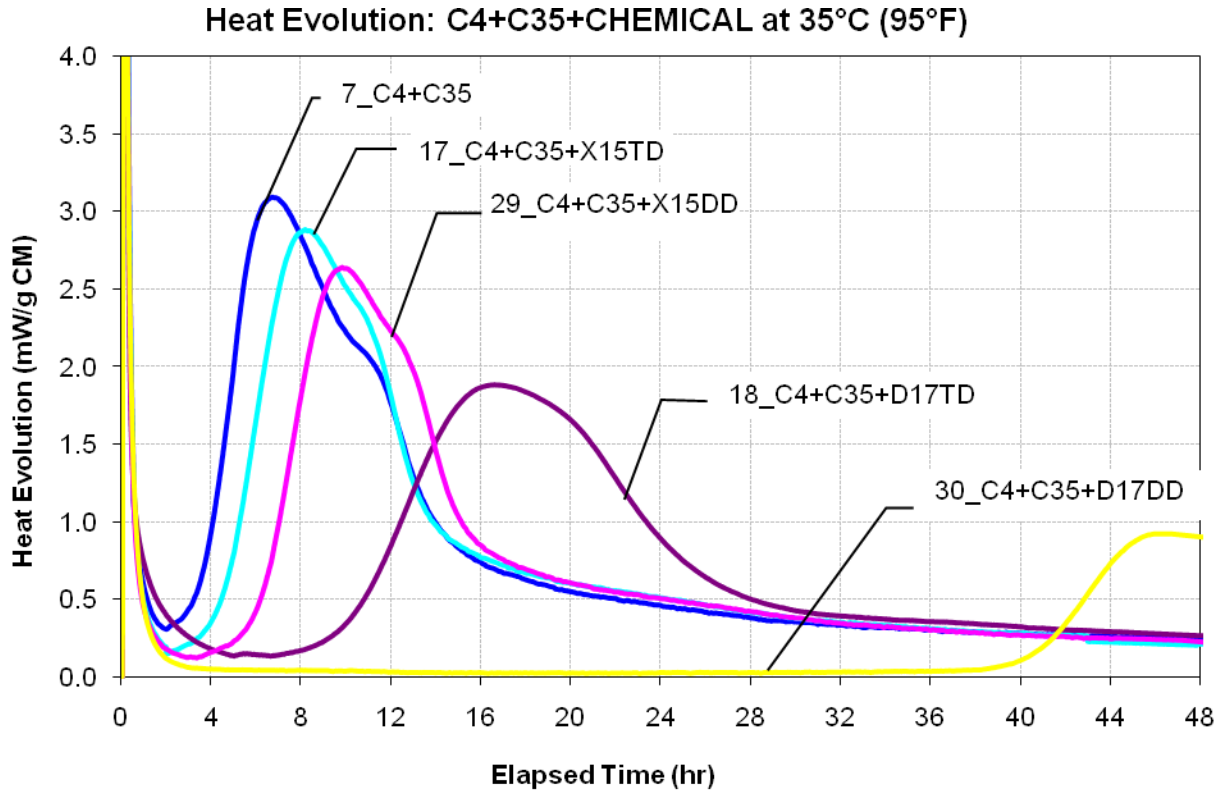
Figure C.15. Heat Evolution (Top) and Integrated Heat Evolution (Bottom) for Cement 4 with Class C Fly Ash System at 35°C.
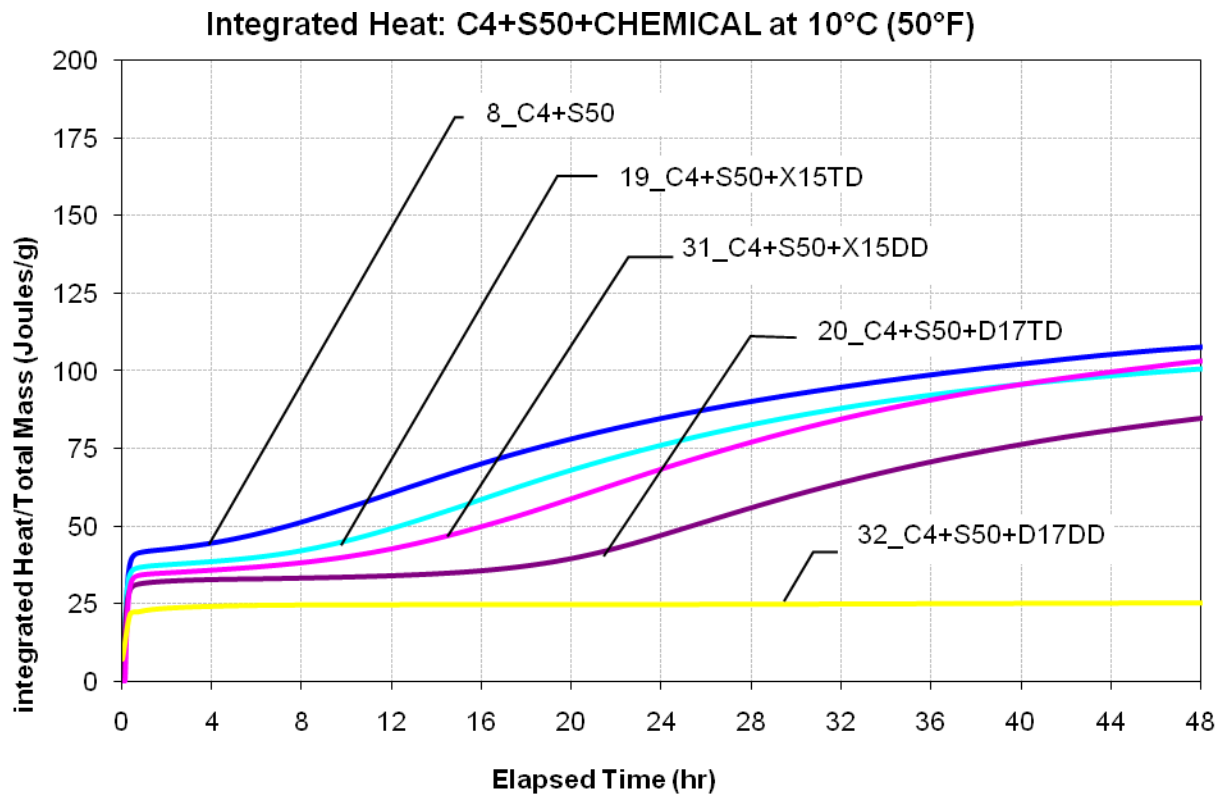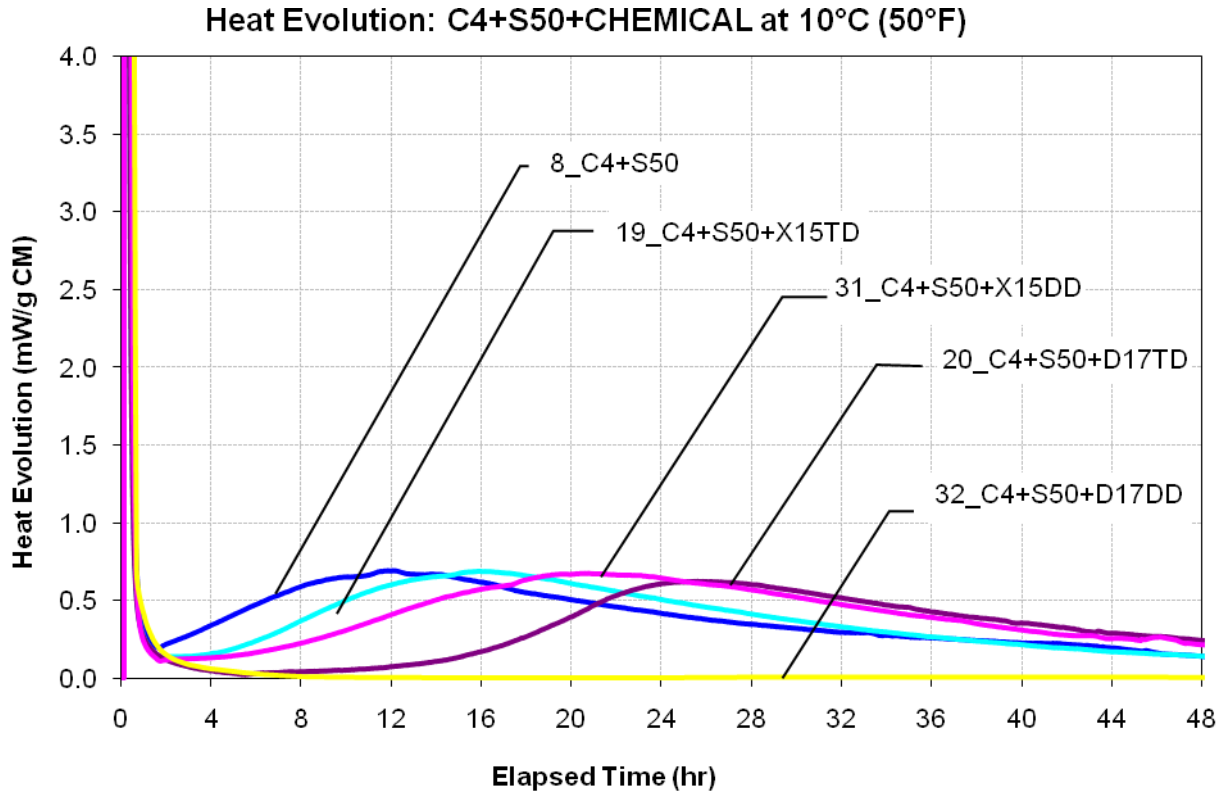
Figure C.16. Heat Evolution (Top) and Integrated Heat Evolution (Bottom) for Cement 4 with Slag System at 10°C.

122
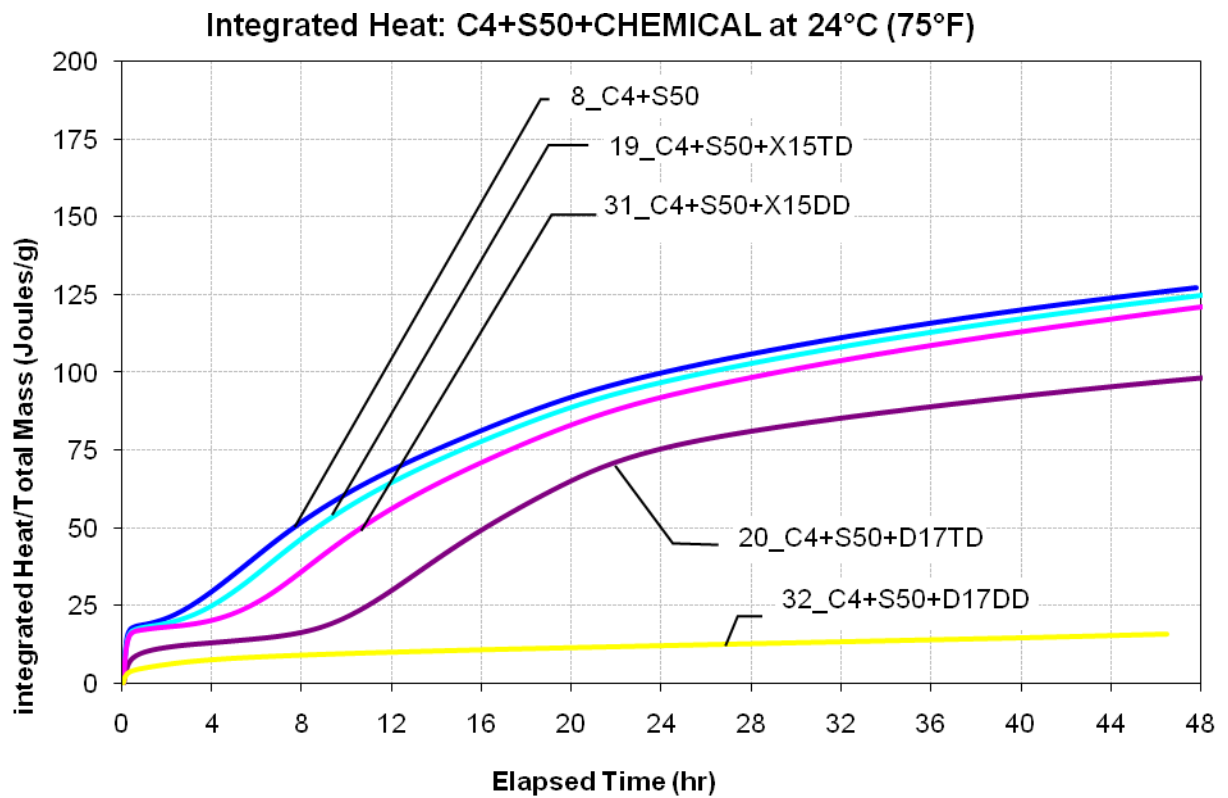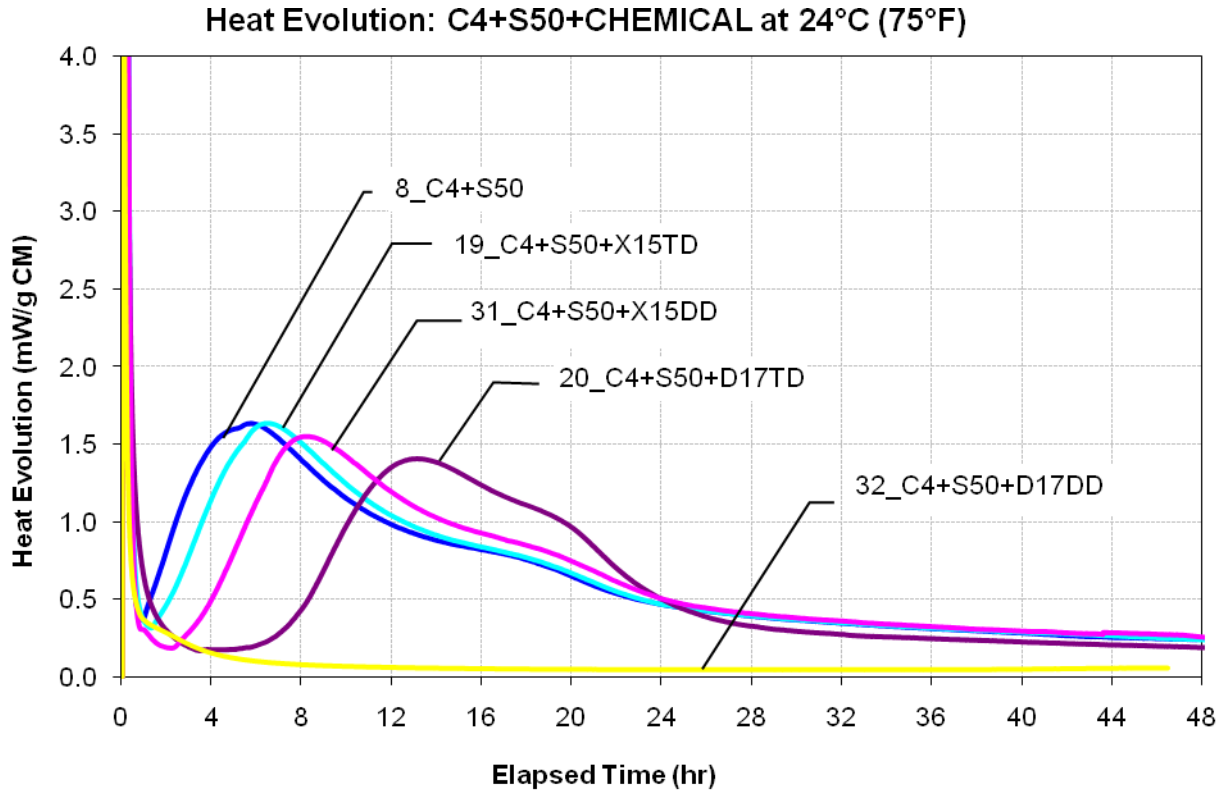
Figure C.17. Heat Evolution (Top) and Integrated Heat Evolution (Bottom) for Cement 4 with Slag System at 24°C.
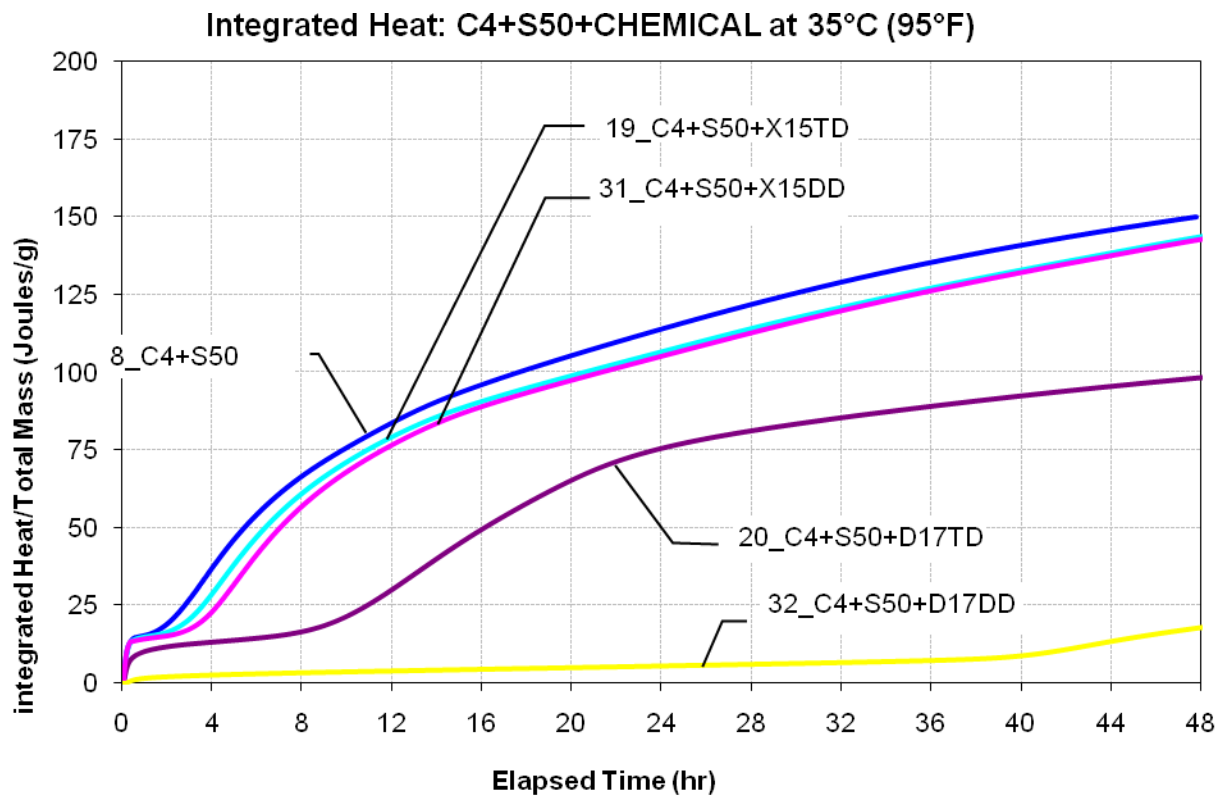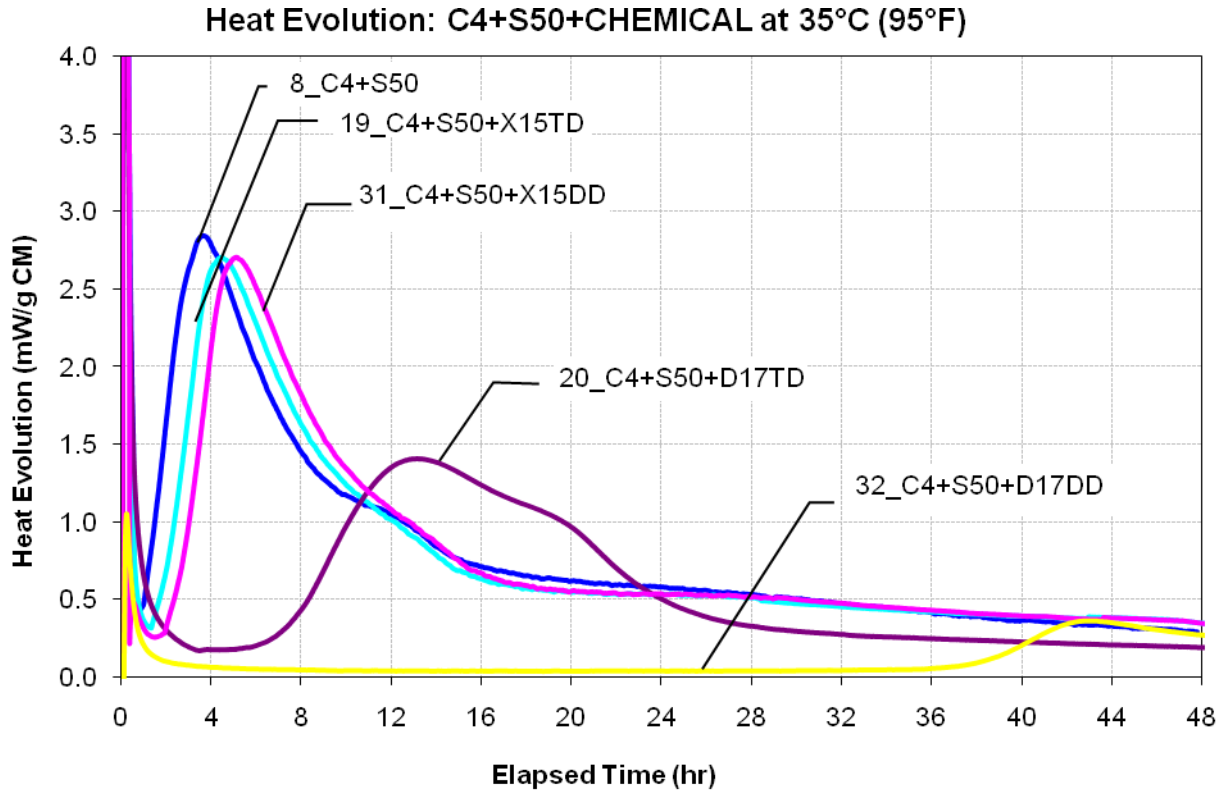
Figure C.18. Heat Evolution (Top) and Integrated Heat Evolution (Bottom) for Cement 4 with Slag System at 35°C.

124

APPENDIX D:

**THE BAR CHARTS OF THE**

RHEOLOGICAL PARAMETERS
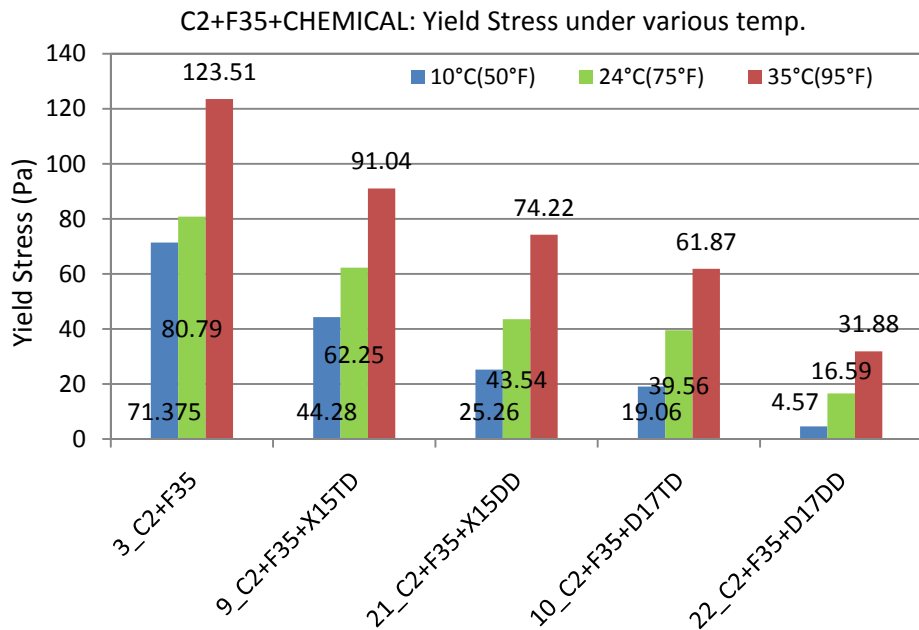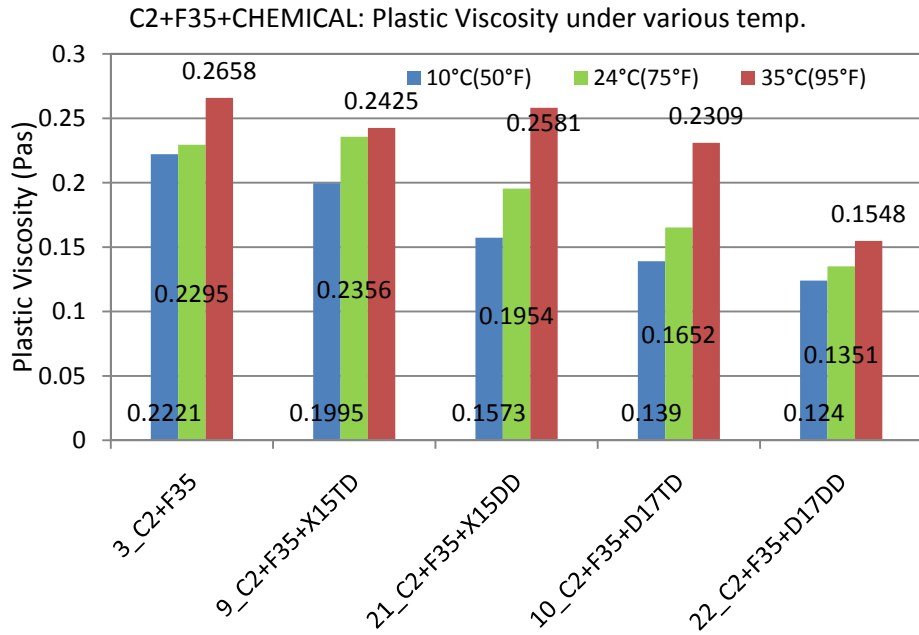
Figure D.1. PV (Top) and YS (Bottom) for C2+F35 System as a Function of Temperature, Admixture Type, and Dosages.
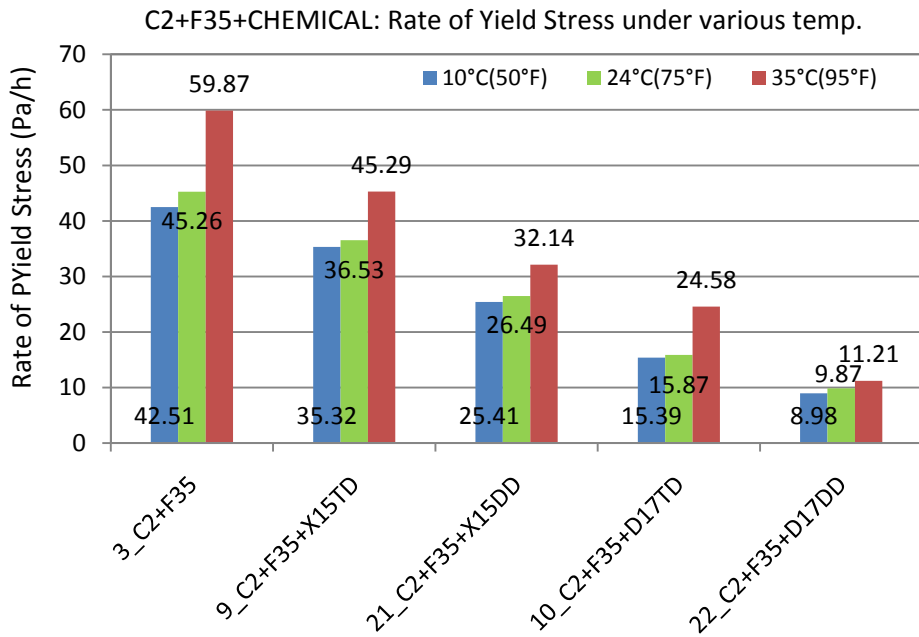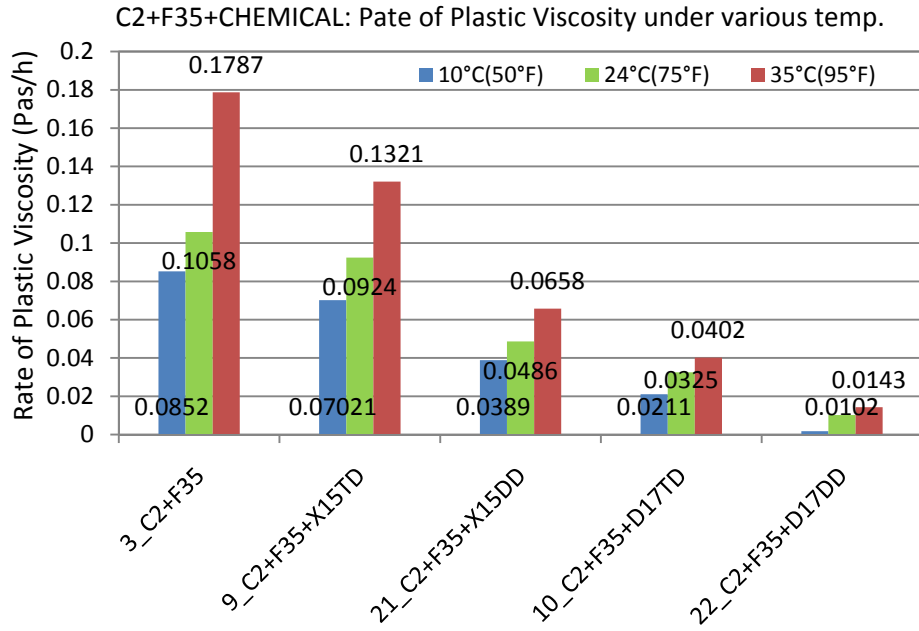
Figure D.2. RPV (Top) and RYS (Bottom) for C2+F35 System as a Function of Temperature, Admixture Type, and Dosages.

C2+C35+CHEMICAL: Plastic Viscosity under various temp.

**C2+C35+CHEMICAL: Yield Stress under various temp.**
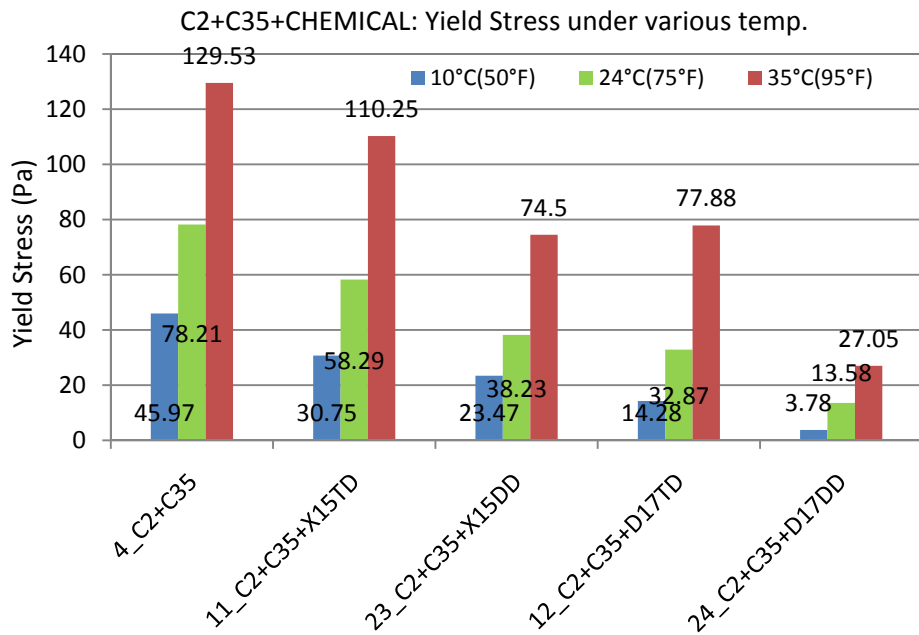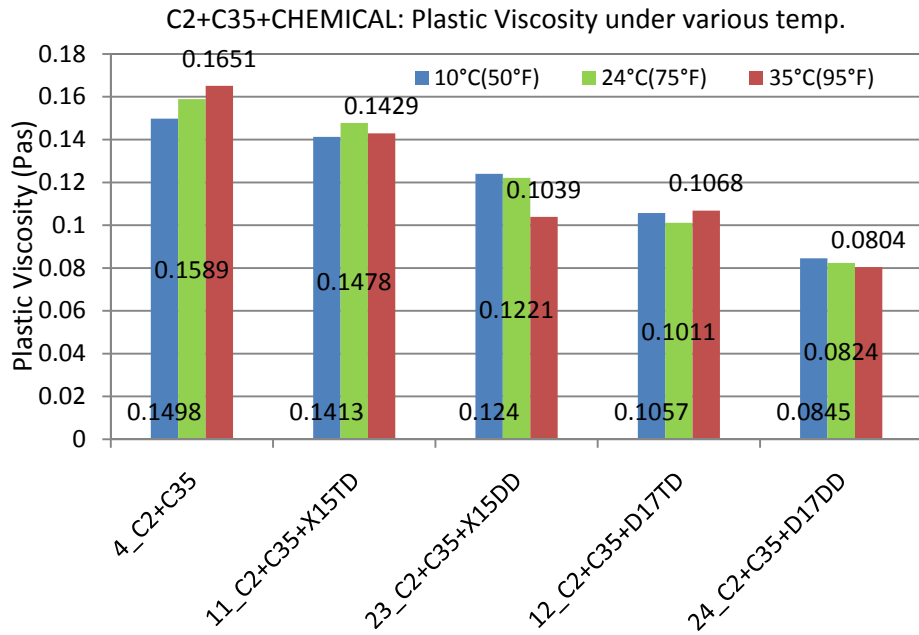
Figure D.3. PV (Top) and YS (Bottom) for C2+C35 System as a Function of Temperature, Admixture Type, and Dosages.
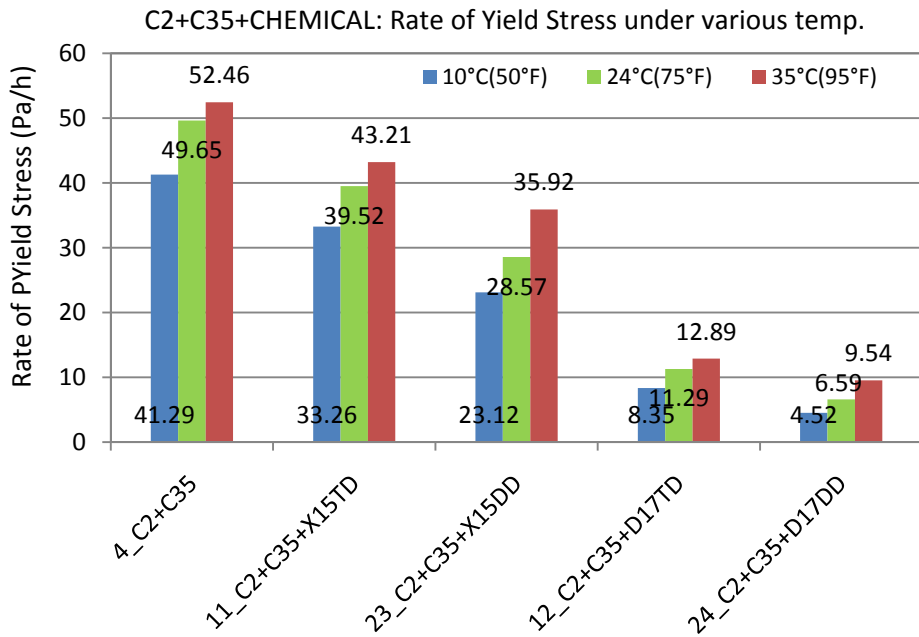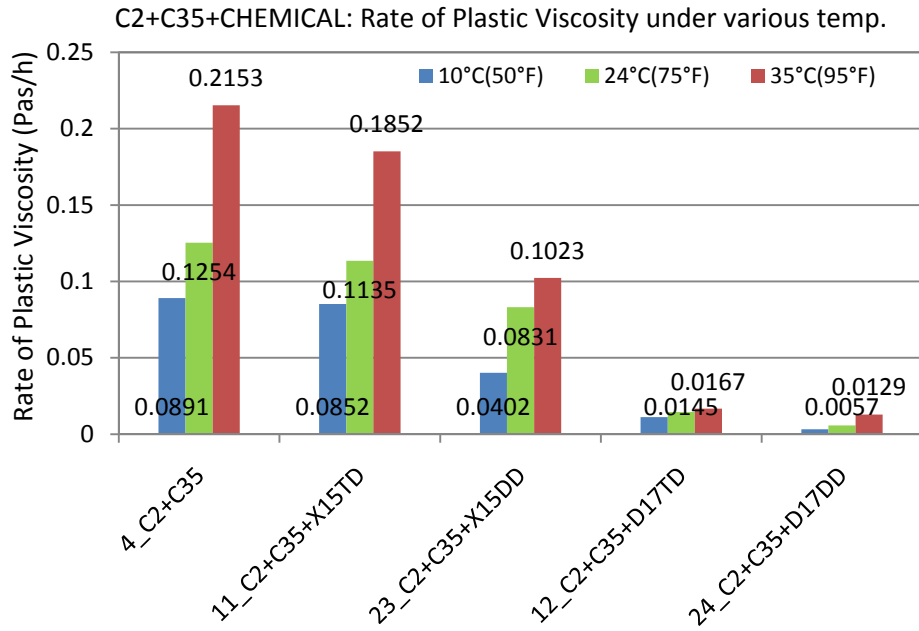
Figure D.4. RPV (Top) and RYS (Bottom) for C2+C35 System as a Function of Temperature, Admixture Type, and Dosages.

C2+S50+CHEMICAL: Plastic Viscosity under various temp.

C2+S50+CHEMICAL: Yield Stress under various temp.
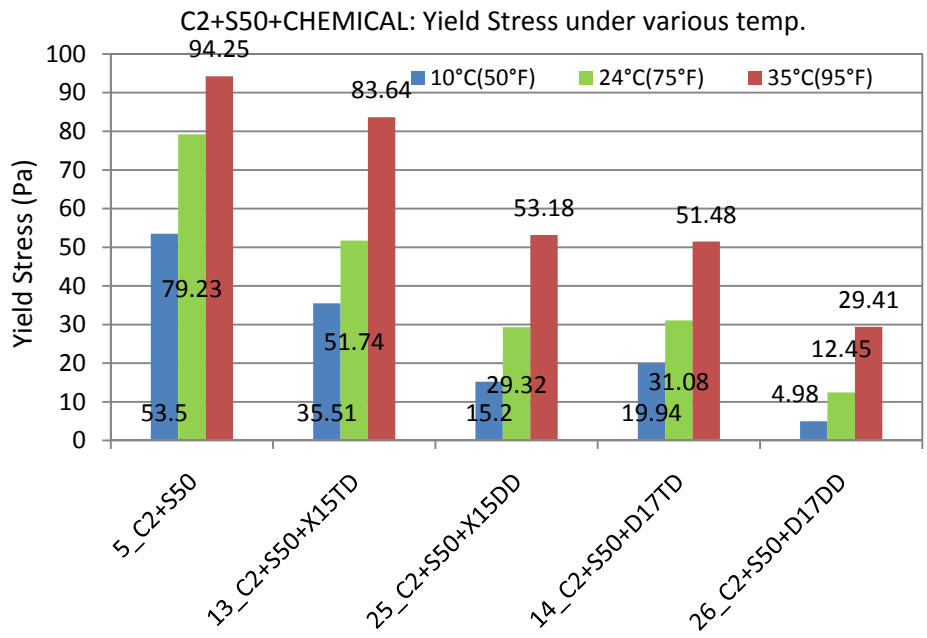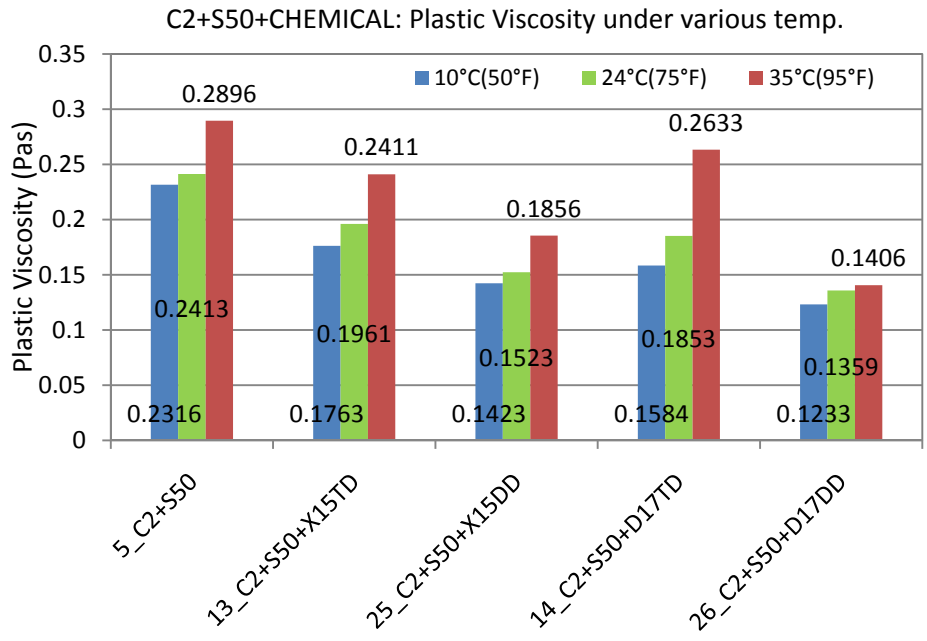
Figure D.5. PV (Top) and YS (Bottom) for C2+S50 System as a Function of Temperature, Admixture Type, and Dosages.
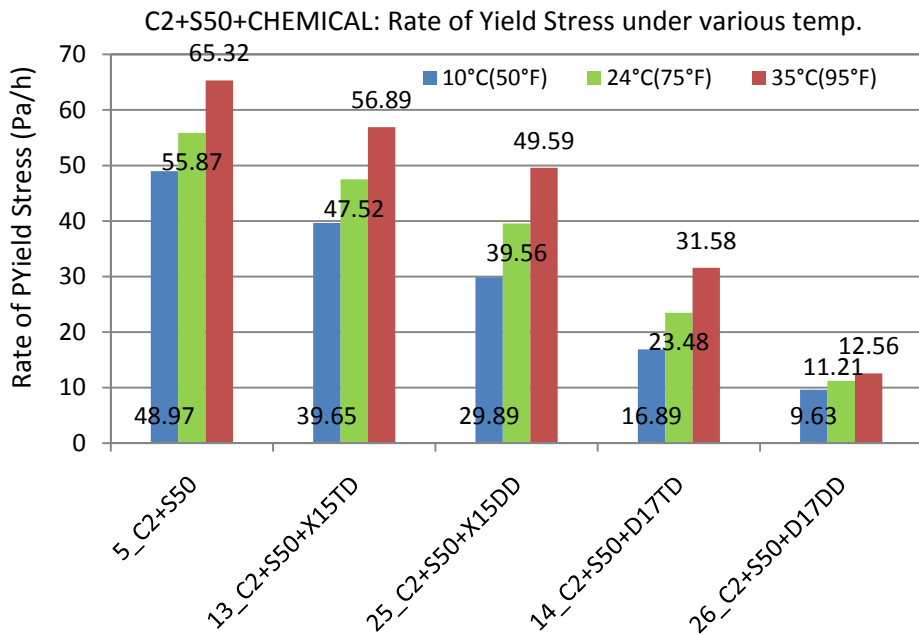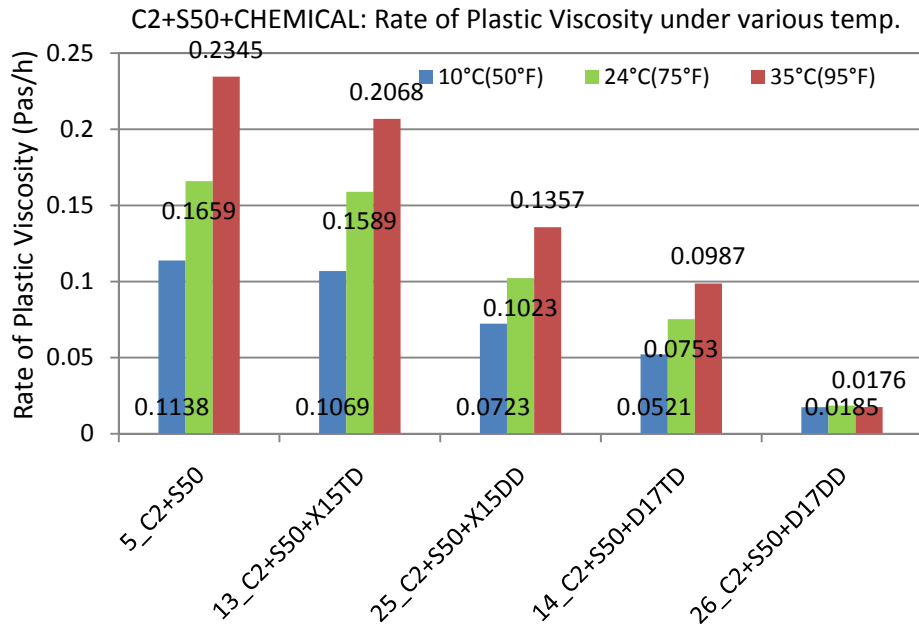
Figure D.6. RPV (Top) and RYS (Bottom) for C2+S50 System as a Function of Temperature, Admixture Type, and Dosages.
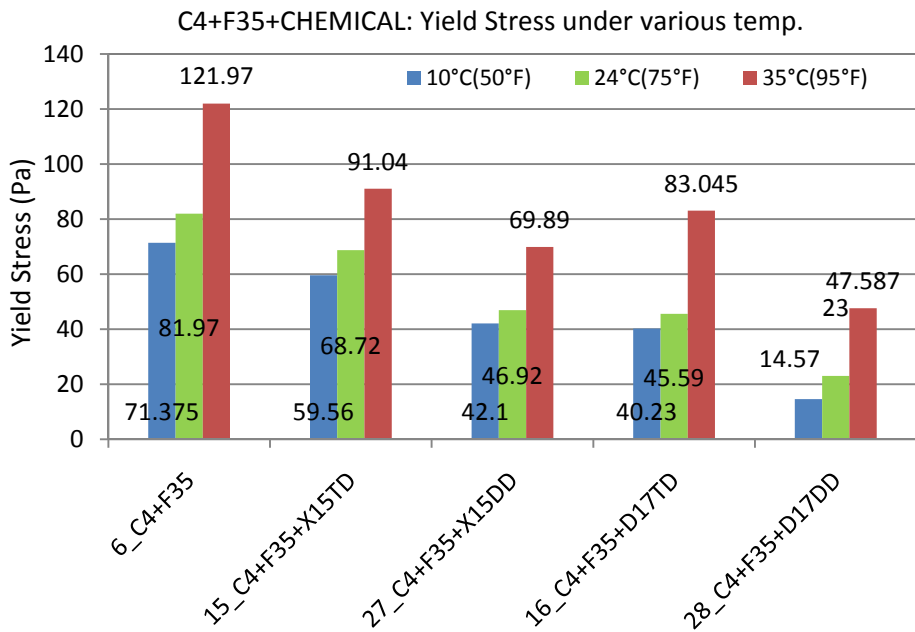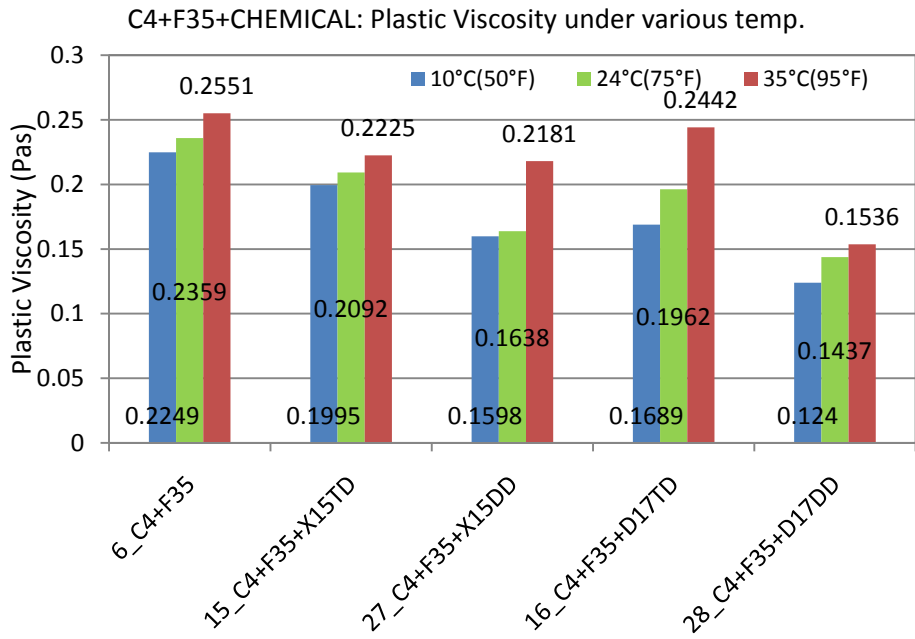
Figure D.7. PV (Top) and YS (Bottom) for C4+F35 System as a Function of Temperature, Admixture Type, and Dosages.
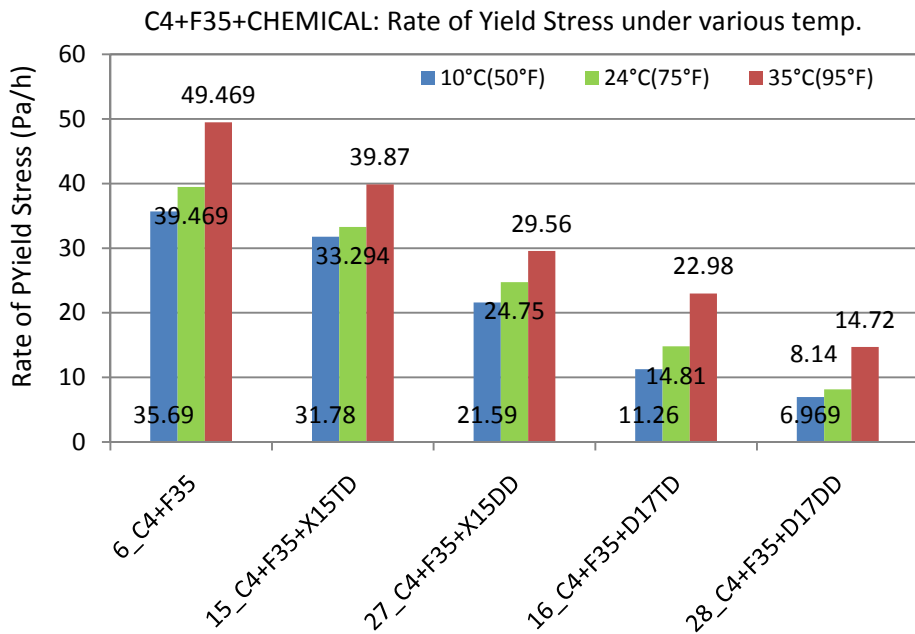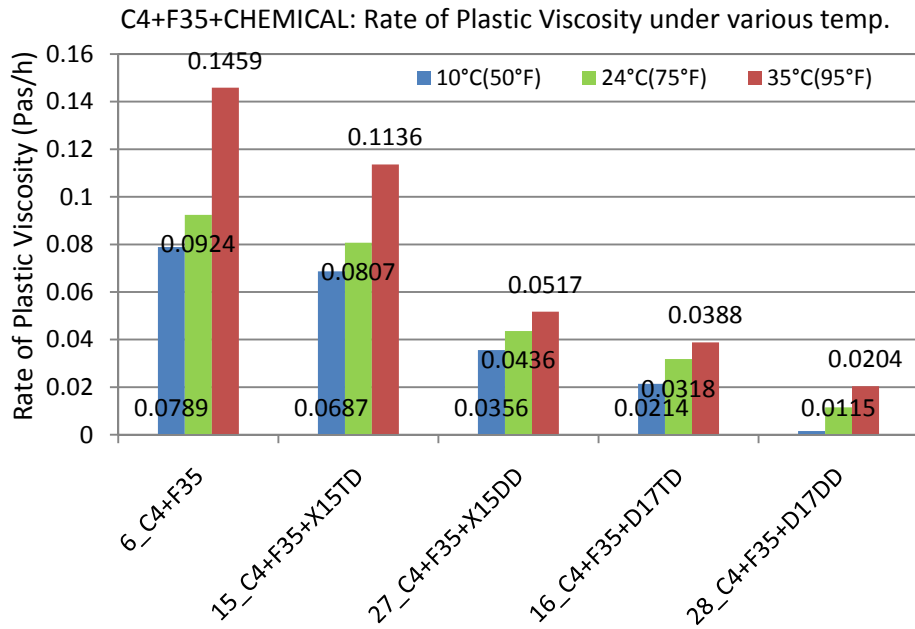
Figure D.8. RPV (Top) and RYS (Bottom) for C4+F35 System as a Function of Temperature, Admixture Type, and Dosages.

C4+C35+CHEMICAL: Plastic Viscosity under various temp.

**C4+C35+CHEMICAL: Yield Stress under various temp.**
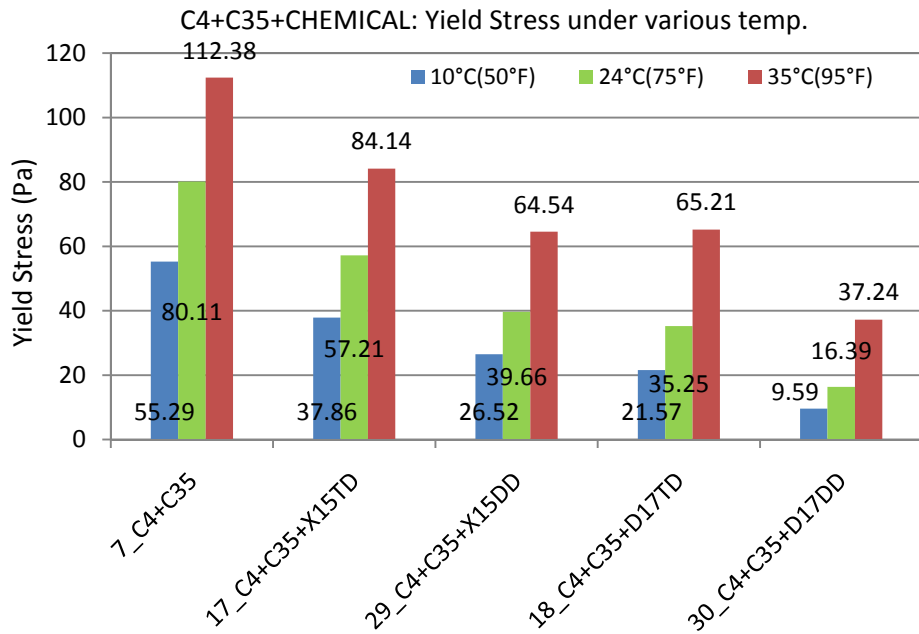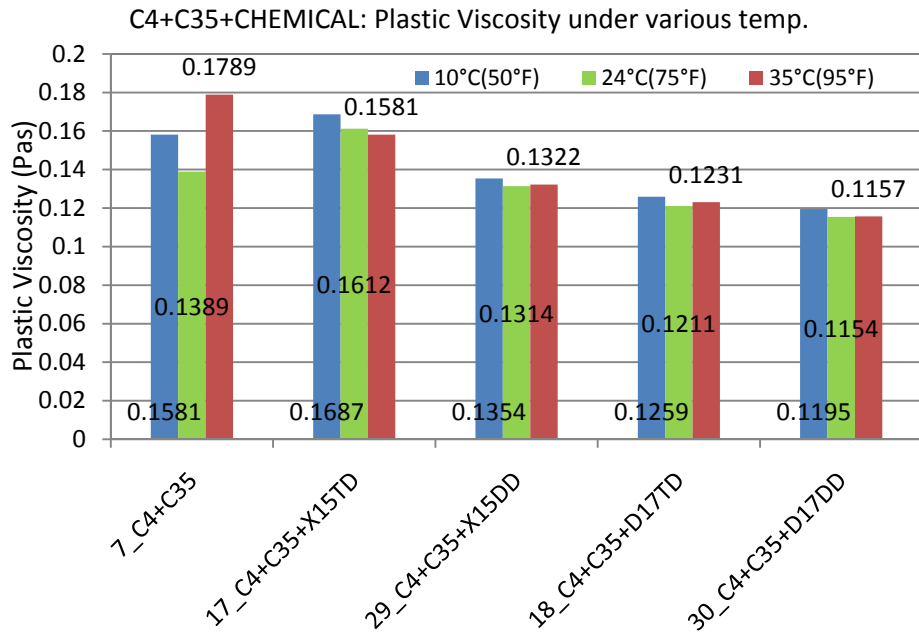
Figure D.9. PV (Top) and YS (Bottom) for C4+C35 System as a Function of Temperature, Admixture Type, and Dosages.
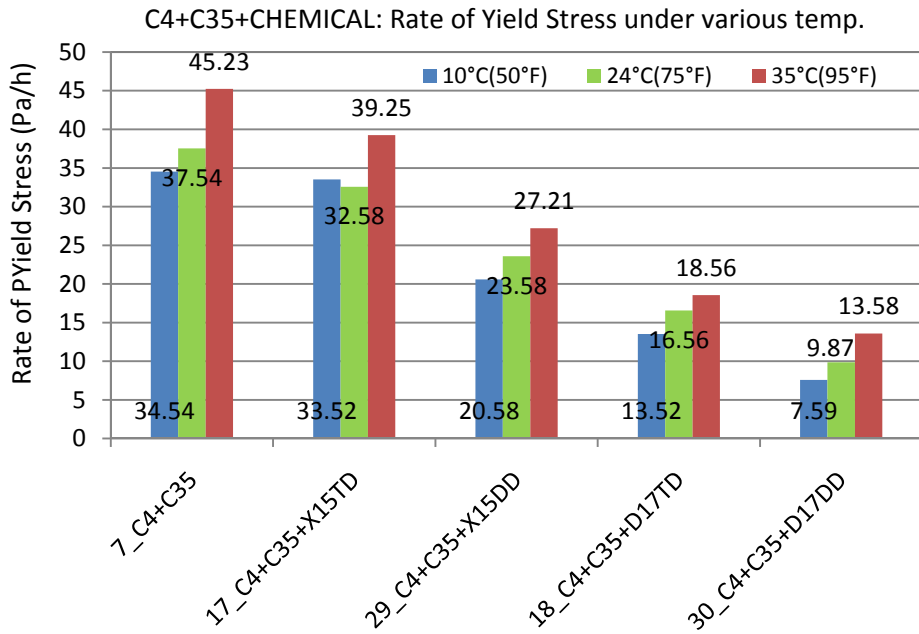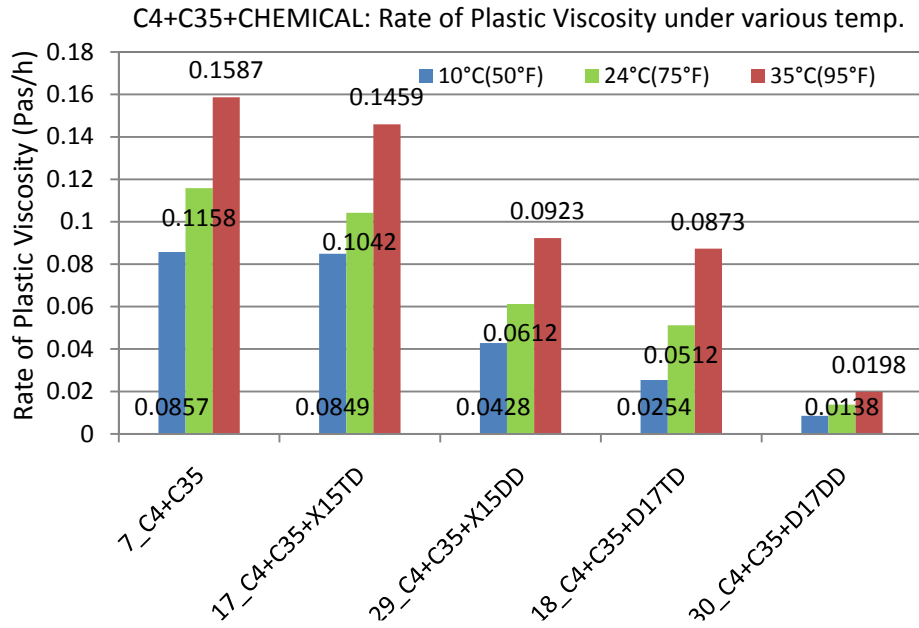
Figure D.10. RPV (Top) and RYS (Bottom) for C4+C35 System as a Function of Temperature, Admixture Type, and Dosages.
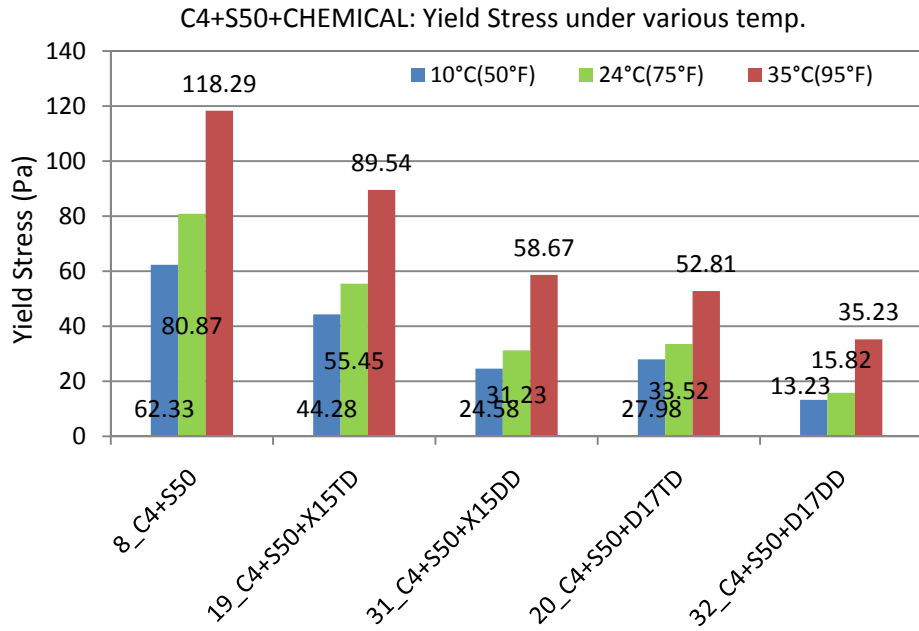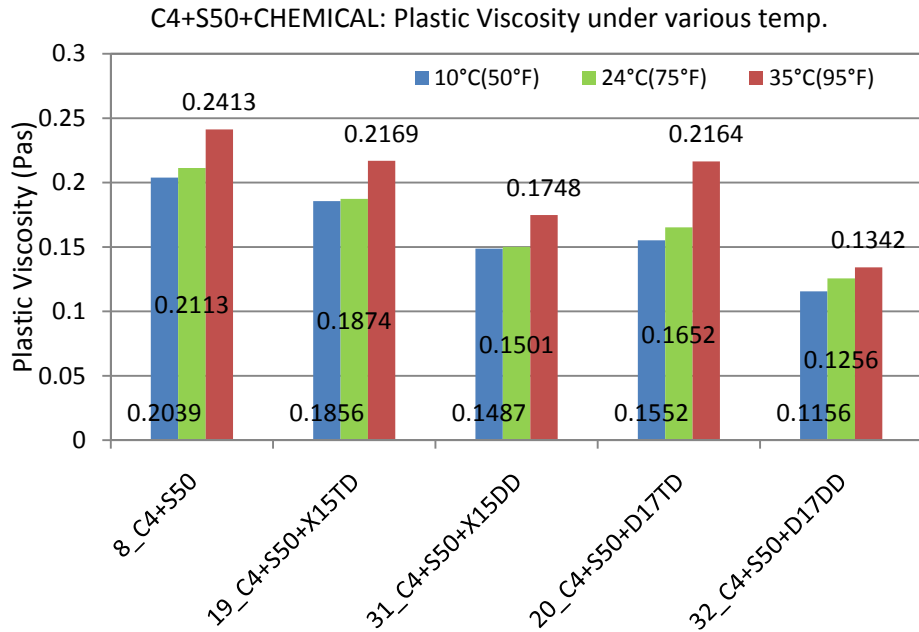
**Figure D.11. PV (Top) and YS (Bottom) for C4+S50 System as a Function of Temperature, Admixture Type, and Dosages.**
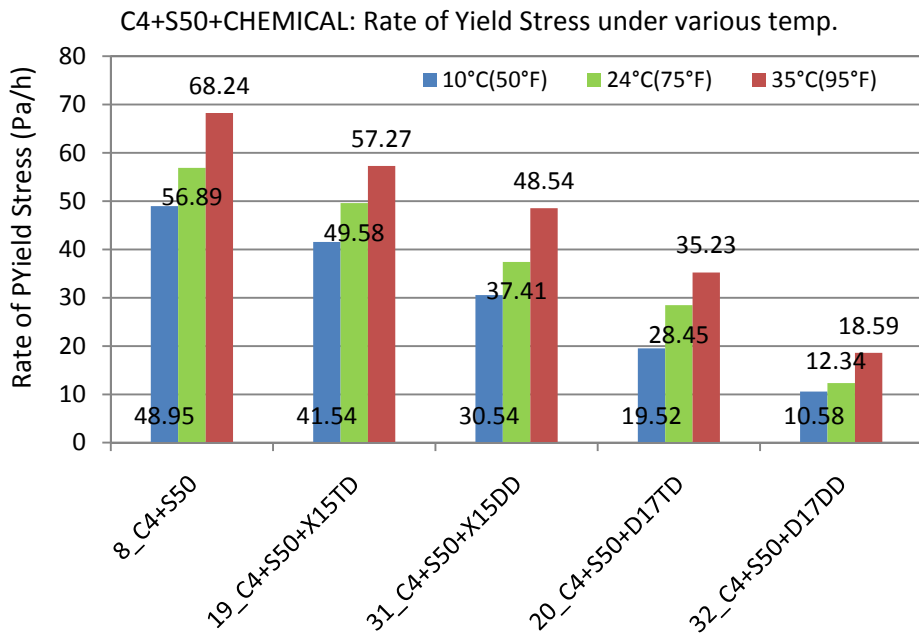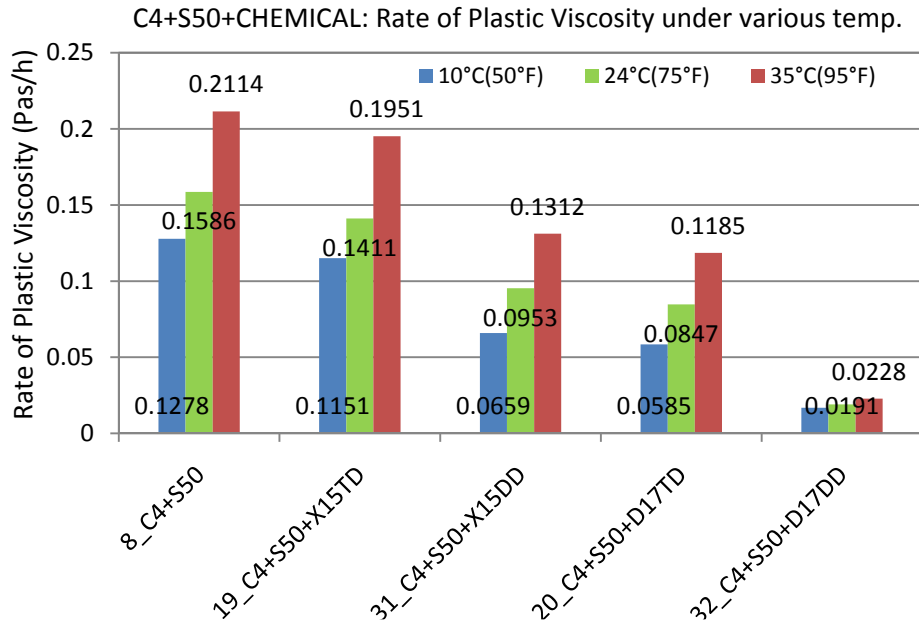
Figure D.12. RPV (Top) and RYS (Bottom) for C4+S50 System as a Function of Temperature, Admixture Type, and Dosages.